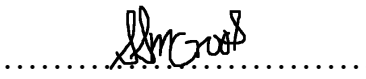




FACULTY OF SCIENCE AND TECHNOLOGY
MASTER'S THESIS

Study programme/specialisation: Offshore Technology, Subsea Technology	Spring semester, 2019 Open / Restricted access
Writer: Sebastian Croos Mariyathas	 (Writer's signature)
Faculty supervisor: Prof. Ove Tobias Gudmestad External supervisor: Dr. Airindy Felisita	
Thesis title: Optimization of Lazy Wave Riser Design	
Credits (ECTS): 30	
Keywords: SCRs, LWRs, Deepwater, Optimization, DNV-OS-F201, Riser configuration, Harsh Environment.	Number of pages: 85 + enclosure: 28 Stavanger, 25 th June 2019 Date/year

Abstract

The objective of this thesis is to optimize the design of a Lazy Wave Riser (LWR) operating at different water depths and in different sea conditions. Design of lazy wave risers involves optimization of the various constituent parts and different parameters which improves the fatigue life and load capacity. The LWR is a concept that is introduced for deepwater applications and milder environmental conditions. The LWR design is well known for its improved fatigue life and feasibility of the operation.

The riser's configurations are analyzed against extreme environmental conditions that occur on the Norwegian Continental Shelf (NCS) to study on the vulnerabilities of the riser. This study analyses the semi-submersible's response to the combination of 100 years wave and 10 years of current and the worst conditions are determined by the maximum allowable utilization of the riser, which is less than unity and hence expresses a safe design. The bending moment and Von Mises stress at the critical sections, sag bend, hog bend and touch down point, are determined. These parameters are used in determining extreme response for the different configurations. Using the basic geometries and parameters, the riser design at different conditions and configurations are optimized using the Orcaflex software.

Four wave directions (0, 45, 90, 180 degrees) are considered as part of the sensitivity study, with a total of 132 combinations being analyzed by Orcaflex. Furthermore, three different water depths were considered with the same set of parameters, tallying up to a grand total of 396 combinations of analyses. From the analysis results, it was found that the 180-degree wave direction to the vessel is giving the maximum downward riser velocity. An increase in the bending moment along the sag-bend area often also contributes to compressive force at the touchdown region due to the associated forces. Overall, this thesis work shows that the response of a production Lazy Wave Riser optimized and designed for deployment in deep waters and harsh environment, is in compliance with the safe design criteria.

Keywords: Water Depth, Lazy Wave Riser, Extreme response analysis

Acknowledgment

The work for this study was carried out at the Department of Mechanical and Structural Engineering and Materials Science, at the Faculty of Science and Technology, University of Stavanger, Norway, under the supervision of Professor Ove Tobias Gudmestad. This thesis is submitted towards the completion of the Master of Science degree in Marine and Offshore Technology.

I would like to take this opportunity to appreciate and thank of Professor Ove Tobias Gudmestad for all the motivation and the timely guidance he provided for this thesis. He has been kind and welcoming in his approach, which was a major source of encouragement. I acknowledge all his provisions and help he provided.

I would also like to make known my deepest gratitude to Dr. Airindy Felisita, who served as my External Supervisor. She has been enormously helpful to me since the initial days, and I owe a lot of the success of this thesis to her. She has been kind in providing me with the preliminary data for the mode, and my comprehension of OrcaFlex has been the result of her graciousness. Her valuable feedback and inputs kept me on the right track throughout the project.

I appreciate the dedication and commitment of all the faculty members, lecturers, and administration officials at the University.

I would also like to make a mention of Antonias Lasut, Akin Adejuwon, and Rohan Joseph and thank them for all the help they provided me with, and Rajiv specifically for the motivation and valuable support that he provided for my thesis.

My family and other friends have been a constant source of encouragement throughout the duration, and I owe them much thanks.

Finally, but most importantly, I thank God and all those whose prayers have seen me through this time and helped me see the light at the end of the tunnel.

Thank you all!

Stavanger, 25 June 2018

Sebastian Croos, Mariyathas

Nomenclature

Greek Characters

α_c	Flow stress parameter accounting for strain hardening
α_{fab}	Manufacturing process reduction factor
γ_A	Load effect factor for accidental factor
γ_C	Resistance factor to account for special conditions
γ_E	Load effect factor for environmental loads
γ_F	Load effect factor for functional loads
γ_M	Material resistance factor
γ_{SC}	Safety class factor
ρ	Water density
ν	Poisson's ratio
σ_e	Von Mises Equivalent Stress

Symbols

A	Cross section area
C_D	Drag coefficient
C_M	Inertia coefficient
E	Young's module
h	Height
H_s	Significant wave height
kg	kilogram
kN	kilo Newton
m	meter
mm	millimeter
s	Second
T_p	Corresponding wave period

Abbreviations

ALS	Accidental Limit State
API	American Petroleum Institute
BOP	Blow-out Preventer
DNV	Det Norske Veritas
DOF	Degree of Freedom
FLS	Fatigue Limit State
FPSO	Floating Production Storage and Offloading
LF	Low Frequency
LRFD	Load and Resistance Factor Design
JONSWAP	Joint Operation North Sea Wave Project
LWR	Lazy Wave Riser Configuration
MODUs	Mobile Offshore Drilling Unit
NCS	Norwegian Continental Shelf
RAOs	Response Amplitude Operators
SCR	Steel Catenary Riser
SLS	Serviceability Limit State
LWR	Lazy Wave Catenary Riser
SMYS	Specified Minimum Yield Stress
TDP	Touchdown Point
ULS	Ultimate Limit State
VIV	Vortex Induced Vibration
WF	Wave Frequency
WSD	Working Stress Design

Table of Contents

Abstract	i
Acknowledgment	ii
Nomenclature	iii
Table of Contents	v
List of Tables.....	viii
List of Figures	ix
1. Introduction.....	1
1.1 Overview and Background	1
1.2 Current research and development	3
1.3 Scope and Objective	4
1.4 Design Considerations	5
2. Deepwater Riser Systems	7
2.1 Introduction	7
2.1.1 Drilling Risers	7
2.1.2 Production Risers	8
2.1.3 Completion Risers	9
2.1.4 Export Risers	9
2.1.5 Injection Risers.....	9
2.2 Flexible Risers	10
2.3 Rigid Steel Risers	11
2.3.1 Steel Catenary Risers (SCRs).....	11
2.3.2 Lazy Wave Risers (LWR)	14
2.4 Hybrid riser.....	15
3. Design Codes and Standards for Riser Systems	16
3.1 Introduction	16

3.2	DNV-OS-F201	17
3.2.1	Limited State Design	18
3.3	Design Load Effects	20
3.4	Resistance Factors	22
3.5	Serviceability Limit State (SLS).....	23
3.6	Ultimate Limit State	24
3.6.1	Bursting	24
3.6.2	Hoop Buckling (Collapse).....	25
3.6.3	Propagating Buckling	25
3.6.4	Combined Loading Criteria.....	26
3.7	Fatigue Limit State (FLS).....	27
3.7.1	S-N curve method.....	28
3.7.2	Fatigue Crack Propagation Method.....	28
3.8	Accidental Limit State (ALS).....	29
3.9	Safety Classes	30
3.10	DNV - Allowable Stress	31
4.	Methodology and Design Premise	34
4.1	Introduction	34
4.2	Metocean Data Study.....	34
4.3	Resonance on Riser	36
4.4	Basic Concepts of VIV	36
4.4.1	Key Parameters	37
4.5	Elements Causing Resonance.....	41
4.5.1	Wave and Current.....	41
4.5.2	Floater Motions	41
4.5.3	Response Amplitude Operator (RAOs).....	44
4.5.4	Hydrodynamic Loading.....	47

4.6	Design Basis	48
4.6.1	Riser Material Properties.....	48
4.6.2	Buoyancy module data	49
4.6.3	Fluid data.....	51
4.6.4	Flex Joint.....	51
4.7	Design Parameters Studies	52
4.7.1	Environmental Data.....	52
4.7.2	Selected Sea State.....	55
4.8	Design Requirement and Acceptance Criteria.....	58
4.8.1	Wall Thickness Criteria.....	58
4.8.2	Acceptance Criteria	59
4.9	LWR Overview.....	61
5.	Extreme Response Analyses	63
5.1	Introduction	63
5.2	Determination for worst Sea state.....	64
5.3	Determination of Critical section for LWRs	68
5.3.1	Static Analysis.....	68
5.3.2	Dynamic Analysis	76
6.	Conclusion	84
	References	86
	Appendix A: Wall Thickness Calculation	89
	Appendix B: Sensitivity Studies for Steel Catenary Riser-OrcaFlex Example.....	92
	Appendix C: OrcaFlex Software Description.....	109

List of Tables

Table 3.1 Description of Load According to DNV-OS-F201 (DNV, 2010a)	21
Table 3.2 Load Effect Factors (DNV, 2010a).....	22
Table 3.3 Safety Class Factor (DNV, 2010a)	22
Table 3.4 Material Resistance Factor (DNV, 2010a).....	23
Table 3.5 Design Fatigue Factors (DNV, 2010a)	28
Table 3.6 Design Check for Accidental Loads (DNV, 2010a)	30
Table 3.7 Classification of Safety Classes (DNV, 2010a)	31
Table 4.1 Steel Pipe Properties (Felisita, 2017).....	49
Table 4.2 Buoyancy Module Properties (Felisita, 2017).	50
Table 4.3 Various Water Depth for LWR.....	52
Table 4.4 Typical Design Sea States for Deep-water area within NCS (Felisita, 2017).....	54
Table 4.5 Typical Current Data for Deep-water Area within NCS (Felisita, 2017).....	54
Table 4.6 Environmental Contour Lines Selected Sea States for Worst Conditions	56
Table 4.7 Thickness of Marine Growth and Biofouling (NORSOK, 2016).....	57
Table 4.8 Hydrodynamic Coefficient (Felisita et al., 2017).....	57
Table 4.9 Riser-soil Interactions (Orimolade et al., 2015).....	58
Table 4.10 Minimum Wall Thickness	59
Table 4.11 Allowable Riser Stress Level (LI, 2014)	60
Table 4.12 Design Case Factor (LI, 2014).....	60
Table 4.13 Parameters of the LWR Configuration	62
Table 4.14 Worst Metocean Condition.....	63
Table 5.1 Selected Worst Condition from the NCS (WD2000m)-Dynamic Analysis	65
Table 5.2 Selected Worst Condition from the NCS (WD1500m)-Dynamic Analysis	66
Table 5.3 Selected Worst Condition from the NCS (WD1000m)-Dynamic Analysis	67
Table 5.4 Summary Results of Lazy-Wave Riser Nominal Static Analysis	71
Table 5.5 Summary Results of Lazy-Wave Riser Nominal Static Analysis	73
Table 5.6 Summary Results of Lazy-Wave Riser Nominal Static Analysis	76
Table 5.7 Summary Results of Lazy-Wave Riser Nominal Dynamic Analysis	77

List of Figures

Figure 1.1 History of Deep-water Development (Shell, 2018)	2
Figure 1.2 Example Composite Drilling Riser (Pangaea Drilling, 2019).....	4
Figure 2.1 Drilling Riser (Hariharan & Thethi, 2007)	8
Figure 2.2 Production Risers (Genesis, 2017)	8
Figure 2.3 Unbonded Cross Section of Flexible Pipe (Gardner, 2017).....	10
Figure 2.4 Steel Catenary Riser (Nakhaee, 2010).....	12
Figure 2.5 Lazy Wave Riser Configuration (Hoffman et al., 2010).....	14
Figure 2.6 Hybrid Riser Configuration (Miller, 2017)	16
Figure 3.1 DNV Standards and RP's for Risers (DNV, 2010a).....	17
Figure 3.2 Design Approach (DNV, 2010a).....	20
Figure 3.3 Hoop Stress and Longitudinal Stress.....	31
Figure 3.4 Curved Element of a Beam (Case et al., 1999).....	33
Figure 4.1 Contour Lines for the Deep-water area for the Metocean Condition in the Norwegian Continental Shelf (NCS) (Felisita, 2017).	35
Figure 4.2 Vortex Shedding: In-line and Cross-flow Response (Kenny, 1993).....	37
Figure 4.3 Plot of Strouhal Number and Reynolds Number for Circular Cylinders (Achenbach & Heinecke, 1981)	38
Figure 4.4 Non-dimensional Amplitude versus Reduced Velocity for three Cylinders with Different Weight (Vikestad, 1998)	40
Figure 4.5 The Six Degrees of Vessel Motions in Sea (Journee & Massie, 2001).....	42
Figure 4.6 Relation between Floater Motions and Waves (Journee & Massie, 2001)	42
Figure 4.7 Semi-submersible Offset Positions (Taheri & Siahtiri, 2017)	43
Figure 4.8 Wave Direction Convention (LI, 2014).....	45
Figure 4.9 RAO for Yaw (lowest value at high period), Roll (next lowest value at high periods), Pitch, Sway, Heave, and Surge (largest value for high periods) (Gudmestad, 2015).....	46
Figure 4.10 The Relation Between Wave Spectrum and RAO for Heave for Three Different Types of Floating Structure (Gudmestad, 2015).	46
Figure 4.11 Buoyancy Modules (Balmoral, 2014).	50
Figure 4.12 Flex Joint Hutchinson Oil and Gas (Knapstad, 2017)	51
Figure 4.13 Flex Joint Implemented for SCR/LWR. (Oil States Industries, 2019).....	52
Figure 4.14 Environmental Contour lines for Selected Sea States (Felisita, 2017).....	55
Figure 4.15 Lazy wave riser Model in OrcaFlex	61
Figure 4.16 Plan View of OrcaFlex LWR Model.....	62
Figure 5.1 Static and Dynamic Stage	64
Figure 5.2 Max Effective Tension for Static Analysis.....	69

Figure 5.3 Max Bending Moment for Static Analysis	69
Figure 5.4 Max Von Mises Stress for Static Analysis	70
Figure 5.5 Max Utilization for Static Analysis	70
Figure 5.6 Max Effective Tension for Static Analysis	71
Figure 5.7 Max Bending Moment for Static Analysis	72
Figure 5.8 Max Bending Moment for Static Analysis	72
Figure 5.9 Max Utilization for Static Analysis	73
Figure 5.10 Max Effective Tension for Static Analysis	74
Figure 5.11 Max Bending Moment for Static Analysis	74
Figure 5.12 Max Von Mises Stress for Static Analysis	75
Figure 5.13 Max Utilization for Static Analysis	75
Figure 5.14 Riser Effective Tension for (WD: 2000m)	78
Figure 5.15 Riser Bending Moment (WD: 2000m)	78
Figure 5.16 Riser Von Mises Stress (WD: 2000m)	79
Figure 5.17 Riser Utilization (WD: 2000m)	79
Figure 5.18 Riser Effective Tension (WD: 1500m)	80
Figure 5.19 Riser Bending Moment (WD: 1500m)	80
Figure 5.20 Riser Von Mises Stress (WD 1500m)	81
Figure 5.21 Riser Utilization (WD: 1500m)	81
Figure 5.22 Riser Effective Tension (WD: 1000m)	82
Figure 5.23 Riser Bending Moment (WD: 1000m)	82
Figure 5.24 Riser Bending Moment (WD: 1000m)	83
Figure 5.25 Riser Utilization (WD: 1000m)	83

1. Introduction

1.1 Overview and Background

The petroleum industry incorporates many globally related processes, such as investigating the hydrocarbon reservoirs, extracting and processing the produced oil and gas, and then shipping the products to the worldwide market. The main products of this industry are gas, LPG, gasoline, and fuel oils. However, developing an oil and gas reservoir is not that easy. Installing an oilrig faces many problems such as high-pressure drilling, high-temperature wells, varying weather conditions, wave, currents and vibrations, unexpected movements of the facilities, etc. In order to overcome these uncertainties and problems, risers are installed between the surface facilities and the process facilities.

Risers are a common sight within the oil and gas industry since the beginning of the petroleum age. They are used for many purposes in this industry, such as, for drilling, production, transportation, and injection. Risers are designed to adhere to safety rules and regulations. Their main function is to safely ship the fluids from one point to another, from the seabed to the oil/gas platform and/or from the platform to the seabed. Risers are attached to one end of the pipeline which lies on the seabed. Using pipelines to transport the oil and gas extracted has been proven to be the safest way of transport according to a study conducted by the Frasier Institute. Between the period of 2003 to 2013, pipelines only experienced an occurrence rate of an accident of 0.049 per million barrels transport, which is considered as extremely low (Green & Jackson, 2015).

Deepwater drilling technology is used to drill oil wells inside the seabed., i.e., under the deep water. There are broad ranges in deep water, below 500 m to more than 2000 m. Oil is not only abundant onshore and shallow waters but also can be found in deep to ultra-deepwater. And to extract the resources from the sea, deepwater drilling technology is introduced.

Deepwater drilling has been used by the Chinese for over 6000 to 7000 years, for drinking water purpose (Angelakis et al., 2012). One interesting thing to notice is that the mathematical and analytical skills used by them were quite advanced. Now there are around 3400 wells drilled in the deep water of the Gulf of Mexico. Due to increasing oil and gas demand, many companies have now started investing in deepwater drilling to find oil resources and to extract them (Bai & Bai, 2005).

Budgeting for the riser systems used in offshore field production development is critical since it contributes to a significant amount of the cost. The first production risers were used in the

1970s, inspired by top-tensioned drilling risers. After which riser have been used for different reason including in drilling or as completion, workover, injection, production and exports lines. (Sparks, 2007). Nowadays, production risers are designed with various configuration rather than the top-tensioned configuration. The common usage and proven riser concepts include SCR (Steel Catenary Riser), flexible risers, and single line or bundled multi-lines hybrid risers (Felisita, 2017). Nowadays, production risers are designed with various configuration rather than the top-tensioned configuration. The common usage and proven riser concepts include SCR (Steel Catenary Riser), flexible risers, and single line or bundled multi-lines hybrid risers (Felisita, 2017).

Steel catenary risers have significantly reduced the cost as compared to conventional rigid and flexible risers. It has aided in the development of a more economic riser design option for fixed platforms (Dikdogmus, 2012). On the other hand, steel lazy wave risers have better advantages for the increasing demand for deep-water developments. Lazy wave risers are feasible and more reliable in deep water for the below reasons (Hopkins, 2015):

- Reduced vessel payload
- Partial decoupling of vessel motions between Touch Down point (TDP) and hang off
- Simplified fabrication and installation compared to freestanding riser solutions

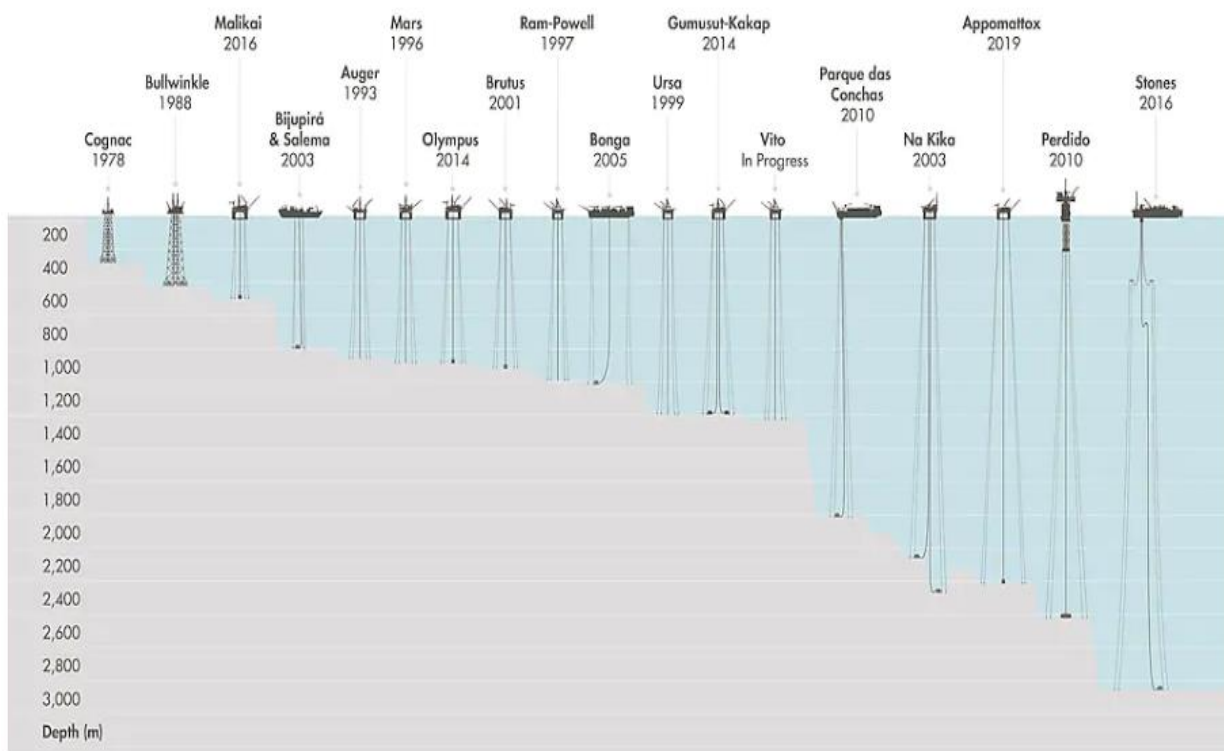


Figure 1.1 History of Deep-water Development (Shell, 2018)

In Figure 1.1 above, various concepts of offshore field development are shown, from the conservative fixed platforms to Floating Production Units (FPUs) in ultra-deep waters.

The different production concepts are illustrated graphically above, ranging from the shallow waters' fixed platform to the deep and ultra-deep waters' FPUs. This thesis is focused on the implementation of lazy wave risers with water depth level ranging between 500 m to 2000 m.

1.2 Current research and development

The most commonly used material for a riser is steel. The riser technology is developing day by day as it is being made to work deeper and deeper. However, the challenges also increase along with the developments. As the water depth goes deeper, risers will be exposed to higher dynamic loads, leading to higher vibrations of the risers (Han & Yan, 2010). This leads to many forces acting on the riser, which in turn reduces the fatigue capacity of the riser. For this purpose, researchers are aiming to develop new materials for risers instead of steel. The desired riser material should have the following qualities:

- Lighter weight
- Ability to withstand pressure at deeper applications
- High damping ability at deeper applications
- Cost-effective
- Easy to install and deploy at any circumstances
- Prolonged life
- High corrosion resistant properties.

Unfortunately, designing a riser to comply with all above-mentioned properties is not possible with the existing materials and technologies. These alternatives are really cost expensive, and it is hard to switch from steel to other material as the current technologies are not favorable. Nevertheless, many companies are trying to develop and manufacture risers by using different materials such as:

- Composite materials (Figure 1.2)
- Aluminum
- Titanium
- Other lighter materials.



Figure 1.2 Example Composite Drilling Riser (Pangaea Drilling, 2019)

The main research on riser technology is to develop technology to drill in the deep-water environment without causing pollution and other environment affecting problems. In terms of production risers, the demands on oil and gas companies are to implement field life extension, as a lot of oil and gas wells are having high amounts of hydrocarbon deposits.

1.3 Scope and Objective

The objective of this thesis is to study thoroughly about the design of Lazy Wave Risers (LWR) and to optimize the riser design at different conditions. The optimization process is done by using the computer program Orca flex; The world's leading package for the dynamic analysis of offshore marine systems software (OrcaFlex Manual, 2012). The study is done by collecting information and information about past research related to LWR design as the basis for further work in this thesis. Based on that, the analysis of a large number of configurations for different water depths and physical conditions will be done to identify the trends in the design when the design basis changes. The parameters are:

- Water depth
- Load conditions
- Environmental conditions
- Design codes
- Fatigue conditions
- Buoyancy modules
- Vessel load conditions

Based on these parameters, the riser design is subjected to optimization. Many mathematical models of the risers and the theory for riser design are studied to assess the behavior of a riser at different conditions. The static and dynamic response of the riser at different conditions are investigated. Optimizing the riser at the earlier stage itself (i.e., at the design stage) helps to reduce cost-related problems.

Along with it, the problems and the difficulties encountered will also be discussed in detail. Finally, the merits of implementing a certain LWR design according to the optimization will be discussed. Therefore, a recommendation of optimized riser design for certain applications (high-pressure drilling riser, low-pressure production riser, etc.) can be presented.

1.4 Design Considerations

Using computer-based techniques, a highly efficient production riser can be designed. There are many parameters, criteria, and considerations when designing a riser. It should be designed under international standards such as API-RP-2RD (API, 1998) or DNV-OSS-302 (DNV, 2010C). These considerations are mainly focusing on the safety of the riser when it is installed on the seabed, the riser stress level, and marine life. A few criteria to be followed while designing a riser are:

- Pipe curvature
- Clearance between the riser and other structures
- Tension prescribed by the pipe manufacturer
- Prescriptions by the pipe manufacturer
- Dynamic response boundaries

The main struggle in designing a riser is to consider all parameters. Due to increased risk and demand for deep-water developments, a large number of data and parameters should be closely monitored to ensure an efficient and safe riser system design. The design criteria for flexible risers are mainly given as fulfilling the below design parameters (DNV, 2010C):

- Strain (polymer sheath, unbonded pipe)
- Creep (internal pressure sheath, unbonded pipe)
- Strain (elastomer layers, bonded pipe)
- Stress/load (reinforcement layers and carcass, bonded pipe)
- Stress (metallic layers and end fittings)
- Hydrostatic collapse (buckling load)

- Mechanical collapse (armor layer induced stress)
- Torsion
- Crushing collapse and vocalization (during installation)
- Compression (axial and effective)
- Service life factors.

There are three stages in the design phase of a riser system. The first stage is about static analysis of the riser and determining the geometrical layout of the riser system. It also involves various studies to ensure a safe design when the design of the riser is changed due to different conditions. i.e., different design parameters such as changing the size and/or geometry, pipe length, and configuration. Finally, a design which satisfies the design criteria is approved. The study will also evaluate the static effects of the current loading and the vessel motion in different directions.

In the second stage, the dynamic response is assessed with a dynamic analysis of the riser. For this, the design and criteria accepted from the first stage are used, as well as selecting the sequences of dynamic load cases. The dynamic load cases include a combination of various conditions such as riser contents and positions, wave and current conditions, and vessel motions to assess the operational ability of the riser at its dynamic state. From the analyses, the parameters are checked and ensured to be within the design limits.

The last stage is about both static and dynamic analysis of particular areas to design certain elements of the riser system. This analysis is relevant for the intermediate connectors and pipes associated with the riser and its minor components. All the parts, even the minor components are checked at different working conditions based on the riser configuration for safer and smoother operations. The design configuration will eventually be determined according to the result of the riser design and its application in the deep water. The above-mentioned stages are the common design procedures at all levels of riser design (Ismail et al., 1992).

2. Deepwater Riser Systems

2.1 Introduction

With the definition of riser already established earlier, the different types of risers based on their applications and configurations are discussed in detail in this chapter. Generally, the risers are classified into five broad categories:

- Drilling risers
- Production risers
- Completion risers
- Export risers
- Injection risers.

2.1.1 Drilling Risers

As the name implies, a drilling riser (Figure 2.1) is used to perform drilling operations in deep water or shallow water. In shallow water, as the pressure is low, standard joints are used, and the need for buoyancy and low top tension is both not necessary. However, in deep-water, high riser tension and special stack-up arrangements should be considered for the drilling operation.

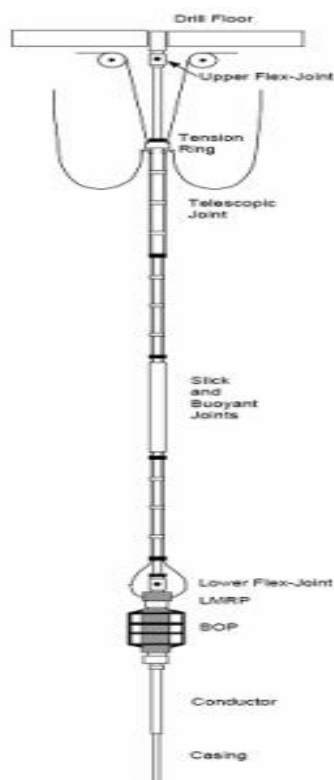


Figure 2.1 Drilling Riser (Hariharan & Thethi, 2007)

Drilling risers are usually vertical risers installed from fixed platforms and jack-up drilling rigs. For shallow water, a free-standing riser is utilized in which the wellhead is positioned above the riser, and the conductor casing acts as an extension of the well's conductor. The blow-out preventer (BOP) is arranged on the wellhead level. This makes the drilling riser to handle the same pressure and fluids as the sub mud line casing elements. For deepwater drilling applications, the risers are vertical Top tensioned risers (TTRs) and are installed from a floating platform.

2.1.2 Production Risers

The purpose of production risers (Figure 2.2) is to transport fluids produced from the reservoir. Production risers, also known as flow line risers, are the pipes which are used for the transportation of unprocessed oil and/or gas to the processing plant at the floating platform.



Figure 2.2 Production Risers (Genesis, 2017)

Production risers are often divided into four types (Bai & Bai, 2005).

- Steel Catenary risers
- Top-tensioned risers
- Flexible risers
- Hybrid risers.

The long-term performance of a riser system is significantly determined by motions in the floating platform. A similar influence is also seen at the floating platform, as the riser will have static and dynamic effects on its response. Therefore, the floating platform, the risers, and the mooring system behave like an entire system with a complex response to environmental loading (Felsite, 2017).

2.1.3 Completion Risers

These risers are vertical risers which give direct access to the wellhead and are intended to accomplish offshore completion, workover, and intervention processes. They are either installed with a fixed platform or floating platform systems. Generally, the completion risers are utilized in combination with the floating MODUs (Mobile Offshore Drilling Units). In some cases, completion risers are used along with subsea completions that use subsea trees.

2.1.4 Export Risers

Export risers are the flow lines for the passage of processed oil and/or gas from the platform to the processing plant, whether it is floating offshore or is located onshore. The export risers are specially designed to carry the hydrocarbons in their oil and gas components while at the same time avoiding the flow assurance problems and difficulties. Hence, these risers are oil or gas export risers without insulation. The use of separate risers for gas or oil components avoids the formation of hydrates while shipping the hydrocarbons.

These risers can be free standing export risers, top-tensioned export risers or catenary export risers based on their applications and configurations. Freestanding export risers are used for shallow water application in a fixed platform. Top-tensioned and catenary export risers are used for deepwater applications installed to a floating production platform.

Usually, the export riser has a single tube, which in turn results in less productivity. However, in the growing riser technology in oil and gas industry, one or more oil or gas components are used to facilitate the required production output in the export riser production facility (Miller, 2017).

2.1.5 Injection Risers

Injection risers serve another purpose, such as transporting fluids to the producing reservoir in order to increase the reservoir pressure and eventually increase the productivity of the well.

In injection risers, brine water is used for injection fluid. The riser is installed on a fixed platform, and the water is used to increase the pressure in the reservoir. It involves drilling wells to increase oil production in shallow and deep water.

2.2 Flexible Risers

A flexible riser (Figure 2.3) is a riser type with properties such as high axial and low bending stiffness. This riser is made from the combination of distinct layers that are divided into two categories that are known as the Un-bonded or Bonded type. The un-bonded riser has independent movement, whereas the bonded type has different layers connected using polymer material. Flexible risers have been available for more than 40 years and are still evolving to meet the demand of a larger production bore, as well as coping with the current challenges of deeper waters (Luppi et al., 2014).

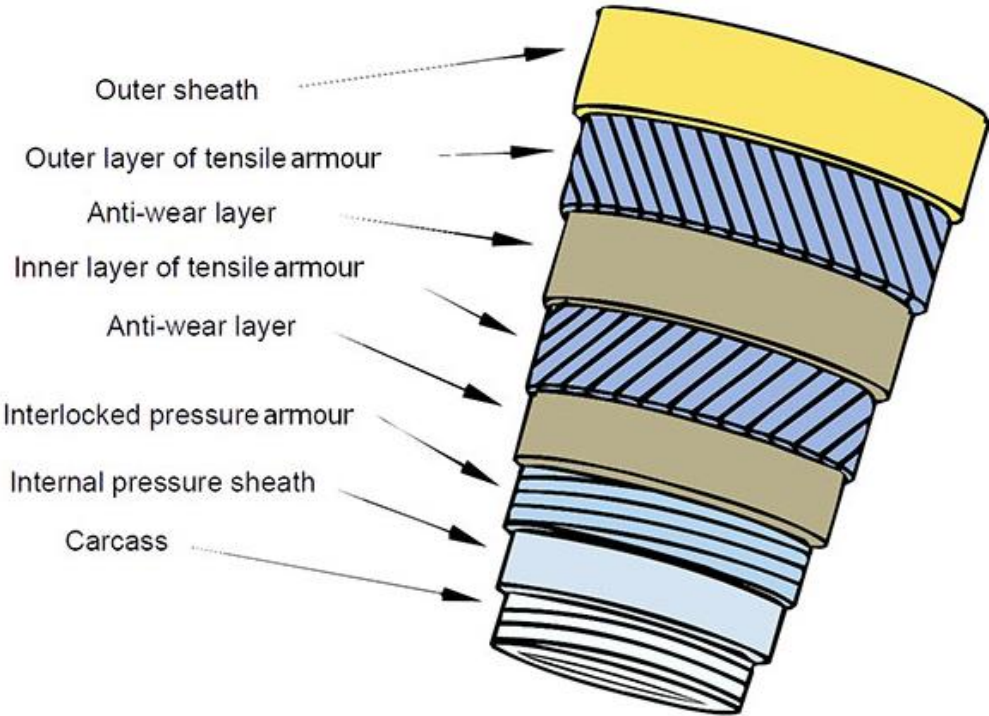


Figure 2.3 Unbonded Cross Section of Flexible Pipe (Gardner, 2017)

Other benefits that flexible risers offer includes, such as it is easy to install, has mobility, and reusability after decommissioning. Recently, composite materials have been introduced as an alternative material for a flexible riser in order to reduce weight, being cost-efficient, and have a higher resistance to corrosion (Kalman et al., 2014).

Despite the advantages that flexible riser provides, its limitation is often observed in deep waters. With the increase of external pressure in deeper waters, the specifications of a production bore are limited (Carter & Ronalds, 1998). Adjustments to the concept selection have to be done, together with the construction cost as compared to rigid steel riser.

2.3 Rigid Steel Risers

Rigid steel risers are usually designed in deep and ultra-deep-water fields using the X60, X65 or X70 steel (Low Carbon). Advantages of the rigid steel risers opposed to the flexible risers include its availability to be designed with larger diameters, ability to be suspended in deeper waters due to its axial strength and lower cost (Huang & Hatton, 1996).

2.3.1 Steel Catenary Risers (SCRs)

A Steel Catenary Riser (SCR) is an extension from a subsea pipeline in a catenary form attached to a floating structure. Initially, SCRs (Figure 2.4) were installed on fixed platforms. SCRs initially appeared at the Auger TLP floating platform in 1994 and now is commonly used in deep-water fields. The SCR's main application is on TLPs, Spars, and semi-submersibles in Brazil, the Gulf of Mexico and West Africa.

The SCR has been widely installed in West Africa FPSO in recent years. This section presents instances of installation (Bai & Bai, 2005) in the Gulf of Mexico. After the first SCRs were installed on Auger TLP, in 1997, the first semi-submersible SCRs were installed in the Marlen Field. Afterwards, in 2001, installation of the first SCRs on truss spars took place on the fields Comoving and Nansen in the Gulf of Mexico. Further, in 2004, the first SCRs were installed on the FPSO vessel in West Africa.

The SCR is commonly used in deep water fields with advantages that include its lower costs, simple design, ability to tolerate the higher temperature and pressure resistance, and improved movement compliance for the floating body. Due to the complicated nature of the marine environment that exists, researching on the SCR theory usually involves fluid dynamics, non-linear mechanics, soil mechanics, and some interdisciplinary related topics

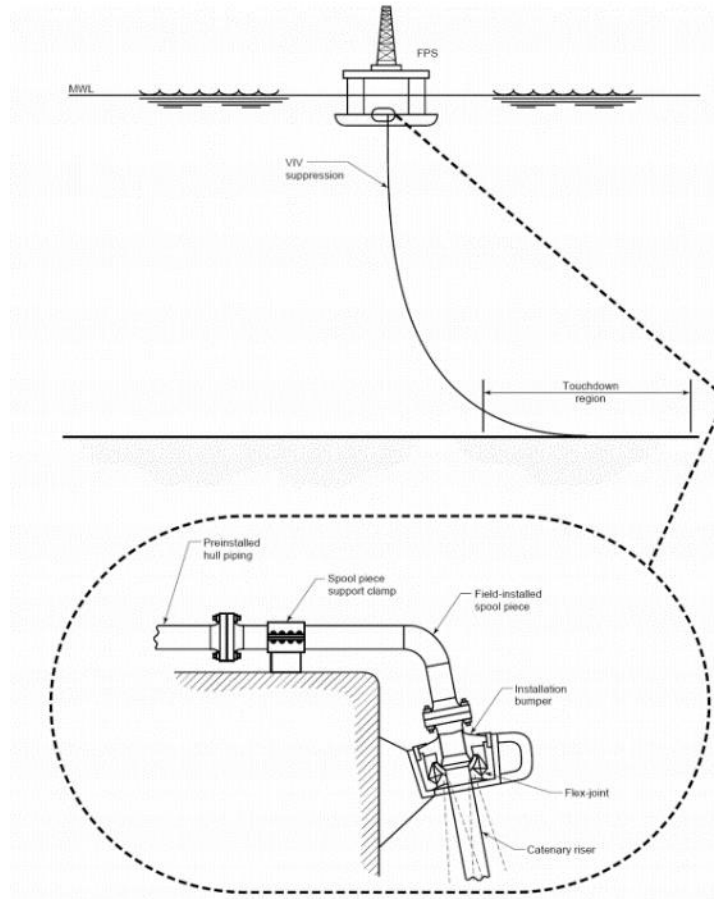


Figure 2.4 Steel Catenary Riser (Nakhaee, 2010)

Strong waves and vessel offsets due to harsh weather conditions has often been cited as a challenge when selecting SCRs model (Legras et al., 2013). The heave, surge and sway usually induce a higher bending force which results in substantial buckling problems along with the touchdown area and fatigue load that is due to the riser soil interaction (Knapstad, 2017). These problems can be tackled by changing the weight along the riser by choosing dissimilar densities for the applied coating. A paper presented by Karunakaran indicated that by increasing the upper section weight while decreasing the cross-sectional weight at the touchdown, the point could improve the dynamic behavior of the SCR sufficiently. However, there is an upper limit on the floater motion, and if the motion is too large, the SCRs option will no longer be a feasible solution. The other design challenge for deep and ultra-deep waters in the high hang-off tension (Karunakaran et al., 2005).

The SCR connects a floating structure to devices like flex joint, J-tube, tapered stress joint, etc. The SCR segment is equipped with a VIV suppression device to reduce Vortex-induced vibration (VIV) (Taggart & Tognarelli, 2008).

Deepwater challenges

The external hydrostatic pressure exerted on the pipeline increases as the water depth increases. Therefore, this becomes an issue when designing pipelines in deep and ultra-deep waters. An extra effort has to be taken to ensure that the pipelines can withstand these extreme forces as the riser descends towards the seabed (Petromin, 2012). The biggest challenge here is the increase in top tension because of the riser increase in diameter and the deeper waters.

The effects that deep waters can have on a riser is summarized below (Howells and Hatton, 1997):

- Increased length and weight
- Increased thickness to resist hydrostatic loading
- Increased spread
- Increased cost

The increase in length is the most significant effect when the depth is increased. While in this case, the weight is often disproportional to the water depth as resistance to collapse due to the hydrostatic force changes (Howells and Hatton, 1997).

The riser spread is also another effect when the depth increases. A typical SCRs have a radial spread that is 1 to 1.5 of the water depths, thus increasing the spread significantly in deeper water (Howells and Hatton, 1997). This is a key factor when selecting the riser system position and production system arrangement.

The challenges related to the design of deep and ultra-deep water SCRs tied back to a floater are (Song and Stanton, 2007):

- Hang-off system limit
- Riser top payload (weight budget) limit
- Hang off angle limit
- Cathode protection design limit; and
- Thermal insulation design limit

2.3.2 Lazy Wave Risers (LWR)

The four different sections of LWRs are:

- Upper Catenary section
- Buoyancy section
- Lower Catenary section,
- Bottom section

Figure 2.5 shows an illustration of the LWR configuration.

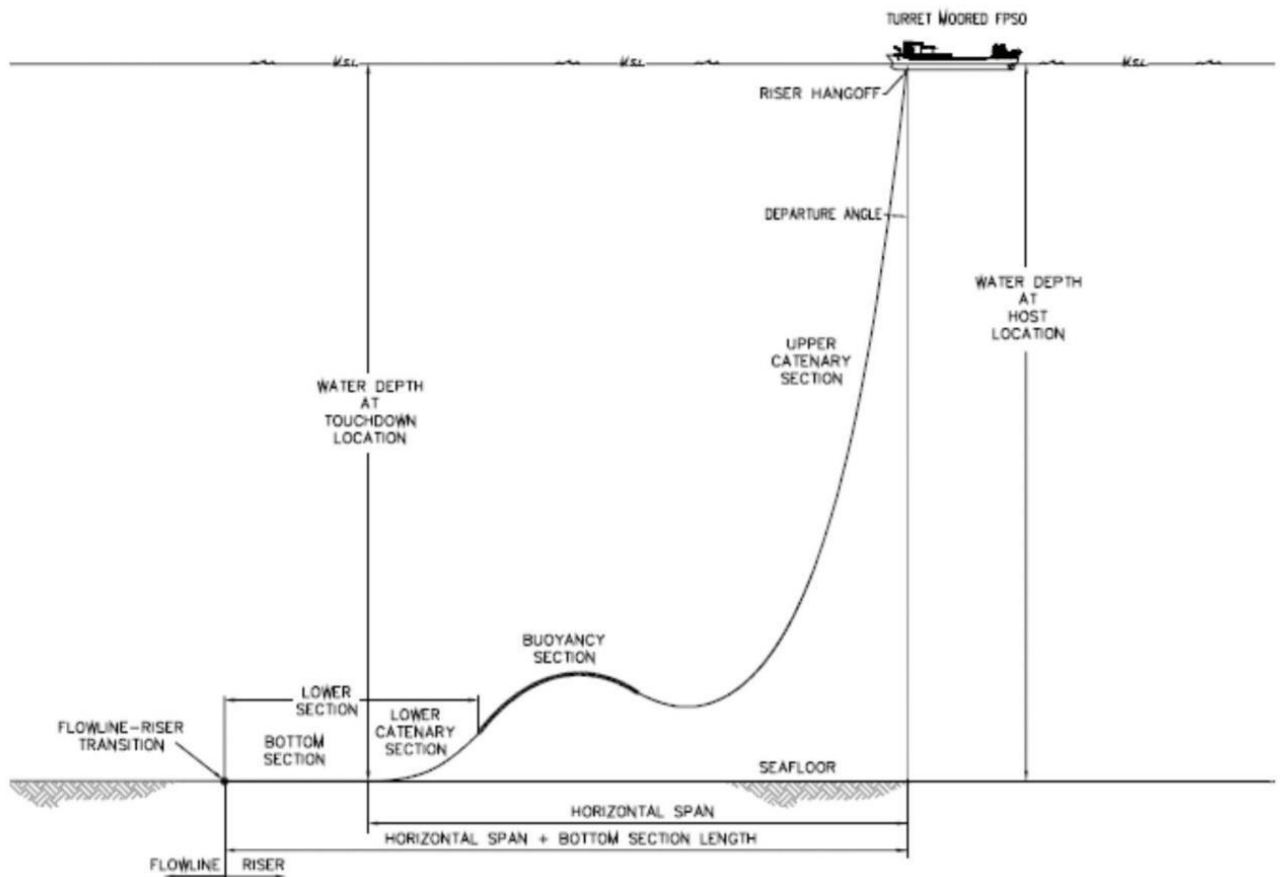


Figure 2.5 Lazy Wave Riser Configuration (Hoffman et al., 2010)

Buoyancy modules are an essential component that was proven to improve the performance of SCRs. The combination of buoyancy modules with the SCR create a distinctive riser configuration called Lazy Wave Riser (LWR). The buoyancy device in the LWR acts as a damper and separates the floater motion from the critical touchdown area, which improves the riser's performance (Felisita et al., 2017).

The fatigue life of LWR is improved significantly by decoupling the forces exerted by the FPU. An ideal configuration would include a low curvature in the hog and sag bend, due to its ability to minimize the static stress normally observed in these sections (Karunakaran et al., 1996). This system was initially introduced in Brazil in 2008 in the BC-10 field. After which, it has been gaining traction and has been successfully installed at different location around the world (Karunakaran & Frønsdal, 2016).

2.4 Hybrid riser

Hybrid riser systems (Figure 2.6) consist of a vertical (or rigid) section, a jumper (or catenary) section, and a submerged buoy near-surface. The development of the hybrid riser resulted from the need to complement the conventional high-stress, flexible, or catenary risers. While in a steel catenary riser, the vertical leg is joined together with a supporting sub-surface buoy, a hybrid riser has integrated steel and flexible pipe technologies that enable the flexible pipe to absorb most of the riser's dynamic motions. These hybrid systems were developed primarily to reduce the effect of decoupling between the risers and floating production unit.

The hybrid system would create more cost-effective, technical solutions, and higher productivity that would provide access to deeper developments in the field. The most commonly used hybrid risers are the Free-Standing Hybrid riser that uses one or many leg configurations bundled as a Hybrid Tower Riser (Tenaris, 2019).

Hybrid risers enable reduction of:

- Riser loads transmitted to the floating production unit to be reduced.
- Minimizing the problems of riser fatigue.
- Riser decoupling of installation planning as the hybrid risers can be pre-installed before the arrival of the floating production unit.

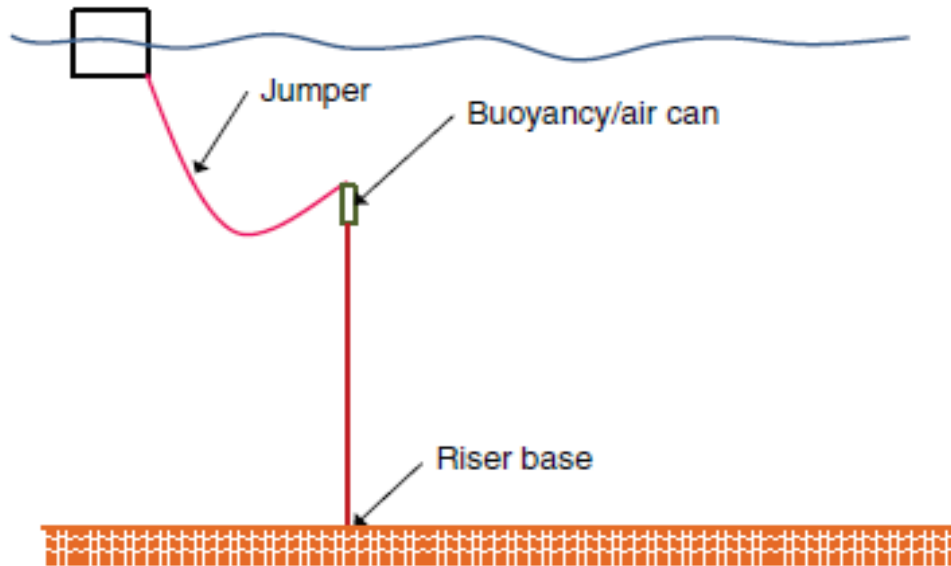


Figure 2.6 Hybrid Riser Configuration (Miller, 2017)

These riser systems are designed to allow riser installation before or after the host platform installation, reduce the riser weight that the host platform must support, and help isolate the riser from the motions of the host platform. The vertical portion of the riser ranges from the riser base on the seafloor to the top riser assembly typically under the submerged buoy (Miller, 2017).

3. Design Codes and Standards for Riser Systems

3.1 Introduction

There are design codes that should be followed for a riser to be implemented in the oil and gas field. These codes will govern the design requirement for the riser to be fit for use on a particular condition and period while capable of sustaining the load effects. Moreover, there are other influences that must be considered during the service life, along with the required durability and maintenance cost during the design process (DNV, 2010).

Two different methods are usually adopted as the design basis for the riser structure. The first one is Working Stress Design (WSD), while the second one is Load and Resistance Factor Design (LRFD). In the WSD methodology, a single safety factor is considered for each of the limit states to accommodate the effect of uncertainty. API-RP-2RD (API, 1998) is the design practice that governs the WSD method for riser design. While in the LRFD, only a partial safety factor is considered for each of the load effect and resistance. DNV-OS-F201 provides the LRFD method for riser design.

In order to ensure the consistency of any design activity, it is important to be consistent in using one design method when analyzing riser design. However, there are some failure modes of a riser such as local buckling which is not related to the riser material, and this is not provided under WSD criterion but LRFD criterion (Xia J., 2008).

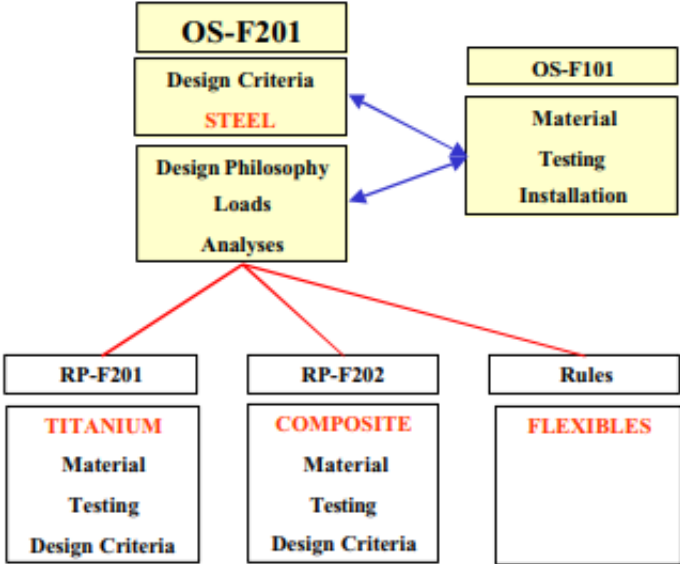


Figure 3.1 DNV Standards and RP's for Risers (DNV, 2010a)

Before designing an LWR system, certain design standards and procedures have to be followed to ensure safe operation. The standards and procedures of both DNV and API are usually different, but it has to be followed while designing a riser system. For our project, we have chosen DNV-OS-F201 published by DNV to design the LWR system for deepwater applications.

The former design format WSD is published by API and the later by DNV and ISO. Therefore, we follow LRFD as we chose DNV-OS-F201 design code.

3.2 DNV-OS-F201

DNV-OS-F201 rules and standard describe that for a certain limit state that is being considered the factorized design load effect should not be more than the factored design resistance, which is the fundamental principle of load resistance factorized design (DNV, 2010a).

The failure modes, coupled with this limit states, are as follows:

- Stress yielding
- Collapse, bursting, propagating buckling for ultimate limit state
- Fatigue failure for fatigue limit state
- The failure caused by accidental loads or by normal loads after accidental events for accidental limit state

3.2.1 Limited State Design

The Limit State Design is followed by other design criteria (DNV, 2010a) such as:

- Serviceability Limit State (SLS)
- Ultimate Limit State (ULS)
- Fatigue Limit State (FLS)
- Accident Limit State or Progress Collapse Limit State (ALS)

Normally, Limited State Design is used along with Load and Resistance Factor Design (LFRD) with concerned equation and safety factors for each failure modes, for a better design.

The principle of the Load and Resistance Factored Design (LRFD) method is to ensure that the factorized design load effects do not exceed the design resistance for any of the limits (i.e., failure modes) considered.

Serviceability Limit State (SLS)

SLS is the ability of the riser to be in service and normal working conditions. The riser pipeline will have to design against the failure mode that follows (DNV, 2010a):

- Clearance
- Excessive angular response
- Excessive top displacement
- Mechanical function

Serviceability requirements are often followed vigilantly to ensure that the operation of the pipe is not hindered. In the case when the SLS is exceeded, proper investigation is done to minimize future damages to the riser.

Ultimate Limit State (ULS)

ULS refers to failures that usually happens due to pipe cross-section yield, collapse, bursting, buckling, or the loss of balance. The riser failure mode is treated as ULS despite not resulting in immediate failure. Usually, risers have no significant hardening effect as they are made using high strength material such as steel or titanium. Therefore, the yield strength has values that are usually not very different from ultimate tensile strength values

It has the limit states as given below (DNV, 2010a):

- Bursting
- Hoop Buckling
- Propagating Buckling
- Gross plastic deformation and local cum hook buckling
- Unstable fracture and gross plastic deformation
- Liquid tightness
- Global buckling
- Gross plastic deformation and local buckling

Fatigue Limit State (FLS)

FLS refers to failure due to fatigue because of the effects of dynamic loading cycle. Three primary problems causing fatigue damage in the riser system are:

- 1st order wave loading, and related float movement
- 2nd order float movement
- Vortex-induced vibrations (VIV) due to the current float movement

Accident Limit State (ALS)

ALS, as the name implies, is accidental and refers to the accidental damage resulting due to dropped object, abnormal corrosion, abnormal environmental conditions, failure of the mooring line, loss of pre-tension, damages to the float, etc. the limit states are same as of the SLS and ULS.

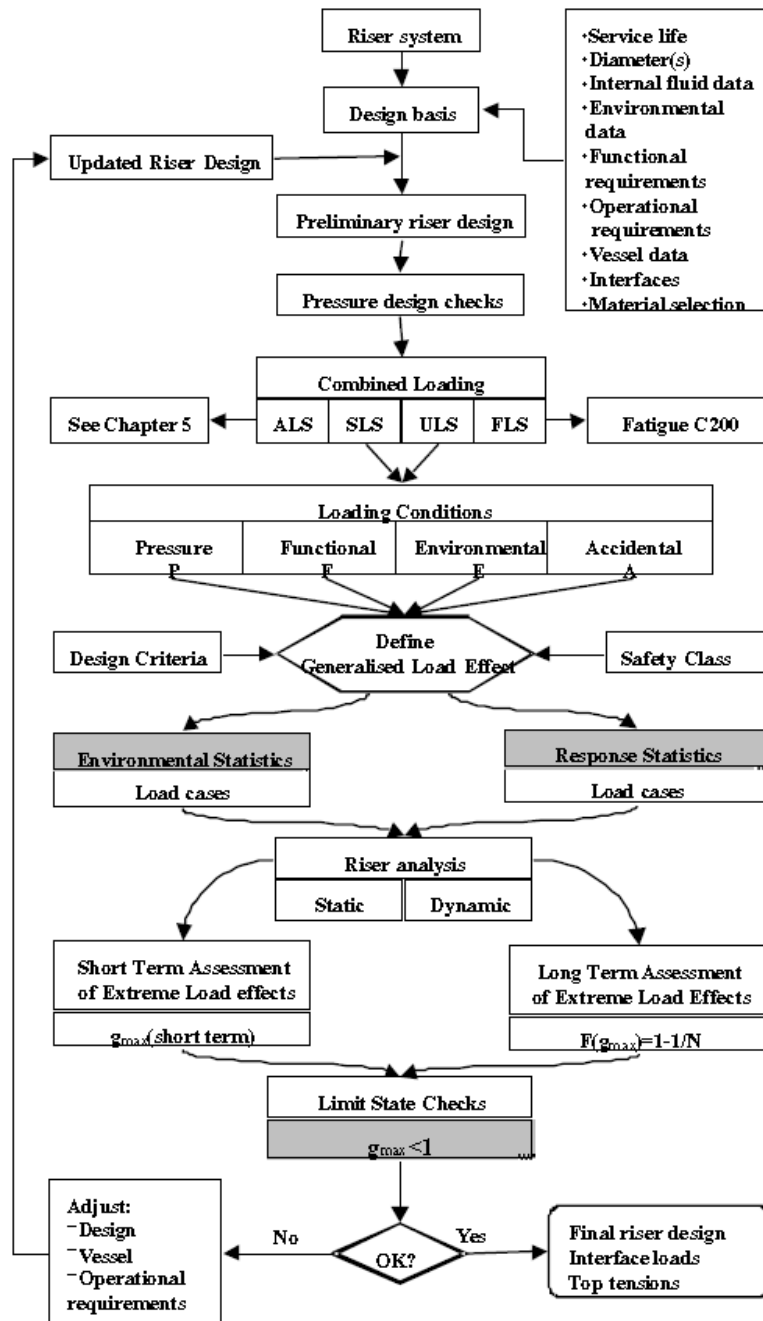


Figure 3.2 Design Approach (DNV, 2010a)

3.3 Design Load Effects

The design load effects are calculated by multiplying the individual load effect by its corresponding load effect factor. Load effects are considered during riser design, to interpret the design bending moment and effective design tension for various load factors. Due to insufficient knowledge or models, leads to the unquantifiable calculation of load effects. Load effect factors usually take into accounts of the natural variability in loads and model uncertainties. The four design loads are:

- Environmental loads
- Functional loads
- Pressure loads
- Accidental loads

Table 3.1 Description of Load According to DNV-OS-F201 (DNV, 2010a)

<i>F-loads</i>	<i>E-loads</i>	<i>P-loads</i> ⁷⁾
Weight and buoyancy ⁶⁾ of riser, tubing, coatings ⁶⁾ , marine growth ²⁾ , anodes, buoyancy modules, contents and attachments Weight of internal fluid Applied tension for top-tension risers Installation induced residual loads or pre-stressing Pre-load of connectors Applied displacements and guidance loads, including active positioning of support floater Thermal loads Soil pressure on buried risers Differential settlements Loads from drilling operations Construction loads and loads caused by tools	Waves Internal waves and other effects due to differences in water density. Current Earthquake ⁴⁾ Ice ³⁾ Floater motions induced by wind, waves and current, i.e.: — Mean offset including steady wave drift, wind and current forces — Wave frequency motions — Low frequency motions	External hydrostatic pressure Internal fluid pressure: hydrostatic, static and dynamic ⁵⁾ contributions, as relevant Water Levels
NOTES 1) Accidental loads, both size and frequency, for a specific riser and floater may be defined by a risk analysis. 2) For temporary risers, marine growth can often be neglected due to the limited duration of planned operations. 3) Ice effects shall be taken into account in areas where ice may develop or drift. 4) Earthquake load effects shall be considered in the riser design for regions considered being seismically active. 5) Slugs and pressure surges may introduce global load effects for compliant configurations. 6) Includes also absorbed water. 7) Possible dynamic load effects from P-loads and F-loads shall be treated as E-loads, e.g. slug flow.		

Table 3.2 Load Effect Factors (DNV, 2010a)

Limit State	F-load effect	E-load Effect	A- load Effect
	γ_F	γ_E	γ_A
ULS	1.1	1.3	-
FLS	1.0	1.0	-
SLS & ALS	1.0	1.0	1.0

Note: 1. If the functional load effect reduces the combined load effects, γ_F shall be taken as 1/1.1
 2. If the environmental load effect reduces the combined load effects, γ_F shall be taken as 1/1.3

3.4 Resistance Factors

It usually accounts for differences in strength and basic variables that include the dimensional tolerances effect and model uncertainties attributed due to the incomplete resistance model. In resistance factors, three types of factors apply

- Safety class factor
- Material resistance factor
- Condition factor

Table 3.3 Safety Class Factor (DNV, 2010a)

Safety class factor γ_{sc}		
Low	Normal	High
1.04	1.14	1.26

Table 3.4 Material Resistance Factor (DNV, 2010a)

Material resistance factor, γ_M	
ULS & ALS	SLS & FLS
1.15	1.0

3.5 Serviceability Limit State (SLS)

State limits on serviceability are often linked with determining acceptable limitations and product usage during normal operation. Often, however, with specific requirements laid out, the engineer must carry out riser serviceability assessments and identify relevant riser system SLS criteria. It is important that the operating procedures highlight and implement all operating limitations and design assumptions. Exceeding an SLS does not always result in the riser failure, but both the ultimate and accidental limit state must not be exceeded for the safety of the riser.

Typically, regular monitoring, maintenance, and inspection are required to identify problems early to ensure the durability of the riser. Serviceability limit states for the behavior of the risers are linked with the limitations on deflection, displacement, pipe's ovalization, and rotation of the pipe's global riser. The limitation for ovalization is given below as an equation

The ovalization should obey the equation below and not exceed more than 3 percent, to avoid local buckling.

$$f_o = \frac{D_{max} - D_{min}}{D_0} \leq 0.03 \quad (3.1)$$

Where,

f_o = ovality

D_{max} = Maximum diameter

D_{min} = Minimum diameter

D_0 = Initial diameter

3.6 Ultimate Limit State

In riser design, the main objective is to define the wall thickness of the pipe and the riser configuration. Related to the ultimate limit state failure modes, the parameters are selected based on their performance. Each failure is discussed in DNV-OS-F201 (DNV, 2010a).

3.6.1 Bursting

At all cross-section conditions of a pipe member which is exposed to net internal pressure, it should satisfy the design criteria shown below.

$$(p_{li} - p_e) \leq \frac{p_b(t_1)}{\gamma_m \gamma_{sc}} \quad (3.2)$$

Where,

p_{li} = Local incidental pressure

$$p_{li} = p_{inc} + \rho_i * g * h$$

p_e = External pressure

γ_m = Material resistance factor

γ_{sc} = Safety class resistance factor

ρ_i = Density of internal fluid

p_{inc} = incidental pressure

$$p_{inc} = 1.1 * p_{design}$$

$p_b(t_1)$ = Burst resistance

$$p_b(t_1) = \frac{2}{\sqrt{3}} * \frac{2 * t_1}{D - t_1} \min \left(f_y; \frac{f_u}{1.15} \right)$$

t_1 = Local incidental pressure

D = Nominal pipe outer diameter

f_y = Material yield strength

f_u = Tensile strength

$$t_1 = t_{nom} - t_{fab}$$

t_{nom} = Nominal/Specified wall thickness

t_{fab} = Fabrication negative tolerance

3.6.2 Hoop Buckling (Collapse)

When subjected to external overpressure, it should be designed according to the given criteria shown below:

$$(p_e - p_{min}) \leq \frac{p_c(t_1)}{\gamma_m * \gamma_{sc}} \quad (3.3)$$

Where

p_{min} = Minimum internal pressure

p_c = resistance for external pressure (hoop buckling)

$p_c(t)$ Is the resistance against hoop buckling given in DNV-OS-F101 as:

$$(p_c(t) - (p_{el}(t)) * (p_c^2(t) - p_p^2(t))) = p_c(t) * p_{el}(t) * p_p(t) * f_0 \frac{D}{t} \quad (3.4)$$

Where,

$p_{el}(t)$ = Elastic collapse pressure

E = Elastic modulus

t = Wall thickness of pipe

ν = Poisson ratio

$p_p(t)$ = Plastic collapse pressure

$$p_p(t) = 2 * \frac{t}{D} f_y * \alpha_{fab}$$

α_{fab} = Manufacturing process reduction factor

f_0 = Initial ovality of pipe, not to be taken less than 0.5%

$$f_0 = \frac{D_{max} - D_{min}}{D}$$

3.6.3 Propagating Buckling

A propagating buckling check ensures buckling remains local, while also ensuring that successive hoop buckling in the adjacent pipe sections are avoided:

$$(p_e - p_{min}) \leq \frac{p_{pr}}{\gamma_m * \gamma_{sc} * \gamma_c} \quad (3.5)$$

Where,

$\gamma_c=1.0$, if no buckle propagation is acceptable.

p_{pr} =Buckling propagation resistance ,

$$p_{pr} = 35 * f_y * \alpha_{fab} * \left(\frac{t}{D}\right)^2$$

3.6.4 Combined Loading Criteria

The combined loading criteria are considered for a pipe member under a combination of bending moment, net internal or external over-pressure, and effective tension.

The designing criteria when subjected to bending moment, net internal overpressure and, effective tension is:

$$\{\gamma_{sc} * \gamma_m\} \left\{ \left(\frac{|M_d|}{M_k} \right) * \sqrt{1 - \left(\frac{p_{ld} - p_e}{p_b(t_2)} \right)^2} + \left[\frac{T_{ed}}{T_k} \right]^2 \right\} + \left(\frac{p_{ld} - p_e}{p_b(t_2)} \right)^2 \leq 1 \quad (3.6)$$

The designing criteria when subjected to bending moment, net external overpressure and, effective tension is,

$$\{\gamma_{sc} * \gamma_m\}^2 \left\{ \left(\frac{|M_d|}{M_k} \right) + \left[\frac{T_{ed}}{T_k} \right]^2 \right\}^2 + \{\gamma_{sc} * \gamma_m\}^2 \left(\frac{p_e - p_{min}}{p_c(t_2)} \right)^2 \leq 1 \quad (3.7)$$

Where,

M_d = Design bending moment

$$M_d = \gamma_F M_F + \gamma_E M_E + \gamma_A M_A$$

$\gamma_{F/E/A}$ = Load effect factors for Functional/Environmental/Accidental

$M_{F/E/A}$ = Bending moment from Functional/Environmental/Accidental loads

T_{ed} = Design effective tension

$$T_{ed} = \gamma_F T_{eF} + \gamma_E T_{eE} + \gamma_A T_{eA}$$

$T_{eF/eE/eA}$ = Effective tension from Functional/Environmental/Accidental loads

T_k = Plastic axial force resistance

$$T_k = M_k = f_y * \alpha_c * \pi * (D - t_2)^2 * t_2$$

M_k = Plastic bending moment resistance

$$M_k = f_y * \alpha_c * (D - t_2)^2 * t_2$$

t_2 = Nominal wall thickness

f_y = Material yield strength

D = Outer diameter

α_c = Flow stress parameter accounting for strain hardening

T_k = Plastic axial force resistance

(t_2) = Burst resistance

$$p_b(t_2) = \frac{2}{\sqrt{3}} * \frac{2 * t_2}{D - t_2} \min \left(f_y; \frac{f_u}{1.15} \right)$$

$p_c(t_2)$ = Hoop buckling capacity

$$t_2 = t_{nom} - t_{corr}$$

t_{nom} = Nominal/Specified pipe wall thickness

t_{corr} = Corrosion/Wear/Erosion allowance

f_u = Ultimate yield strength

p_{ld} = Local internal design pressure

p_e = Local external pressure

3.7 Fatigue Limit State (FLS)

Sufficient fatigue safety must be ensured within the riser system's service life. All the cyclic loading that is imposed during its entire lifetime is considered along with both the magnitude and number of cycles large enough to cause such damage. Temporary phases such as installation, running, hang-off, transport, and towing also must be considered.

There are two fatigue assessment methods:

- S-N curve method
- Fatigue crack propagation method

3.7.1 S-N curve method

The following are to be considered while using the S-N curve method during the calculation.

- Short-term distribution assessment of nominal stress range
- Selection of suitable S-N curve
- Incorporation of the thickness correction factor
- Determination of stress concentration factor (SCF) not included in the S-N curve, see, e.g., DNV-RP-C203
- Accumulated fatigue damage determination D_{fat} overall short-term conditions

The criteria for fatigue are expressed as:

$$D_{fat} * DFF \leq 1 \quad (3.8)$$

Where

D_{fat} = Accumulated fatigue damage (Palmgren-Miner rule)

DFF = Design fatigue factor according to the Table (3.5) given below

Table 3.5 Design Fatigue Factors (DNV, 2010a)

Safety Class		
Low	Medium	High
3.0	6.0	10.0

3.7.2 Fatigue Crack Propagation Method

The fatigue damage is usually seen by the presence of crack propagation. The crack if present should ideally stay within an accepted length and not grow beyond the critical dimensional size during the initial inspection period or service life. The crack propagation calculations typically follow the step below:

- Determination of nominal stress range long - term distribution.

- Select the right crack growth law with appropriate parameters for crack growth. Average growth parameters (characteristic resistance) plus 2 standard deviations are to be determined.
- Estimation of initial crack size and geometry and/or any time for initiation cracking. The best estimate shall be applied to the initial crack size (mean value). Crack initiation time for welds is usually neglected.
- Determining cyclic stress in the growth plane of the prospective crack. The mean stress is determined for non-welded components.
- Final or critical cracks size determination.
- Integration of the fatigue cracks propagation relationship with long - term stress range distribution to determine the fatigue crack growth life (through the thickness, unstable fracture/gross plastic deformation).

The condition to design the fatigue crack growth life is:

$$\frac{N_{tot}}{N_{cg}} * DFF \leq 1 \quad (3.9)$$

Where

N_{tot} = total number of applied stress cycles during service or to in-service inspection

N_{cg} = Number of stress cycles necessary to increase the defect from the initial to the critical defect size

DFF = Design fatigue factor, according to Table (3.5)

3.8 Accidental Limit State (ALS)

ALS is a limit state that occurs due to accidental events or loads. Such events usually occur during technical failure, incorrect operations, or an abnormal condition, which is usually the result of bad planning or unplanned actions

The following design checks are normally applied:

- Resistance to direct accidental charge. (Typically, discrete events with an annual occurrence frequency of less than 10^{-2})
- Ultimate resistance and impact assessment due to the excess of the SLS introduced to define operational limitations.

- Post-accidental resistance to environmental loads (if resistance is reduced due to structural damage caused by accidental loads).

Accidental loads can be grouped into:

- Environmental events (earthquake, Tsunami, Glaciers or huge icebergs)
- Collision of risers, riser components and/or floater systems
- Fire accidents
- Hook load
- Excess internal pressure loads (overpressure)
- Failure of components and/or systems
- The design against accidental loads can be carried out either directly or indirectly by calculating the effects of the loads on the structure.

Table 3.6 Design Check for Accidental Loads (DNV, 2010a)

Probability of occurrence	Safety Class		
	Low	Normal	High
$> 10^{-2}$	Accidental loads may be regarded similar to environmental loads and may be evaluated similar to ULS design check		
$10^{-2} - 10^{-3}$	To be evaluated on a case by case basis		
$10^{-3} - 10^{-4}$	$\gamma_c = 1.0$	$\gamma_c = 1.0$	$\gamma_c = 1.0$
$10^{-4} - 10^{-5}$	Accidental loads or events may be disregarded	$\gamma_c = 1.0$	$\gamma_c = 1.0$
$10^{-5} - 10^{-6}$			$\gamma_c = 1.0$
$< 10^{-6}$			

3.9 Safety Classes

The safety classes of a riser system are considered according to several requirements. The consequences of failure can determine the structural safety requirement of a riser system.

Those consequences are divided into three main concern:

- Risk to human life
- Risk to environment
- Political and economic consequences

The safety class levels, namely, low, normal, and high, are shown in Table 3.7. To select the safety class of a riser, below consideration is to be taken into account:

- The fluid category of the riser content
- The location of the part of the riser that is being designed
- Whether the riser is in its operating phase or in a temporary phase

DNV-OS-F201 is used as the basis for the riser design to make sure that the application of safety class methodology is considered. This methodology links acceptance criteria to the consequence of failure. The descriptions on each safety classes provided by DNV are shown in Table 3.7 below.

Table 3.7 Classification of Safety Classes (DNV, 2010a)

Safety Class	Definition
Low	Where failure implies low risk of human injury and minor environmental and economic consequences.
Normal	For conditions where failure implies risk of human injury, significant environmental pollution or very high economic or political consequences
High	For operating conditions where failure implies high risk of human injury, significant environmental pollution or very high economic or political consequences

3.10 DNV - Allowable Stress

Von Miss Equivalent stress

Von Mises stress can be calculated according to DNV with working stress design (WSD) and shall be calculated as below:

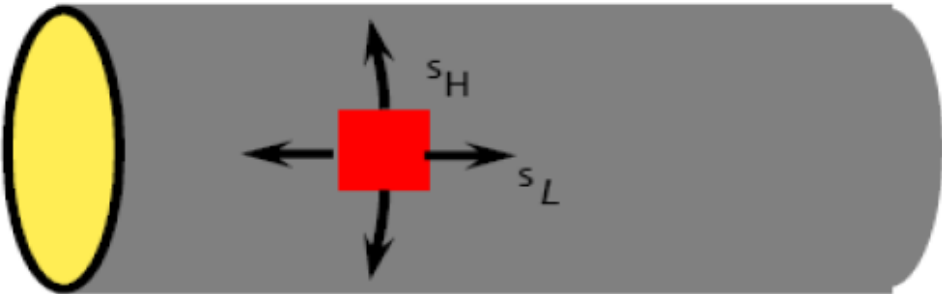


Figure 3.3 Hoop Stress and Longitudinal Stress

Here hoop stress S_H is statically determinate.

Longitudinal stress S_L is not statically determinate and depends on whether the pipeline moves longitudinally.

Use simplified Von Mises equation given by:

$$\sigma_{eq} = \sqrt{(\sigma_h^2 + \sigma_l^2 - \sigma_h \sigma_l)} \quad (3.10)$$

External pressure (p_{ex}) = $\rho * g * H$

Internal pressure (p_{in}) = 34.5 MPa (*selected for this thesis, to be updated for any other value of the internal pressure*)

$S_H = \sigma_h$

$S_L = \sigma_L$

Hoop Stress Calculation (σ_h) = $(p_{in} - p_{ex}) * \frac{D_o}{2*t}$

Longitudinal stress (σ_l) = axial stress + bending stress = $\frac{N}{A_z} + \frac{M}{f}$

A_z = cross-section area

N = True pipe wall force

OD, ID = Outer and inner pipe diameter

p_{in}, p_{ex} = Internal and External pressure,

H = Water depth

Bending Stress

Pure bending stress in a beam normally assumes that the cross-sections keep plane and keep normal direction to the longitudinal of the beam after bending. Moreover, the beam is made from linear elastic material according to Hooke's Law, and it is also homogeneous (Case et al., 1999).

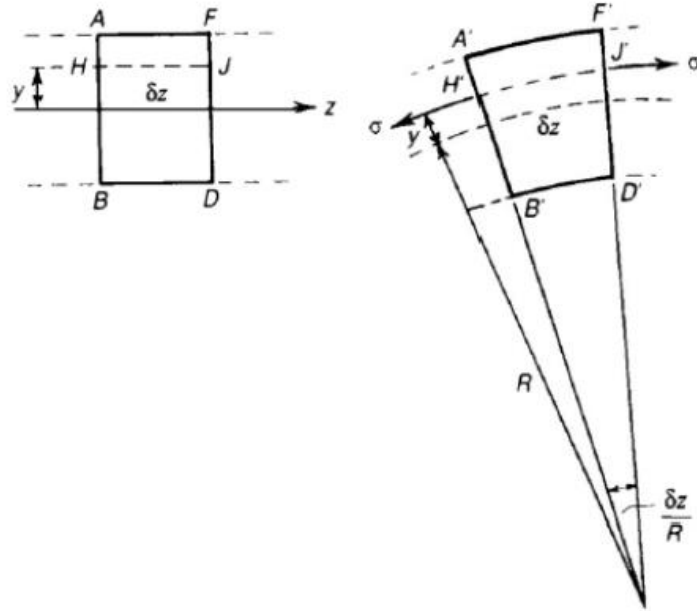


Figure 3.4 Curved Element of a Beam (Case et al., 1999).

$$\text{Stress } \sigma = E * \varepsilon = \frac{E y}{I}$$

$$\text{Moment } M = \int_{-\frac{h}{2}}^{\frac{h}{2}} \sigma y b dy = \frac{E}{R} \int_{-\frac{h}{2}}^{\frac{h}{2}} y^2 b dy = \frac{E b h^3}{R 12} = \frac{E I}{R}$$

$$\frac{\sigma_b}{Y_{max}} = \frac{E}{R} = \frac{M}{I}$$

$$\text{Bending stress } \sigma_b = \frac{M}{f} = M \frac{Y_{max}}{I}$$

Where

$$Y_{max} = \frac{OD}{2}$$

E= Young's modulus

I = moment of inertia

M = Bending moment

f = Pipe section modulus

Allowable stress

As per DNV with working stress design, the below yield criteria shall be used as the allowable stress in the pipeline:

$$\sigma_{allowable} = \eta * \sigma_y \quad (3.11)$$

σ_y = Yield strength (SMYS)

η = 0.96 (including environmental load) or 0.72 (without environmental load)

4. Methodology and Design Premise

4.1 Introduction

The basis to determine an initial configuration of the LWR will be presented in this chapter. The environmental data for extreme weather conditions used in this thesis comes from the deep-water semi-submersible in the Norwegian Continental Shelf. The procedure to determine the worst sea state based according to the vessel response is also explained.

OrcaFlex is used as the software to simulate the dynamic analysis of the LWR, starting from modeling the riser, changing the parameters, and running the analysis. Further analysis and comparisons are carried with Microsoft Excel. The target of the design is to verify that the design acceptance criteria. The main parameter that is going to be changed in this thesis is the water depth. Therefore, the impact of various water depth to the maximum bending moment and von Mises stress are observed, along with the maximum utilization. In the other hand, sensitivity analysis will also be observed by looking at the different output according to the direction of the wave towards the semi-submersible.

Codes and Standards

The LWR design methodology is according to DNV-OS-F201 and associated recommended practices. The standard and recommended practices followed in this thesis are enlisted below:

- DNV-OS-F101 - Submarine Pipeline Systems
- DNV-OSS-302 - Offshore Riser Systems
- API-RP-2RD - Design of Risers for Floating Production Systems (FPSs) and Tension-Leg Platforms (TLPs)

4.2 Metocean Data Study

There are various deep-water locations with the harsh environment that can be taken into account for the analysis. However, in this thesis, one location is selected to represent the condition of a deep-water in the Norwegian Continental Shelf (NCS). The typical deep-water areas in the NCS are in the range of 1500 - 2000 m (Felisita, 2017).

In this thesis, below steps to apply the environmental contour line was the approach recommended by (Haver, 2007):

- Determine the q -probability contour or surface according to the metocean characteristics. In this work, the environmental contour line is used according to the typical contour line for the deep-water area in the NCS, as shown in Figure 4.1
- Choose the most unfavorable metocean condition together with the q -probability contour or surface related to the extremes of the current response problem.
- Determine the distribution function of the 3-hour maximum response for the most unfavorable metocean condition.
- The result will be the estimation of the q -probability response value by the α -quantile of the determined extreme value distribution.

The environmental condition in the long-term for the deep-water area in the NCS is estimated using contour lines diagram, as shown in Figure 4.1 below.

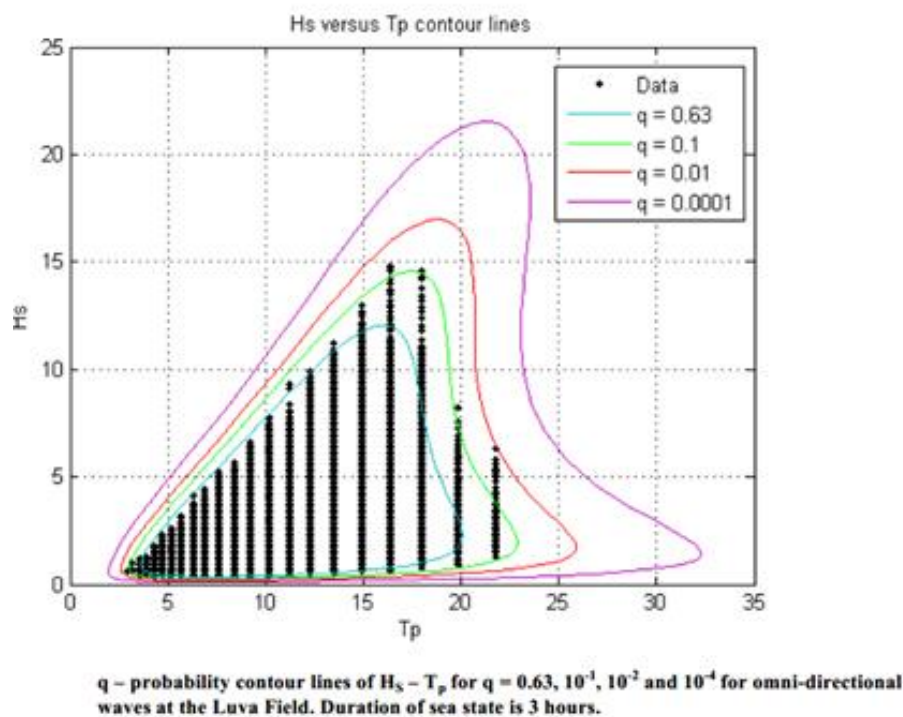


Figure 4.1 Contour Lines for the Deep-water area for the Metocean Condition in the Norwegian Continental Shelf (NCS) (Felisita, 2017).

4.3 Resonance on Riser

Resonance is a phenomenon when a structure or material oscillates naturally at a high amplitude at a specific frequency. This frequency is called a structural resonant frequency. Normally, a structure has a lot of resonant frequencies.

When a structure has small damping, the resonant frequencies are nearly the same as the natural frequencies of the structure. Resonance is the condition when the natural frequency of a structure and the excitation frequency are equal or approximately equal. This makes the structure or material to vibrate at a high amplitude. This is also called the classical resonance state. This resonance state usually leads to unwanted behavior of the structure or material.

Each structure has its own set of frequency, which is correlated to the makeup composition of the material, and this is normally referred to its lowest natural frequency. The mass or density of the material is inversely proportional to the fundamental frequency of vibration. The lesser mass or density, the higher the fundamental frequency of the structure.

Research on longitudinal resonant vibration of a riser by (Sparks et al., 1983) showed that there are two important parameters to be carefully considered. The first was the hydrodynamic damping of the riser, because of the discontinuity of the riser buoyancy units around connectors. The second that would be applied to the riser was the actual heave excitation close to its fundamental frequency. The research also mentioned that the natural frequencies are important to determine the dynamic behavior of a suspended riser, and modifying the riser configuration might significantly change the natural frequencies.

4.4 Basic Concepts of VIV

Vortex Induced Vibration (VIV) is a common phenomenon that needs to be considered when dealing with slender flexible structures such as mooring anchors and marine risers. VIV can cause big oscillations and fatigue failure, usually when facing an environment with the severe current. Therefore, it is a very important design issue related to the possibility of resonance.

The formation of VIV starts when fluid passes a submerged blunt cylindrical body. It will create vortices downstream of it. From both sides of the body, these vortices are shed periodically, resulting in the Von Karman vortex (Figure 4.2). The alternating shedding induces vibration with similar frequency as the vortex shedding creating a harmonic load. A regular and recurring pattern of vortices moves downstream after the shed with subsequent

dissipation of energy. The interaction between both the vortices and the cylinder is called VIV (Sumer & Fredsøe, 2006).

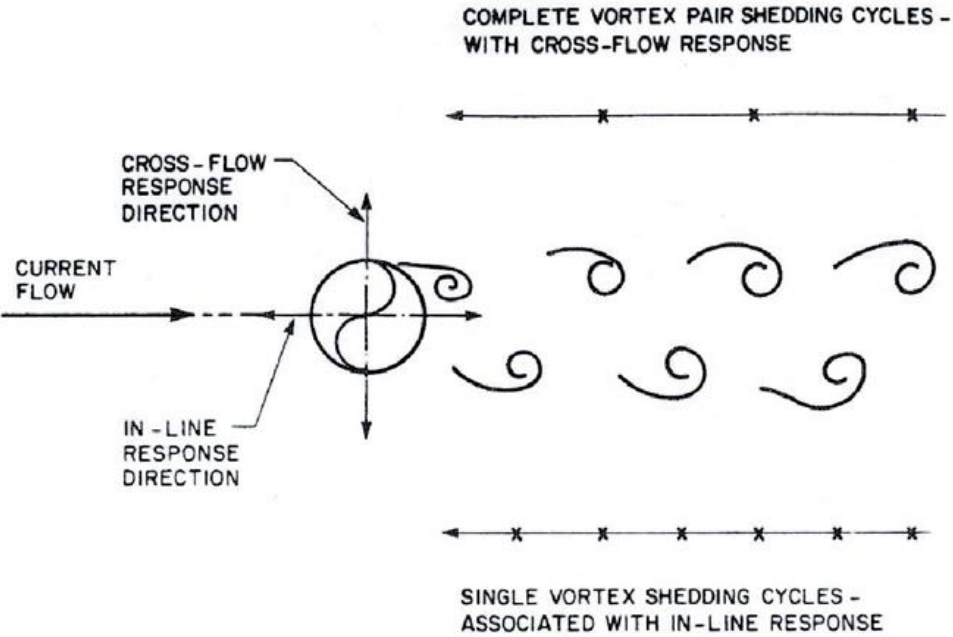


Figure 4.2 Vortex Shedding: In-line and Cross-flow Response (Kenny, 1993)

4.4.1 Key Parameters

The parameters used to characterize the process of vortex-induced vibrations are as below:

Reynolds number, Re

Reynolds number is a dimensionless quantity used to aid in forecasting the flow pattern in differing flow situations. It represents the relation of inertia and friction forces that act on a body, as well as defines the vortex pattern for different flow regimes.

Strouhal number, St

Strouhal number is a dimensionless number relating to oscillating flow mechanisms, defining the vortex shedding frequency of a fixed cylinder.

$$St = \frac{f_v D}{U} \tag{4.1}$$

Where:

f_v : vortex shedding frequency for a fixed cylinder

D: diameter of the cylinder

U: the velocity of the flow

As illustrated in Figure 4.3, the Strouhal number varies significantly for different values of the Reynolds number.

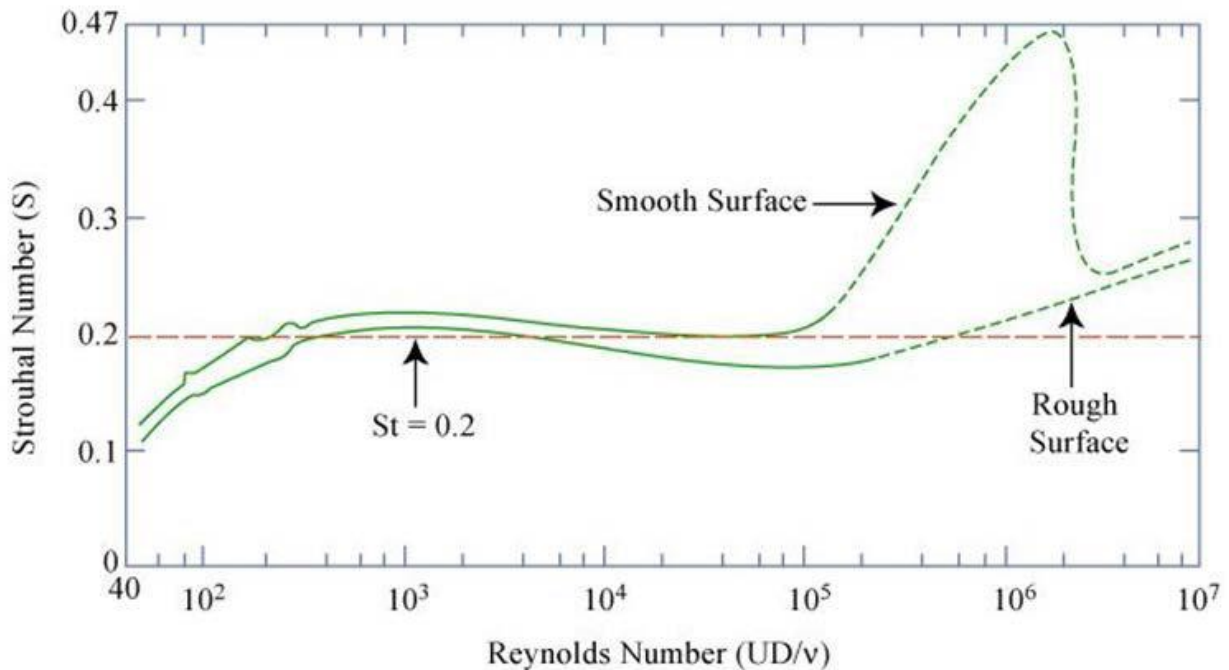


Figure 4.3 Plot of Strouhal Number and Reynolds Number for Circular Cylinders (Achenbach & Heinecke, 1981)

As seen in Figure 4.3 above, the value of the Strouhal number is stable and near 0.2 in the sub-critical regime, due to the short-ranged vortex shedding. In the critical regime, the value of Strouhal number changes due to wide-ranged vortex shedding. On the other hand, in the supercritical regime with high Reynolds number, the wake is highly turbulent and aperiodic. At even higher Reynolds number, the vortex shedding becomes periodic.

Reduced velocity, V_r

Reduced velocity is defined as the ratio between the path length per cycle and width.

$$V_r = \frac{\text{path length per cycle}}{\text{width}} = \frac{U}{f_0 D} \quad (4.2)$$

The oscillation frequency of the structure:

$$f_{osc} = \frac{1}{2\pi} \sqrt{\frac{k}{m+m_a}} \quad (4.3)$$

Where:

K : stiffness,

m : The mass of the cylinder,

m_a : The added mass in still water.

If the oscillation frequency is considered in still water, V_r will be as below:

$$V_r = \frac{U}{f_o D} = \frac{1}{\hat{f}} \quad (4.4)$$

In still water, the Eigen frequency of the structure is as below:

$$f_0 = \frac{1}{2\pi} \sqrt{\frac{k}{m+m_{a0}}} \quad (4.5)$$

Non-dimensional frequency, \hat{f}

This frequency is the parameter to define the condition of a cylinder with forced motions. Moreover, it is an important parameter to control the added mass.

$$\hat{f} = \frac{f_{osc} D}{U} \quad (4.6)$$

Roughness ratio, k/D

Roughness ratio characterizes the surface of the cylinder.

$$Roughness\ ratio = \frac{k}{D} \quad (4.7)$$

Where:

k : surface roughness.

In the critical flow regime, the Strouhal number is dependent on surface roughness, illustrated above in Figure 4.3.

Mass ratio, $m/\rho D$

The mass ratio for a cylinder is a relation between its mass per unit length m and ρD^2

$$\text{mass ratio} = \frac{m}{\rho D^2} \quad (4.8)$$

The mass ratio is a key parameter for the value of added mass on the cylinder. This is shown in Figure 4.4, where the non-dimensional response amplitude A/D is presented as a function of the reduced velocity.

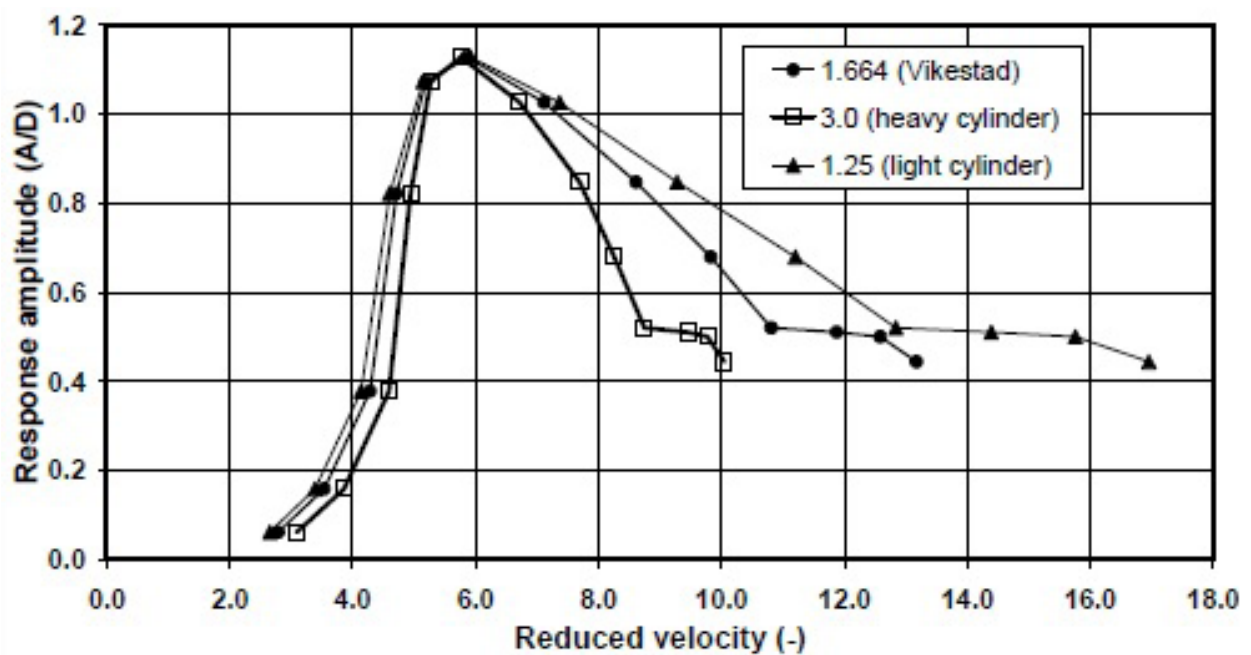


Figure 4.4 Non-dimensional Amplitude versus Reduced Velocity for three Cylinders with Different Weight (Vikestad, 1998)

Non-dimensional displacement amplitude ratio, A/D

The displacement amplitude ratio is the parameter defining the free vibrational experimental displacement amplitude to the forced experimental oscillation amplitude.

$$\left(\frac{A}{D}\right)_{IL/CF} \quad (4.9)$$

4.5 Elements Causing Resonance

In this chapter, the basic theories and understanding of riser analysis related to resonance will be presented. Afterward, the knowledge and theory of riser analysis will be utilized as the basis to improve the understanding of riser design, especially for Lazy Wave Riser. Those backgrounds are the knowledge of waves and currents, vessel responses, hydrodynamic effects, and soil and riser interaction.

4.5.1 Wave and Current

Wave and current are the main environmental conditions affecting the riser's dynamic response. Riser design should consider withstanding the worst environmental condition during its lifetime. Usually, it is driven by the combination of a 100 Years Wave with the associated 10 Years Current that is relevant to the location where the riser will be installed. These conditions will be determined by the floater response analysis.

4.5.2 Floater Motions

The motions of a floater in the sea are influenced by environmental factors such as the wind, wave, and current. The motion response due to those conditions are divided into two kind of motions, which are translational and rotational motions, and each of them has three directions on 3D space. Therefore, there are 6 degrees of freedom (DOF) for the floater motions. Surge, sway and heave that is known as the translational motions. It correlates to the linear movement in x, y, and z-direction respectively. Whereas roll, pitch, and yaw represent the rotational motions. It correlates to the rotation movement along the x, y, and z-direction respectively.

Figure 4.5 below shows an illustration of the translational and rotational motions.

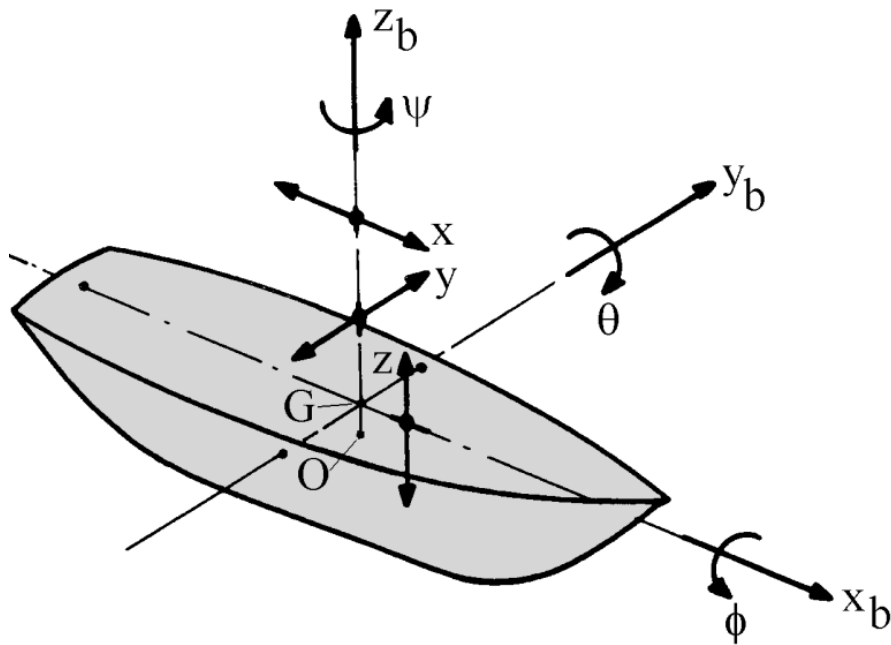


Figure 4.5 The Six Degrees of Vessel Motions in Sea (Journée & Massie, 2001)

The relationship between waves and floater motions can be explained by Figure 4.6 below, showing the block diagram of the three components along with the time when waves are coming, hitting the floating structure, and finally generate the motions.

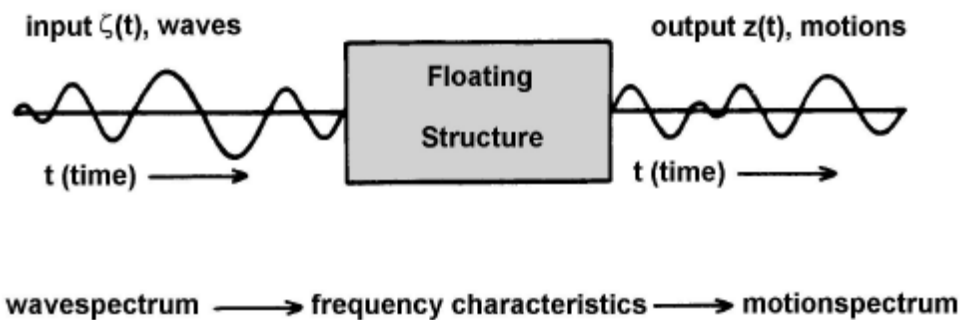


Figure 4.6 Relation between Floater Motions and Waves (Journée & Massie, 2001)

The irregular wave is the energy distribution over the wave frequencies that provide the input for a linear characteristic in the illustration above. The floating structure frequency characteristics are calculated using model experiments or the computations. The motions of the floating structure are the output of the system. However, these motions have an irregular behavior similar to the wave that caused the motion in the first place.

As indicated by Journée & Massie (2001), in a lot of circumstances, the floater motions generally have a linear behavior. This implies the constant proportion of both the motion and

wave amplitudes at each of the frequencies together with the phase shift between both the waves and motions. By merging the results from regular waves of differing frequencies, amplitude, and direction, it is possible to determine an irregular wave's resulting motion. Using the wave energy spectra and floater's frequency characteristic response, it is possible to calculate the response spectra.

Both the static loading and the dynamic loading on the riser is determined by the floater motions and together with its offsets.

Figure 4.7 below shows an illustration of the Semi-submersible offset Positions

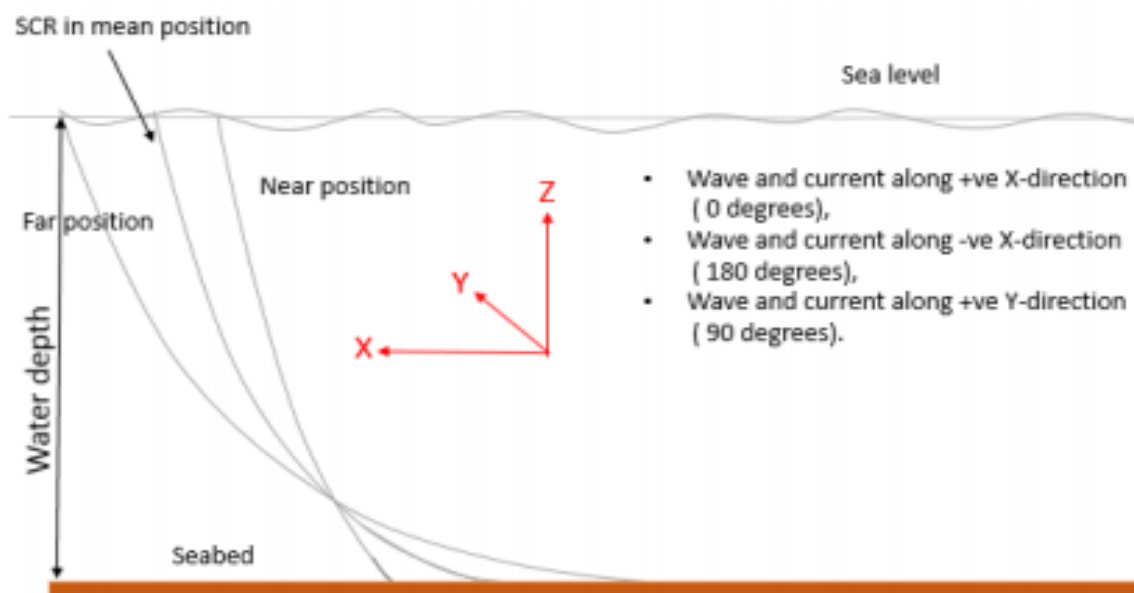


Figure 4.7 Semi-submersible Offset Positions (Taheri & Siahtiri, 2017)

On the other side, the two terms of floater motions characteristic are as follows: Wave frequency (WF) and Low frequency (LF). The definitions of these terms as explained on (DNV, 2010):

- **Wave Frequency motion (WF):** The motions due to the 1s order wave force that acts on the floater. The platform typically moves with a period that is between 3-25 seconds.
- **Low-Frequency motion (LF):** The motions due to the 2nd order wave forces, where the frequency is below the wave frequency close to the surge, sway and yaw eigen period values of the floaters. Such motions typically result in a period that is in between 20 to 300 seconds.

4.5.3 Response Amplitude Operator (RAOs)

RAOs are transfer functions which connect the floater motion response to the spectrum of wave energy. Floater motions have six degrees of freedom with their own RAOs, which must be inputted to the analysis software in order to generate the floater response.

The variation of RAOs depends on the types of the floater, the draught of a specific type of floater, wave period, wave direction, etc. RAOs are normally presented in tables or graphs and produced from a computer program such as OrcaFlex.

RAOs can be defined by various conventions such as the OrcaFlex convention, by using response amplitude, length unit for translation and degree unit for rotation, and per unit wave amplitude. The other convention, for example, using phase lag at the time when wave crest passes through the RAO origin up to when the maximum positive excursion is attained (OrcaFlex Manual, 2012).

$$X = A \cdot RAO \cdot \cos(\omega t - \psi) \quad (4.10)$$

Where,

X = Vessel displacement

A = wave amplitude

RAO = response amplitude operator

ω = wave frequency (rad/s)

T = time (s)

Ψ = phase angle of response.

RAOs convention, as used in OrcaFlex, is according to the wave directions and the origin.

The convention for wave direction (LI, 2014):

- **Following sea:** 0° direction of the wave, defined as the propagation of the wave along the positive x-axis (bow direction)
- **Beam sea:** 90° direction of the wave, defined as the propagation of the wave along the positive y-axis (starboard direction)
- **Head sea:** 180° direction of the wave, defined as the propagation of the wave along the negative x-axis (stern direction)

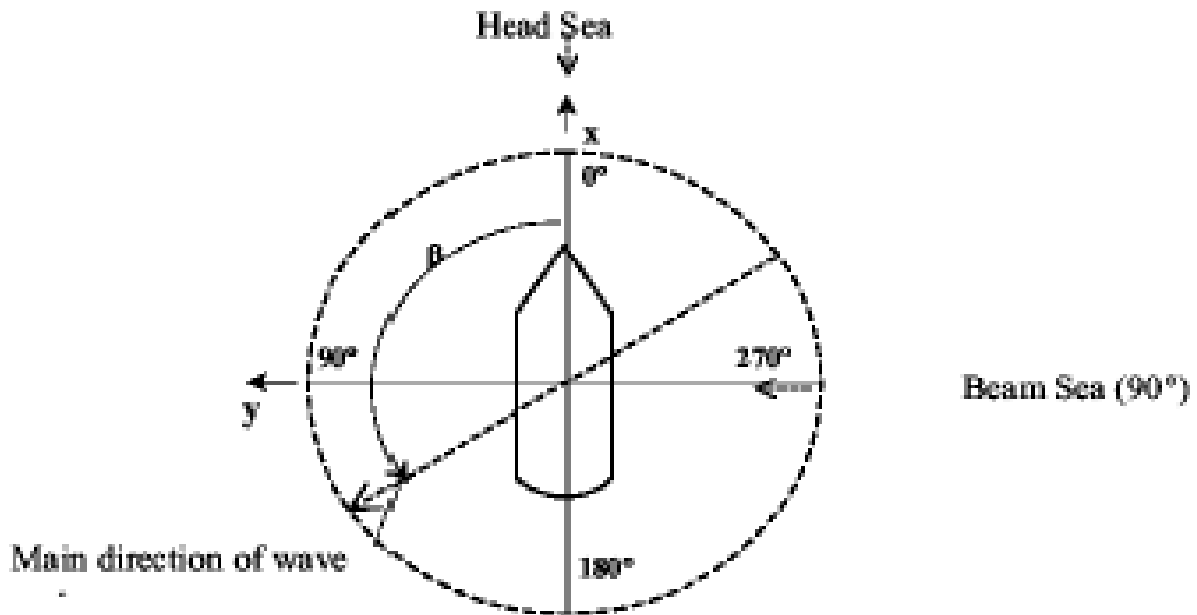


Figure 4.8 Wave Direction Convention (LI, 2014)

The convention used to denote the RAO origin is situated along the floater centreline axis that is along the water plane line:

- The positive x-direction towards the floater's bow
- The positive y-direction towards the floater's port side
- The positive z-direction vertically upwards from the floater

According to the floater RAOs, the rigid body motions will be assigned in Orcaflex, to the riser attachment point to the floater. The floater alignment will be considered concerning the inbound wave direction, and then the corresponding RAO will be computed.

The response of a floating structure exposed to the wave can be presented in a graph showing the RAO according to the heading of the wave. To understand the RAO for the six degrees of freedom, an example from (Gudmestad, 2015) for a particular direction of the wave is shown as below:

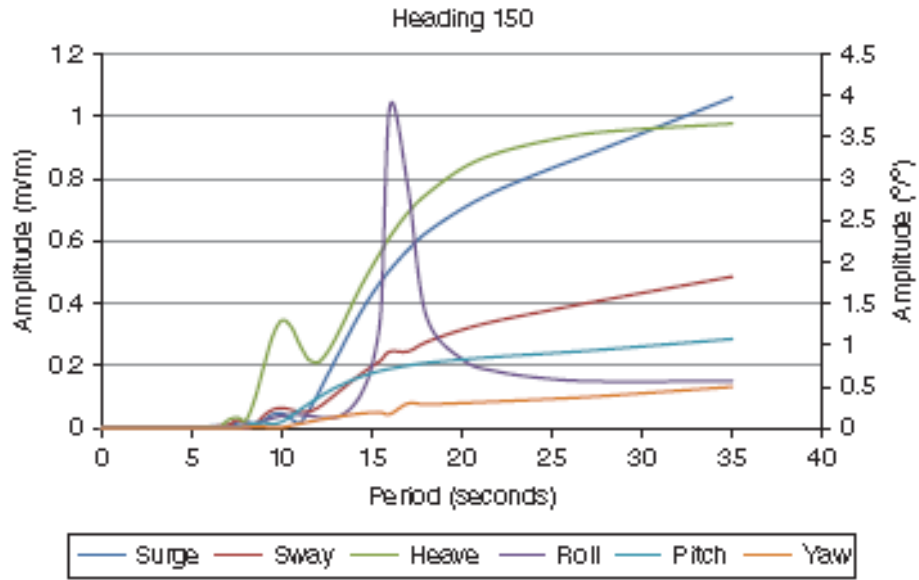


Figure 4.9 RAO for Yaw (lowest value at high period), Roll (next lowest value at high periods), Pitch, Sway, Heave, and Surge (largest value for high periods) (Gudmestad, 2015).

For three different types of floating structures, the relation between the wave spectrum and the RAO for heave is shown in Figure 4.10

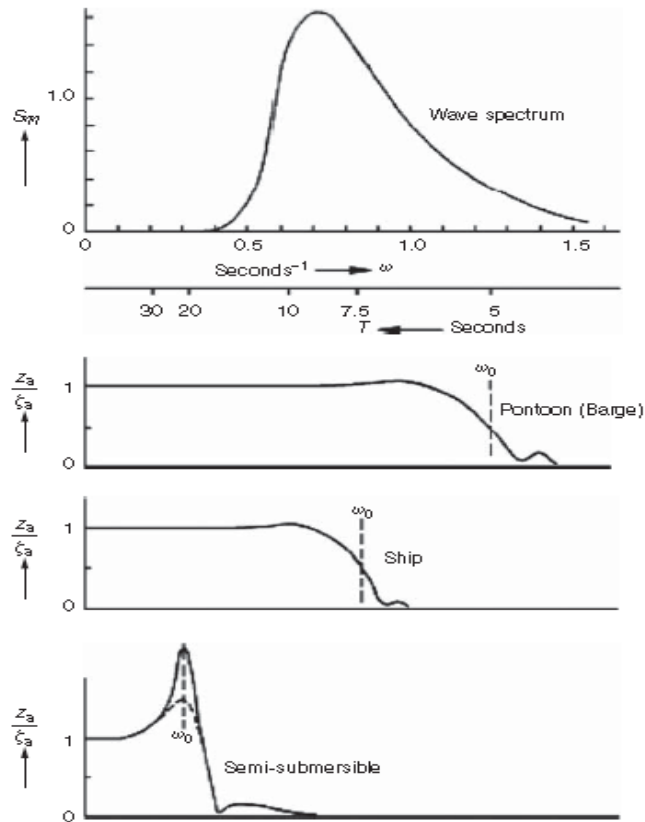


Figure 4.10 The Relation Between Wave Spectrum and RAO for Heave for Three Different Types of Floating Structure (Gudmestad, 2015).

The natural frequencies of a floater depend on its dimension and shape. As shown in Figure 4.10 above, a large pontoon (barge) has high natural frequency and substantial RAO values across a big part of the normal wave frequency range. The reason is that a big portion of the wave energy will be converted into the heave motion, resulting in a large motion spectrum. Meanwhile, a ship has lower natural frequency will transfer a lesser amount of energy than a barge, with moderate wave energy converted into heave motions. Finally, a semisubmersible has very low natural frequency because of its high mass and the small intersection with the waterline. Therefore, a small portion of the wave energy is converted into heave motions.

Thus, the natural frequency is an essential phenomenon which will affect the behavior of the structure in waves. The natural frequency should be adjusted not to interfere with the wave frequency range.

4.5.4 Hydrodynamic Loading

The hydrodynamic loading of LWR is formulated by the Morison equation for the relative interaction of fluid-structure velocities and accelerations. Below is the Morison equation, according to DNV-OS-F201:

$$f_n = \frac{1}{2} \rho C_D^n D_h |v_n - \dot{r}_n| (v_n - \dot{r}_n) + \rho \frac{\pi D_b^2}{4} C_M^n \dot{v}_n - \rho \frac{\pi D_b^2}{4} (C_M^n - 1) \ddot{r}_n \quad (4.11)$$

$$f_t = \frac{1}{2} \rho C_D^t D_h |v_t - \dot{r}_t| (v_t - \dot{r}_t) + \rho \frac{\pi D_b^2}{4} C_M^t \dot{v}_t - \rho \frac{\pi D_b^2}{4} (C_M^t - 1) \ddot{r}_t \quad (4.12)$$

Where,

f_n	Force per unit length in normal direction
f_t	Force per unit length in tangential direction
ρ	Water density
D_h	Hydrodynamic diameter
D_b	Buoyancy diameter
v_n, \dot{v}_n	Fluid velocity and acceleration in normal direction
\dot{r}_n, \ddot{r}_n	Structural velocity and acceleration in tangential direction
C_D^n, C_M^n	Drag and inertia coefficients in normal direction

C_D^t, C_M^t	Drag and inertia coefficients in tangential direction
v_t, \dot{u}_t	Fluid velocity and acceleration in tangential direction
\dot{r}_t, \ddot{r}_t	Structural velocity and acceleration in tangential direction

There are coefficients in the Morison equation, i.e., the drag and inertia coefficient, which depend on different parameters such as the Keulegan-Carpenter number, Reynolds number, and the surface roughness of the body. Those coefficients are stated in the DNV-OS-F201, for example in a selected type of pipe like the cylindrical bare pipes which has a drag coefficient between 0.7 to 1.0 and inertia coefficient of 2.0. Besides that, rough cylinders, have a drag coefficient of 1.05 can be taken to consider the presence of marine growth (NORSOK, 2007).

4.6 Design Basis

4.6.1 Riser Material Properties

The typical material used for risers is API 5L X60, X65, and X70 carbon steel. Another thing to consider for riser material selection is the property of the hydrocarbon fluid in the reservoir. Corrosive fluids such as CO₂ and H₂S can influence the fatigue performance of a riser. In that case, corrosion resistant alloy (CRA) materials are normally used to make sure the required fatigue life for some deep-water steel riser will be achieved.

In this work, an X65 grade carbon steel material is used as the riser material, with specified minimum yield strength (SMYS) equal to 448 MPa. The details of the riser material properties used in this thesis are shown in Table 4.1 below:

Table 4.1 Steel Pipe Properties (Felisita, 2017).

Parameter	Design Value	Unit
Internal diameter (10" pipe)	254	mm
Riser Wall Thickness	26	mm
Coating Thickness	76	mm
Riser material	Carbon Steel, grade X65	
Steel Material Density	7850	kg/m ³
Young's modulus E	207000	MPa
Safety class	High	-
Specified Minimum Yield Strength (SMYS)	448	MPa
Design Pressure	34.5	MPa
Poisson Ratio	0.3	
Internal fluid density	800	kg/m ³
Coating Density	700	kg/m ³

4.6.2 Buoyancy module data

Especially for LWR, the riser is connected to buoyancy elements along a differing section along the riser. This is done to minimize the payload and improve fatigue life of the riser. These buoyancy elements normally come in the form of a synthetic foam which has a lesser density than water, thus allowing it to float. Moreover, every buoyancy module is equipped with a clamp to ensure that they are securely connected to the riser. The lazy wave configuration is complete by spreading out these modules over the middle section of the entire pipe at a particular distance between them known as the pitch. Thus, allowing the end design configuration to contain enough buoyancy force to carry both the weight of the riser and its content.

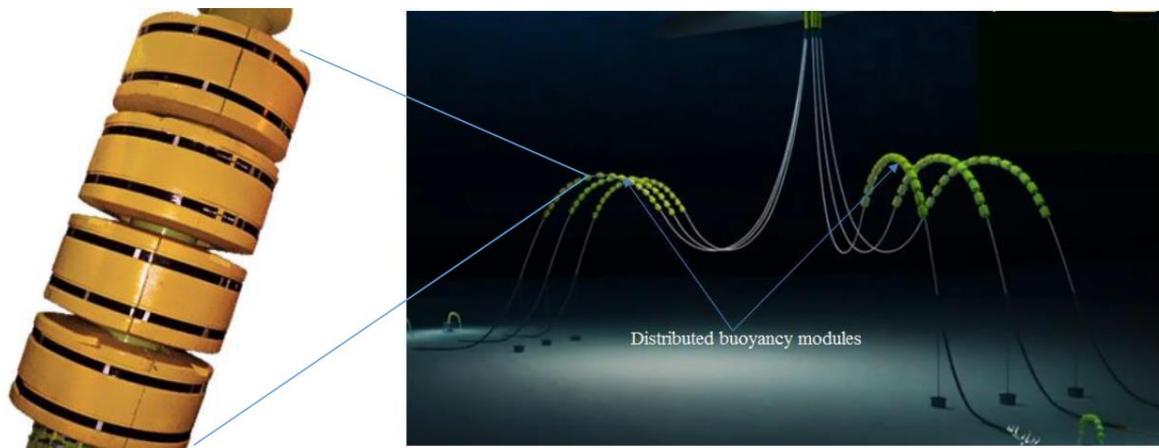


Figure 4.11 Buoyancy Modules (Balmoral, 2014).

Various values and dimensions of buoyancy modules are included on the risers. Buoyancy module data are shown in Table 4.2 below. Each riser configurations have a similar length but different diameter in the buoyancy section.

Table 4.2 Buoyancy Module Properties (Felisita, 2017).

Riser configurations	Outside Diameter (m)	Length (m)
1	1,81	1,8
2	1,87	1,8
3	1,92	1,8
4	1,96	1,8
5	1,76	1,8
6	1,57	1,8
7	1,875	1,3
8	1,935	1,3
9	1,99	1,3
10	1,8	1,3
11	1,74	1,3
12	1,684	1,684
Material Density	500 kg/m ³	
Distance between modules (Pitch)	12 m	
Clamp Weight	50 kg	

4.6.3 Fluid data

In this thesis, the density of the internal fluid is used at 800 kg/m³, and the related design pressure at the seabed is chosen at 34, 5 MPa. Furthermore, sensitivity study will be done by considering the empty LWR (no-fluid condition). However, water-filled is not considered because of not enough related environmental data.

4.6.4 Flex Joint

In this work, the connection of the riser to the floater is presumed to be fitted with a flex joint. This assumption was also implemented by (Bai & Bai, 2005). As in their analysis, where the riser is joined with a semi-submersible by a flex-joint so that the riser can rotate with minimal bending moment. This joint typically consist of an alternating lamination of spherically shaped steel together with rubber components inside a steel structure welded to the riser, as shown in Figure 4.12 below. Such configuration allows flexibility in rotation along with the vertical and horizontal directions (Grealish et al., 2007).

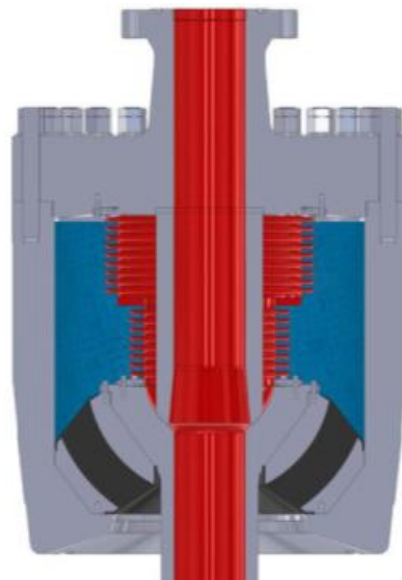


Figure 4.12 Flex Joint Hutchinson Oil and Gas (Knapstad, 2017)

As the flex joint is connected to the riser termination point, the global analysis of this top end of the riser is modeled as pinned support. For extreme loading, the stiffness at the flex joint will not influence the response. However, rotational stiffness of the flex joint need to be considered for its fatigue analysis since it will influence the fatigue response at the riser cross

section near to the flex joint (Legras et al., 2013). For the analysis examined, the rotational stiffness is set to 10 kNm/degree and is considered to be a realistic estimation of the actual stiffness in the conventional flex joint. Figure 4.13 below shows the flex joint implemented for SCR/LWR.



Figure 4.13 Flex Joint Implemented for SCR/LWR. (Oil States Industries, 2019)

4.7 Design Parameters Studies

4.7.1 Environmental Data

Water depth

Table 4.3 Various Water Depth for LWR.

Case	Water Depth (m)	Density (kg/m ³)
1	2000	1025
2	1500	1025
3	1000	1025

Wave and Current data

The wave and current data are used according to the condition in the Norwegian Sea, with the extreme sea state using the JONSWAP wave spectrum for the representation of irregular waves. In Table 4.4 and Table 4.5 below, the wave and current data are shown for the 100 Years Sea State along with the 10 Years Current Velocity.

The JONSWAP range is a refinement of the Pierson-Moskowitz range for a sea-state, and is given by (DNV, 2010b):

$$S_J(\omega) = A_\gamma S_{PM}(\omega) \gamma^{\exp\left(-0.5\left(\frac{\omega-\omega_p}{\sigma\omega_p}\right)^2\right)} \quad (4.13)$$

Where:

$S_{PM}(\omega)$ = Pierson-Moskowitz spectrum

γ = non-dimensional peak shape parameter

σ = spectral width parameter

$$\sigma = \sigma_a \text{ for } \omega \leq \omega_p$$

$$\sigma = \sigma_b \text{ for } \omega > \omega_p$$

A_γ = $1-0.287 \ln(\gamma)$ a normalizing factor

γ = non-dimensional peak shape parameter

$$\gamma = 5 \quad \text{for } \frac{T_p}{\sqrt{H_s}} \leq 3.6$$

$$\gamma = \exp\left(5.75 - 1.15 \frac{T_p}{\sqrt{H_s}}\right) \quad \text{for } 3.6 < \frac{T_p}{\sqrt{H_s}} < 5$$

$$\gamma = 1 \quad \text{for } 5 < \frac{T_p}{\sqrt{H_s}}$$

In (DNV, 2010b), the Pierson-Moskowitz is given as:

$$S_{PM}(\omega) = \frac{5}{16} H_s^2 \omega_p^4 \omega^{-5} \exp\left(-\frac{5}{4} \left(\frac{\omega}{\omega_p}\right)^{-4}\right) \quad (4.14)$$

Where:

$$\omega_p = \frac{2\pi}{T} \text{ (Angular spectral peak frequency)} \quad (4.15)$$

Table 4.4 Typical Design Sea States for Deep-water area within NCS (Felisita, 2017)

Parameter	100-year sea state data
Wave Data	
Significant wave height, H_s (m)	17
Corresponding wave period, T_p (s)	18.9
Wave Spectrum	JONSWAP
Wave Load Modelling	Irregular Wave

Table 4.5 Typical Current Data for Deep-water Area within NCS (Felisita, 2017)

Current Data	
Water Depth	10-Year
(m)	Current Velocity (m/s)
-10	1.65
-50	1.26
-100	1.25
-200	1.09
-300	0.83
-400	0.74
-500	0.73
-600	0.6
-800	0.6
-1000	0.55
-1200	0.55
-3 m above sea bottom	0.46

4.7.2 Selected Sea State

Metocean data that are used in this thesis consist of meteorological and oceanography data for the long-term environmental condition in the deep-water of the Norwegian Continental Shelf (NCS). They are estimated using standard contour lines diagram, as shown in Figure 4.14 below. It shows the distribution of sea states along the upper peak of the $q=10^{-2}$ contour line. Those sea states were used to select the most unfavorable metocean condition.

Different options of sea states are also shown in Figure 4.14 to select the harshest metocean condition.

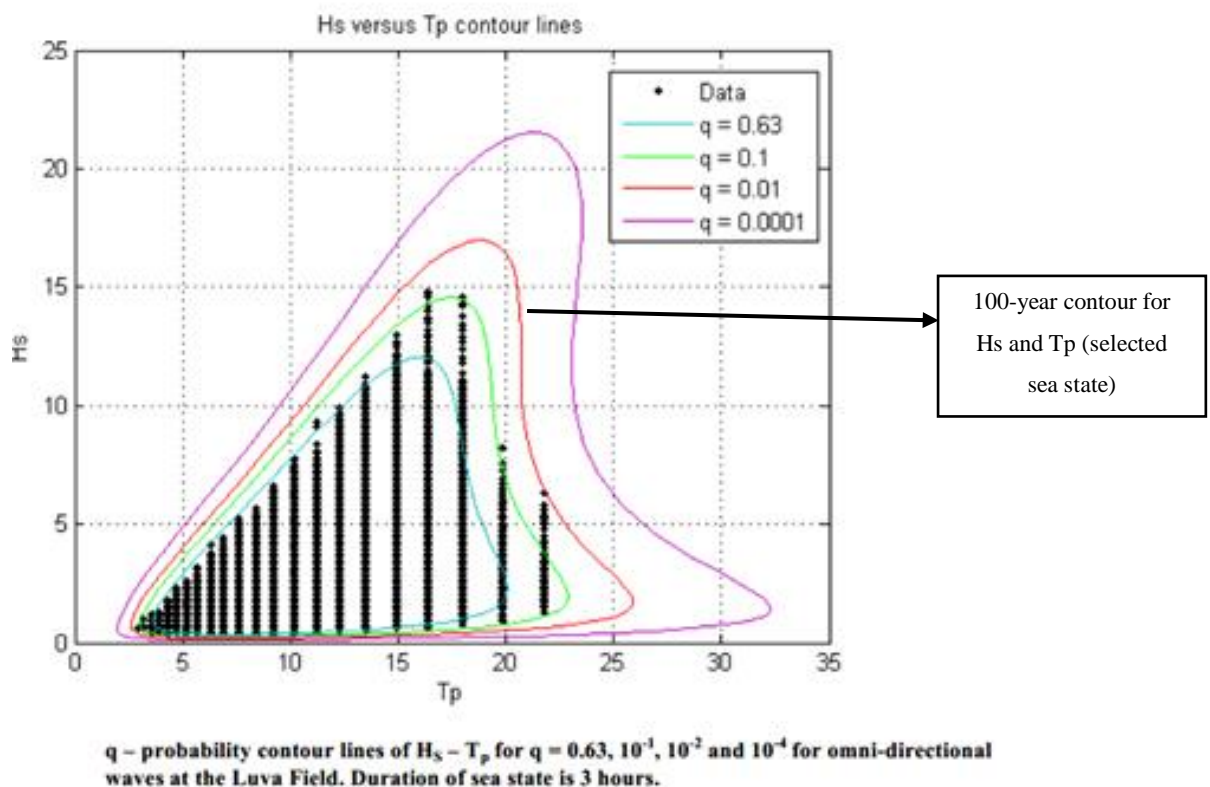


Figure 4.14 Environmental Contour lines for Selected Sea States (Felisita, 2017)

The significant wave height (H_s) and peak period (T_p) provide information to the JONSWAP spectrum to run the simulation of the irregular wave. In this case, the peak shape parameter (γ) is formed by the relationship formula of H_s range of 6.2 m to 17.1 m and T_p range of 18s to 22s as provided in section 4.6.5.

Table 4.6 Environmental Contour Lines Selected Sea States for Worst Conditions

Load Cases	Hs (m)	Tp (s)	γ
1	17	18	2.087
2	17.1	18.7	1.732
3	17	19	1.569
4	16.4	20	1.073
5	15	20.5	1
6	15	21	1
7	14.6	20.5	1
8	12.3	20.7	1
9	10	20.8	1
10	8	21	1
11	6.2	22	1

Marine growth

Marine growth factor for all submerged structures is to be taken into account as per NORSOK N-003. In the standard, it is specified that 13000 N/m³ mass density of marine growths is used in the air (NORSOK, 2007). The marine growth thickness is used corresponding to Table 4.7 below, only if the scheduled maintenance for cleaning the submerged structures is not scheduled. The marine growth thickness is considered uniform along the pipe surface, and the water depth value is measured using the mean water level as reference.

Various thicknesses of marine growth are considered up to a water depth of 275 m (Felisita, 2017). Those thicknesses are shown in Table 4.7 below:

Table 4.7 Thickness of Marine Growth and Biofouling (NORSOK, 2016).

Depth (m)	Thickness t (mm)	Density ρ_{mg} (kg/m ³)	Submerged weight W_{mg}^{**} (kN/m ³)
Above +2	0	-	-
-15 to +2	60	1325	2,94
-30 to -15	50	1325	2,94
-40 to -30	40	1325	2,94
-60 to -40	30	1100	0,74
-100 to -60	20	1100	0,74
Below -100	10*	1100*	0,74

*) Cold water corals can build up local colonies with no limitation regarding size in water depths between 100 and 800 m. Cold water corals are assumed not to occur for temperatures below 2 °C, i.e. for the Norwegian continental shelf it may be assumed that these occur in water depths between 100 m and 450 m. The density of the marine growth should be taken as 1300 kg/m³ in the whole water depth range where cold-water corals can be found.

**) Submerged weight per unit volume (dry weight minus buoyancy), assuming sea water density 1025 kg/m³

Hydrodynamic Coefficients

The hydrodynamic coefficients are carefully selected based on several parameters which have been listed in Chapter 4.3, to get an accurate hydrodynamic load effect acting on the riser. The hydrodynamic coefficients that are used in this thesis can be seen in Table 4.8.

Table 4.8 Hydrodynamic Coefficient (Felisita et al., 2017).

Hydrodynamic coefficient	
Parameters	Value
Drag Coefficient (CD), SCRs	1.1
Added Mass Coefficient (CM), SCRs	1.0
CM, SCRs with buoy	1.0

Soil-Riser Interaction

There are complex interactions between the riser pipe movements, soil resistance, and the pipe penetration into the seabed, at the location when the riser is exposed to the oscillatory

movement (Bai & Bai, 2005). Both the riser fatigue life and the out-of-plane motions of the riser at the touchdown point area is influenced by these interactions.

Thus, riser-soil interactions should be defined to determine riser's fatigue performance. The parameters of the riser-soil interaction used in this thesis are as shown below:

Table 4.9 Riser-soil Interactions (Orimolade et al., 2015)

Parameter	value
Axial friction Coefficient	0,3
Lateral friction Coefficient	0,5
Horizontal lateral/axial soil stiffness	200 kN/m^2
Vertical soil stiffness	50 kN/m^2

4.8 Design Requirement and Acceptance Criteria

4.8.1 Wall Thickness Criteria

Wall thickness is an important property to consider when designing a riser. The wall thickness that can be utilized must be able to withstand external hydrostatic pressure, internal overpressure, and combined loading. In this study, the minimum wall thickness is approximated according to the pressure containment, collapse, and combined loading criteria according to DNV-OS-F201.

This minimum required wall thickness can be verified using the Pipeline Engineering Tool (PET) software by DNV, and PET will calculate the thickness based on DNV-OS-F101. The formula for wall thickness is the same as in DNV-OS-F201.

Table 4.10 below shows the summary of wall thickness assessment. The highest minimum wall thickness was found to be required for water depth 2000 m for the buckle propagation criteria. The wall thickness check is also done for 1000 m and 1500 m but shown to be not as significant as the 2000 m water depth. However, the buckle propagation criteria are usually not chosen as the parameter to determine the thickness because buckling at risers can be avoided by including buckle arrestors. Based on the assessment, 26 mm is used in this study. The complete parameters used to calculate the wall thickness by using PET are shown in Appendix A.

Table 4.10 Minimum Wall Thickness

Water Depth (m)	Burst (Operating Condition) (mm)	Burst (System Test) (mm)	Collapse (mm)	Propagating Buckling (mm)
2000	7.51	6.61	18.35	26.49
1500	9.73	8.37	15.25	23.08
1000	12	10.16	12.22	19.11

4.8.2 Acceptance Criteria

The riser design should comply with the design acceptance criteria to ensure that the design is safe. Below are the acceptance criteria:

Buckling Utilization Factor

Based on DNV-OS-F201, the correlation between the tension and moment is vital for all the acceptance criteria in the combination loading for the LRFD. To guarantee the riser design follows the design acceptance criteria, utilization or generalized loading expressed by the following equation from DNV should be considered.

$$g(t) = g(M_d(t), T_{ed}(t), \nabla_p, R_k, \Lambda) \leq 1 \quad (4.16)$$

Where

- M_d : Bending moment
- T_d : Effective tension
- ∇_p : Load difference pressure
- R_k : Vector of cross-sectional capacities
- Λ : Vector of safety factors

$$g(t) \leq 1 : \text{Safe}$$

The maximum buckling utilization factor must be less than 1 to ensure the design is safe for all limit state design. The computation for the LRFD is programmed in Orcaflex, and it is part of the analysis in the software.

Compression

Compression (negative tension) is undesirable. Therefore, to comply with design acceptance criteria, compression needs to be avoided and should be kept at an absolute minimum.

Fatigue

250 years is the minimum fatigue life that must be attained in the fatigue response analysis.

Strength Criteria

The maximum allowable static stress is set to 298 MPa in the thesis, corresponding to 2/3 of SMYS. While in the ULS design, the maximum allowable stress is 358 MPa based on a design factor that is 0.8. An ALS design will have maximum allowable stress of 448 MPa based on a design factor that is 1.0. The maximum allowable stress is with the accordance of API-RP-2RD (Orimolade et al., 2015)

The allowable stress levels and the design case factor C_f are given in Table 4.11 and Table 4.12.

Table 4.11 Allowable Riser Stress Level (LI, 2014)

Stress Category	Allowable Stress	Reference
Primary membrane (Von Mises)	$C_f \sigma_a$	API RP 2RD
Primary membrane plus bending	$1.5 C_f \sigma_a$	API RP 2RD
Primary membrane plus bending plus secondary	$2 \sigma_y^1$	API RP 2RD

Note: σ_y = SMYS, σ_a = basic allowable stress = 2/3 σ_y

Table 4.12 Design Case Factor (LI, 2014)

Load Category	Design Case Factor, C_f
Operating	1
Extreme	1.2
Temporary	1.35
Survival	1.5
Installation	1.2

4.9 LWR Overview

A lazy wave configuration involves the use of buoyancy modules along a section of the riser length to influence its free-hanging configuration. The system under consideration consists of a lazy wave riser connected to a semi-submersible. Here in this study, the major differences are water depth and riser length. The riser buoyancy section of length is approximately the same. The LWR model configuration as shown in Figure 4.15

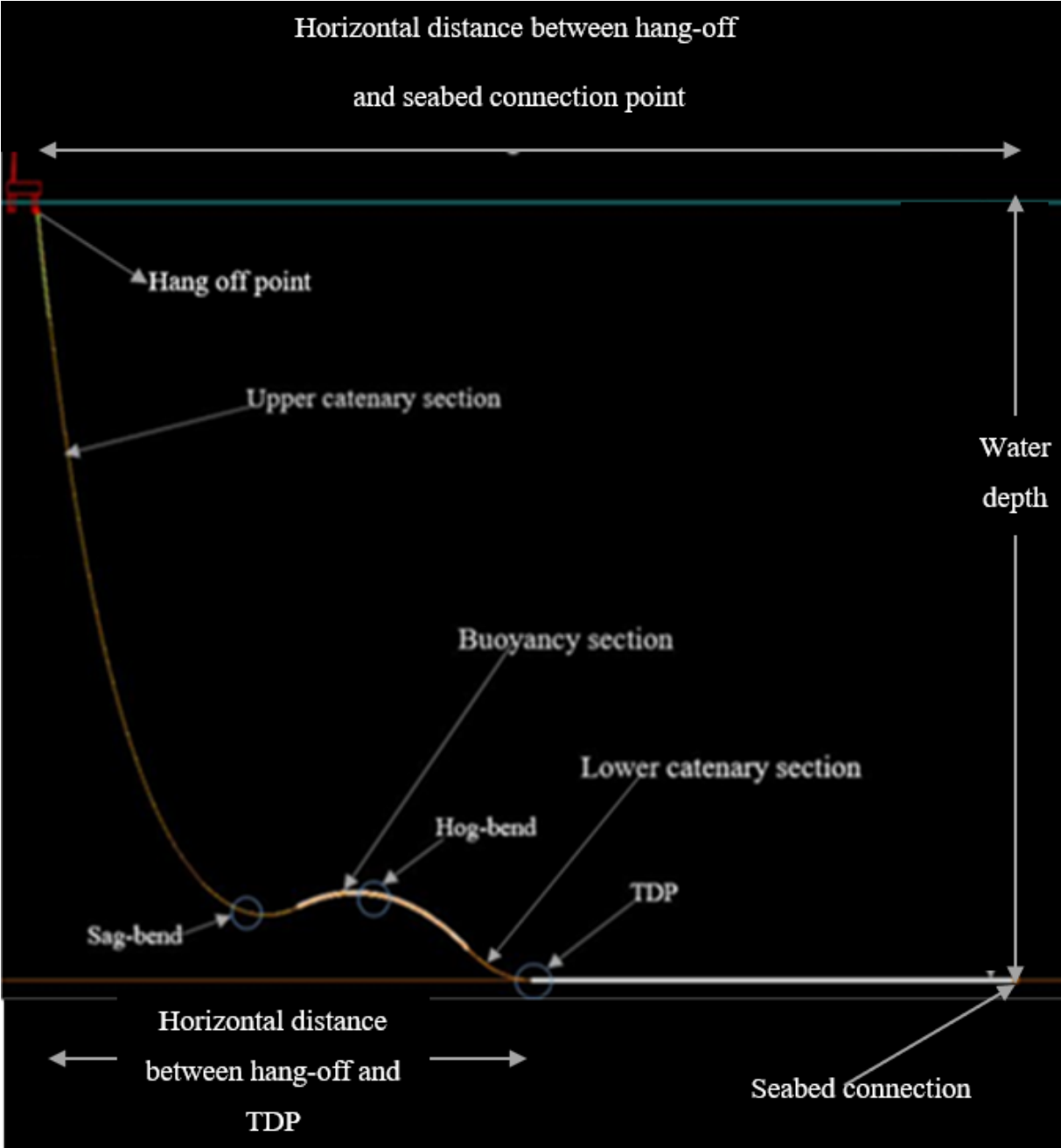


Figure 4.15 Lazy wave riser Model in OrcaFlex

Table 4.13 Parameters of the LWR Configuration

Water Depth				
Parameters	2000m	1500m	1000m	Unit
Upper Catenary Length	2180	1750	1375	m
Buoyancy section length	600	600	600	m
Lower Catenary Length	1830	1830	1830	m
Total Riser Length	4610	4180	3805	m

Both the vessel and the riser are configured to the worst-case scenarios in a combination of extreme wave and currents directions. The X direction is shown in Figure 4.16 below, indicates both the wave and current direction, while the Y-axis indicates the 90-degree direction of the wave and current. Since only the worst-case scenarios are analyzed, the maximum impact will only occur to the riser at 0 and 180 degrees, which are the two directions that are being considered in this analysis.

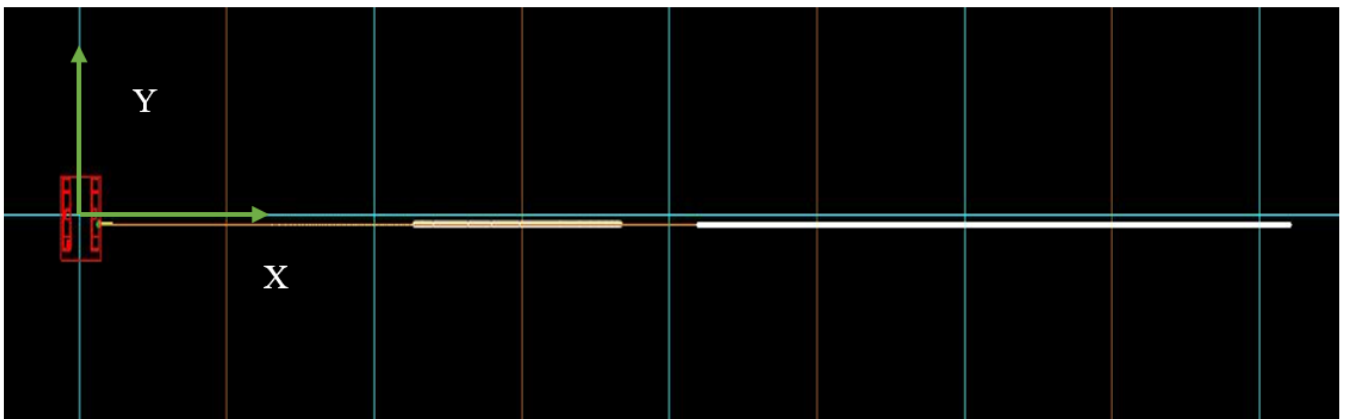


Figure 4.16 Plan View of OrcaFlex LWR Model

From the analysis results, it was found that the 180-degree wave direction to the vessel is giving the maximum downward riser velocity, as shown in Table 4.14 below

Table 4.14 Worst Metocean Condition

Water depth (m)	Hs (m)	Tp (s)	Wave direction (degree)
2000	17	19	180
1500	17	19	180
1000	17	19	180
Wave Spectrum			JONSWAP
Wave Load Modelling			Irregular Wave

5. Extreme Response Analyses

5.1 Introduction

Different load cases (Environment Load: Wave and Current Load) will be tested on different riser models to gain a better understanding and knowledge of the extreme responses. The worst sea state used is from a 100 years wave and 10 years current, since it yields the maximum downward velocity according to the various parameters.

In this study, three different water depth is examined for the LWR configuration. The analysis part is subdivided into two categories. The first being the static analysis while the second being the dynamic analysis. In order to establish a static equilibrium, the static analysis is initially performed. After that, the dynamic analysis is stimulated to obtain the motion of the vessels for different wave frequencies. The design parameter and limitation used are referred from DNV OS F201 (DNV, 2010a).

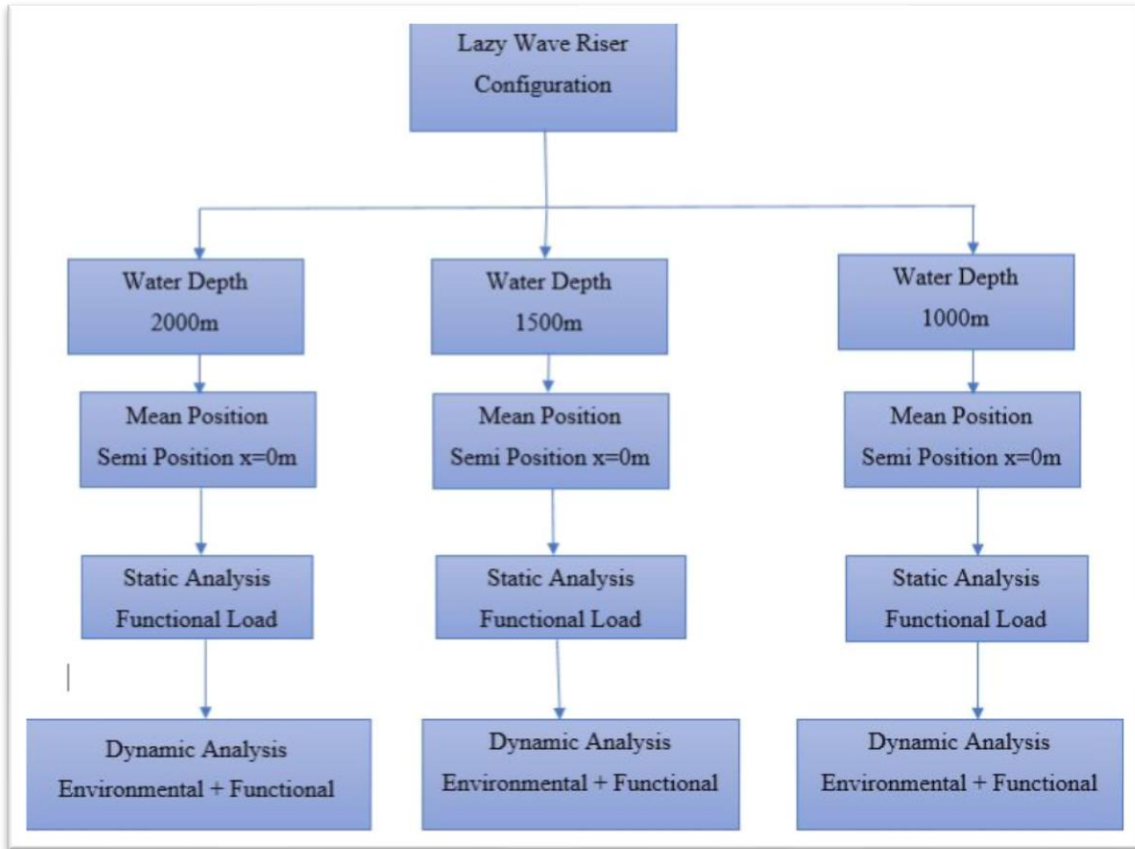


Figure 5.1 Static and Dynamic Stage

5.2 Determination for worst Sea state

In the dynamic analysis, a different combination of H_s and T_p from the metocean data study is used to evaluate the response from the semi-submersible during the 100 years wave and 10 years current. There was four-wave direction (0, 45, 90, 180) that was used as the parameter in this study. Orcaflex ran a total of 132 combination values to gain a better understanding of the issues presented.

Additionally, three different water depth was computed together with the same sets of parameters. That brings it up to a total combination that was analyzed to 396. The study was conducted with a three-hour storm stimulation to replicate the extreme sea state conditions.

Case 1:

Table 5.1 Selected Worst Condition from the NCS (WD2000m)-Dynamic Analysis

Water Depth (m)	Hs (m)	Tp (s)	Wave Direction (deg)	Max von Mises Stress (MPa)	Max Bending Moment (kNm)	Max Utilization
2000m	17,0	18,0	0	231	269	0,27
			45	203	210	0,152
			90	216	273	0,28
			180	222	309	0,38
	17,1	18,7	0	231	253	0,247
			45	204	205	0,152
			90	215	264	0,26
			180	226	300	0,35
	17,0	19,0	0	256	308	0,38
			45	228	215	0,22
			90	246	321	0,41
			180	257	353	0,52
	16,4	20,0	0	304	259	0,251
			45	196	213	0,154
			90	208	288	0,33
			180	220	318	0,38
	15,0	20,5	0	213	250	0,23
			45	195	203	0,15
			90	202	247	0,24
			180	214	275	0,28
	14,6	20,5	0	210	245	0,23
			45	192	201	0,15
			90	200	243	0,22
			180	211	268	0,27
	12,3	20,7	0	191	218	0,18
			45	178	190	0,13
			90	145	215	0,16
			180	192	229	0,18
	10,0	20,8	0	173	200	0,142
			45	164	184	0,12
			90	168	197	0,14
			180	174	205	0,153
	8,0	21,0	0	158	189	0,125
			45	152	179	0,106
			90	154	186	0,124
			180	160	191	0,13
	6,2	22,0	0	145,3	180	0,11
			45	140,7	175	0,105
			90	142	179	0,106
			180	146	180	0,107
15	21	0	213	245	0,23	
		45	192	200	0,142	
		90	200	240	0,22	
		180	212	265	0,22	

Case 2:

Table 5.2 Selected Worst Condition from the NCS (WD1500m)-Dynamic Analysis

Water Depth (m)	Hs (m)	Tp (s)	Wave Direction (deg)	Max von Mises Stress (MPa)	Max Bending Moment (kNm)	Max Utilization
1500m	17,0	18,0	0	198	247	0,24
			45	171	194	0,138
			90	191	253	0,247
			180	214	284	0,32
	17,1	18,7	0	200	237	0,21
			45	176	195	0,138
			90	190	246	0,23
			180	215	272	0,236
	17,0	19,0	0	221	286	0,32
			45	198	206	0,156
			90	219	306	0,38
			180	248	330	0,46
	16,4	20,0	0	195	248	0,24
			45	164	209	0,16
			90	189	271	0,29
			180	208	292	0,33
	15,0	20,5	0	186	232	0,201
			45	161	192	0,13
			90	179	231	0,198
			180	205	254	0,245
	14,6	20,5	0	185	228	0,194
			45	158	189	0,13
			90	177	226	0,19
			180	202	246	0,23
	12,3	20,7	0	171	205	0,153
			45	144	176	0,113
			90	161	201	0,15
			180	184	212	0,16
	10,0	20,8	0	158	186	0,125
			45	131	167	0,097
			90	147	182	0,12
			180	168	190	0,13
8,0	21,0	0	146	172	0,107	
		45	125	162	0,093	
		90	136	172	0,105	
		180	154	174	0,11	
6,2	22,0	0	137	163	0,095	
		45	123	15	0,086	
		90	126	164	0,095	
		180	142	166	0,096	
15	21	0	187	229	0,19	
		45	157	188	0,127	
		90	176	225	0,19	
		180	203	242	0,22	

Case 3:

Table 5.3 Selected Worst Condition from the NCS (WD1000m)-Dynamic Analysis

Water Depth (m)	Hs (m)	Tp (s)	Wave Direction (deg)	Max Von Mises (MPa)	Max Bending Moment (kNm)	Max Utilization
1000m	17,0	18,0	0	215	267	0,24
			45	165	197	0,143
			90	181	244	0,23
			180	222	256	0,252
	17,1	18,7	0	219	261	0,21
			45	169	198	0,144
			90	181	243	0,23
			180	222	257	0,258
	17,0	19,0	0	237	297	0,34
			45	178	211	0,17
			90	206	282	0,32
			180	255	296	0,38
	16,4	20,0	0	214	261	0,24
			45	165	214	0,17
			90	185	266	0,27
			180	217	268	0,28
	15,0	20,5	0	202	231	0,19
			45	159	190	0,13
			90	171	228	0,2
			180	214	245	0,23
	14,6	20,5	0	198	225	0,23
			45	158	187	0,13
			90	169	224	0,19
			180	212	239	0,22
	12,3	20,7	0	183	196	0,145
			45	151	169	0,103
			90	157	195	0,14
			180	195	206	0,16
	10,0	20,8	0	171	175	0,11
			45	144	158	0,09
			90	146	174	0,105
			180	178	180	0,12
	8,0	21,0	0	159	162	0,1
			45	139	151	0,08
			90	138	161	0,09
			180	164	164	0,093
	6,2	22,0	0	149	150	0,078
			45	134	146	0,076
			90	131	152	0,081
			180	153	154	0,085
15	21	0	203	230	0,19	
		45	161	186	0,127	
		90	169	222	0,186	
		180	213	240	0,22	

In the results, the extreme metocean condition occurred at $H_s=17$ m and $T_p =19$ s for all the three cases. It is observed that the highest wave height is usually not the worst results since the riser system is interdependent on its dynamics. The pipe utilization is measured by the effective tension, bending moment, and pressure exposure, as indicated in section 3.6.4. The maximum DNV LRFD utilization value was 0.52, 0.46, and 0.38 at each respective 2000m water depth, 1500 water depth, and 1000 water depth for the LWR. Also, the 180-degree wave direction experienced the maximum downward velocity. These forces resulted in a more significant bending moment in the sag-bend area and caused by the compressive forces in the touchdown region. All configuration is acceptable since the utilization of less than 1. To summarize, the abovementioned observation in the deep-water or harsh conditions indicated that all the response is within the safe and allowable design criteria.

5.3 Determination of Critical section for LWRs

5.3.1 Static Analysis

Similarly, as described earlier, the static equilibrium of the LWR configuration is calculated through static analysis. Both the functional load and the nominal offset position is considered, while the environmental load is not considered. The maximum effective tension, bending moments DNV LRFD utilization was observed along the length of the riser. Table 3.1 and Section 3.3 describes the functional loads that were considered. The most unfavorable metocean values from the result calculated were $H_s=17$ m and $T_p =19$ s.

The critical sections of the LWR at different water depths (1000, 1500 and 2000m) was presented as a summary of the results.

Case 1 WD: 2000m

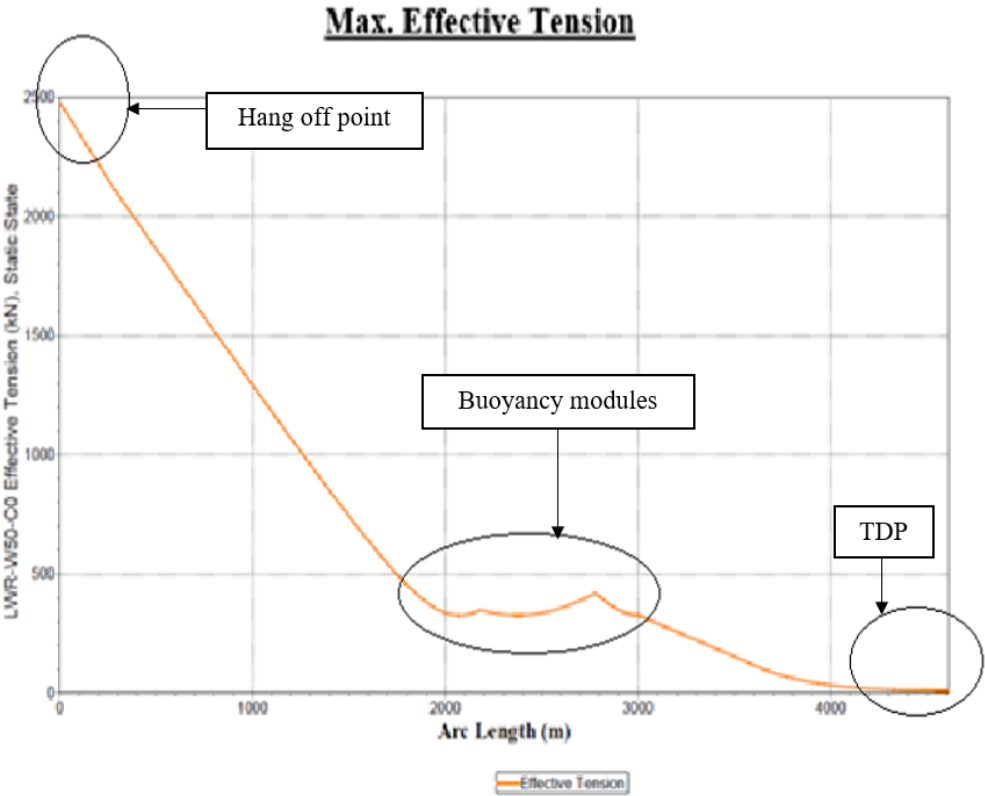


Figure 5.2 Max Effective Tension for Static Analysis

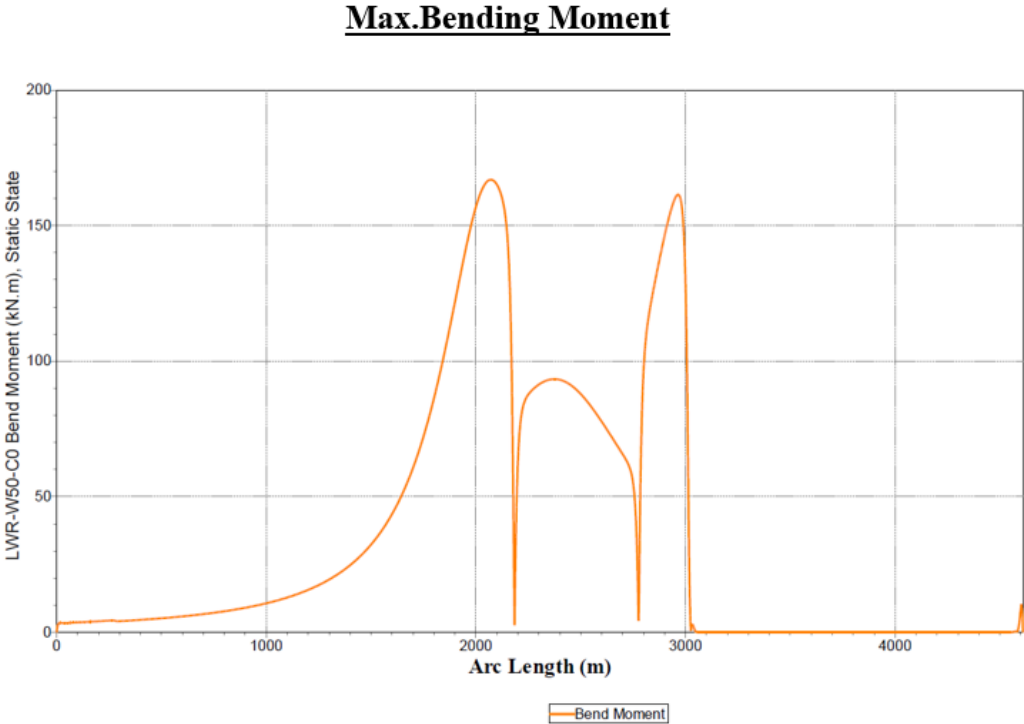


Figure 5.3 Max Bending Moment for Static Analysis

Max Von Mises Stress

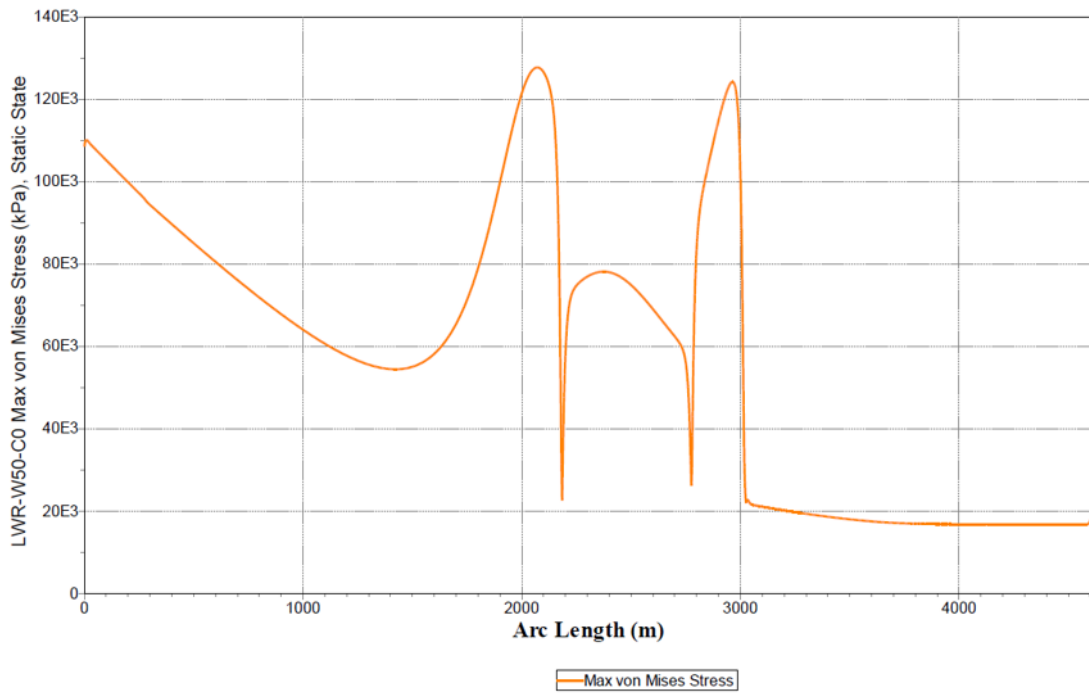


Figure 5.4 Max Von Mises Stress for Static Analysis

Max.DNV LRFD Utilization

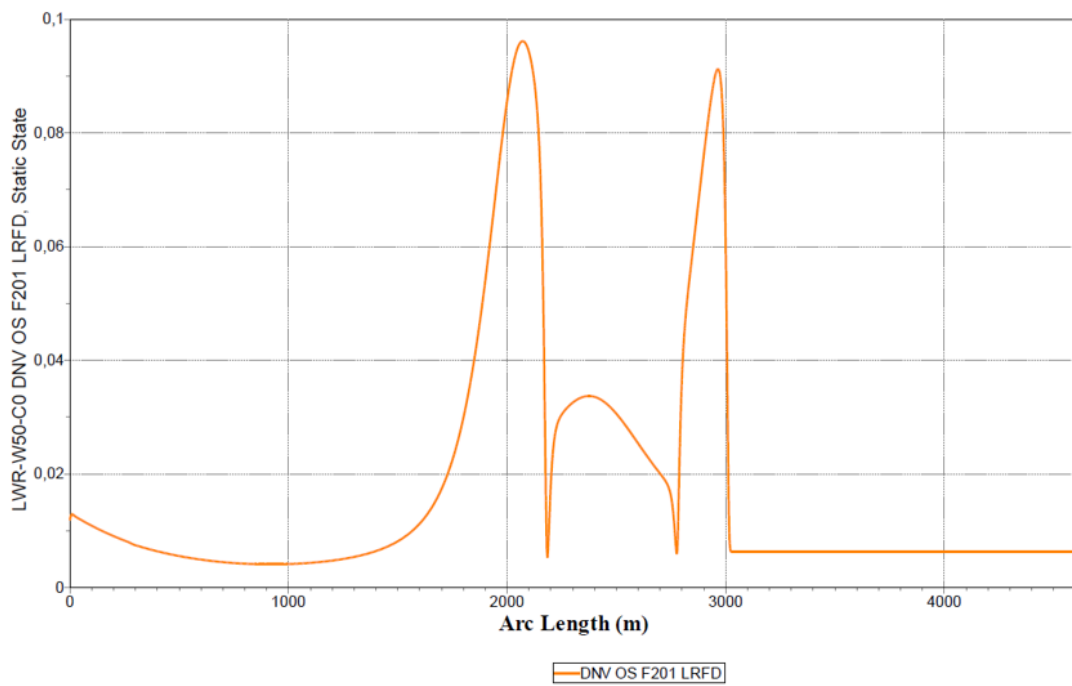


Figure 5.5 Max Utilization for Static Analysis

The static analysis results for Semisubmersible Nominal Position are presented in Table 5.4 to Table 5.6

Table 5.4 Summary Results of Lazy-Wave Riser Nominal Static Analysis

Semisubmersible Nominal Position (Hs:17 m / Tp:19 s) (Wave direction-180⁰)				
Water depth: 2000m				
Top Tension (kN)	2458			
Hang-off Angle (degree)	8 ⁰			
Critical Locations	Unit	Sag-bend	Hog-bend	TDP
Effective Tension	kN	326,04	326,02	329,64
Bending Moment	kN.m	166,8	93,2	161,42
Von Mises Stresses	MPa	127,68	78,12	124,21
DNV Utilization	-	0,096	0,033	0,091

Result Discussion of the Static analysis

The effective tension experience is identical for all the three locations. The maximum utilization is found in the sag-bend area, but utilization is very low at all location. All the critical location has low static stress, and it is safely below the allowable limit.

Case 2 WD: 1500m

Max. Effective Tension

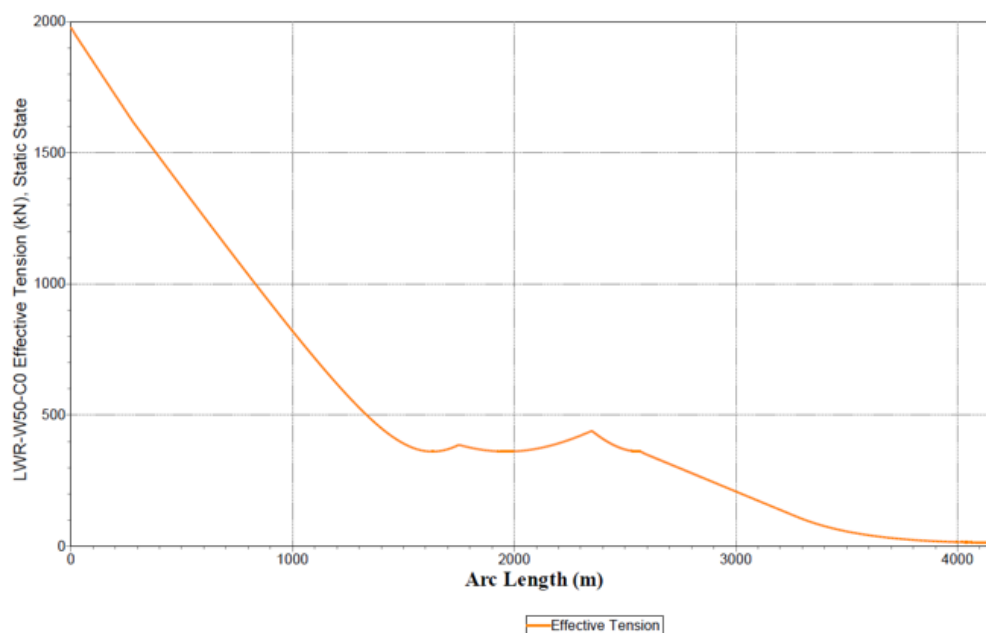


Figure 5.6 Max Effective Tension for Static Analysis

Max Bending Moment

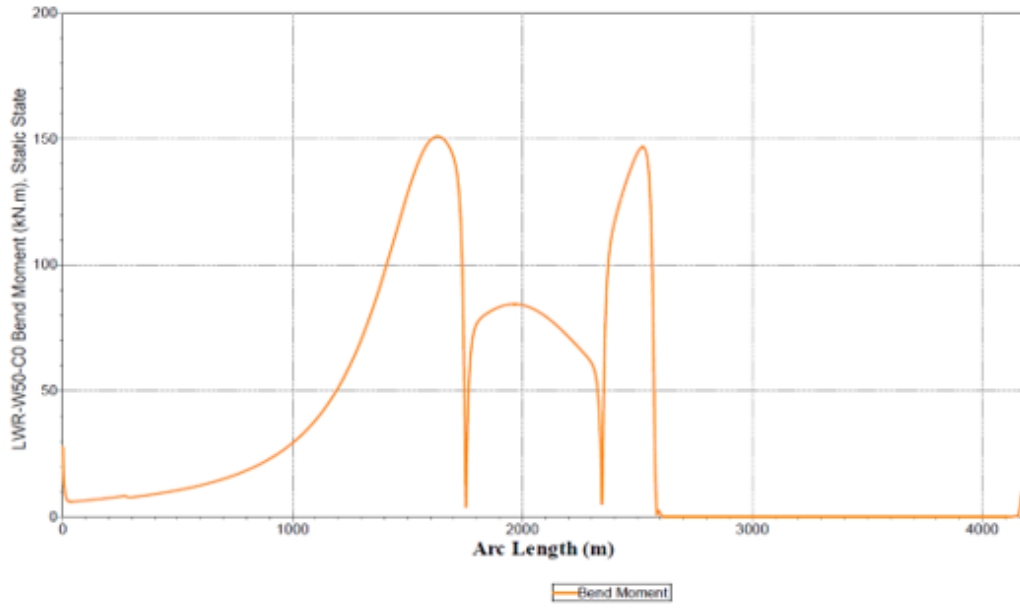


Figure 5.7 Max Bending Moment for Static Analysis

Max Von Mises Stress

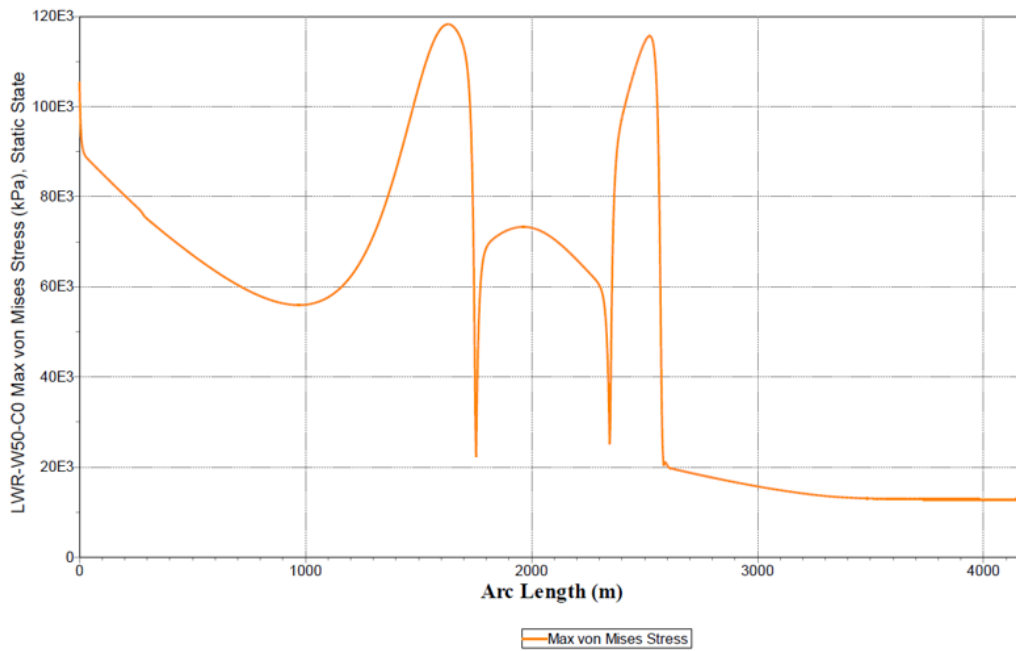


Figure 5.8 Max Bending Moment for Static Analysis

Max DNV LRFD Utilization

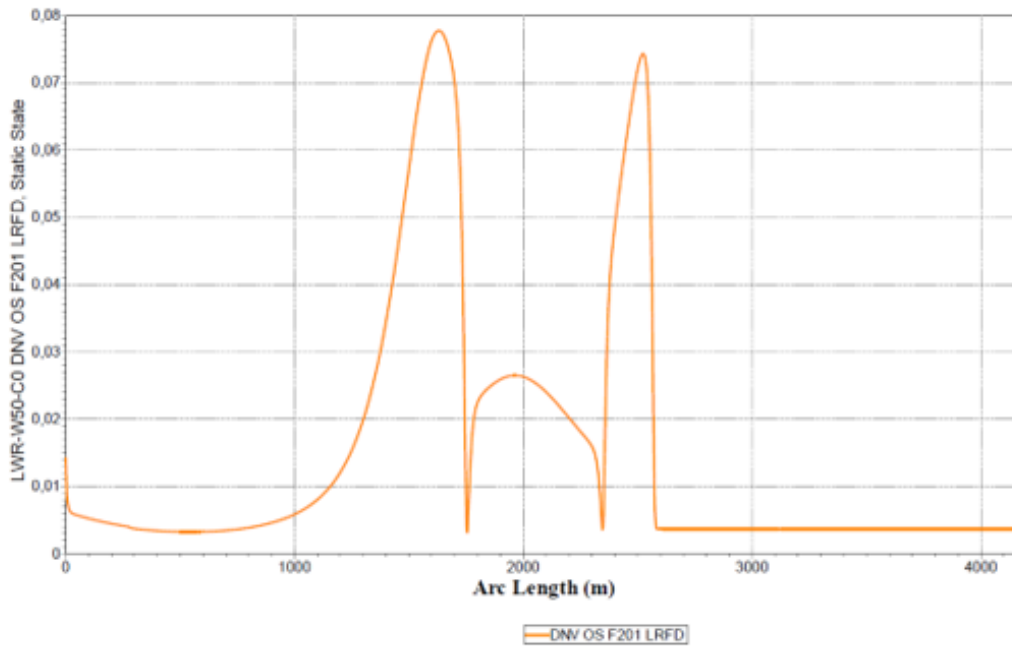


Figure 5.9 Max Utilization for Static Analysis

Table 5.5 Summary Results of Lazy-Wave Riser Nominal Static Analysis

Semisubmersible Nominal Position (Hs:17 m / Tp:19 s)				
(Wave direction-180^o)				
Water depth: 1500m				
Top Tension (kN)	1956			
Hang-off Angle (degree)	11,5			
Critical Locations	Unit	Sag-bend	Hog-bend	TDP
Effective Tension	kN	361	360,85	362,5
Bending Moment	kN.m	150,82	84,34	145,7
Von Mises Stresses	MPa	118,15	73,27	114,8
DNV Utilization	-	0,077	0,026	0,073

Result Discussion of the Static analysis

Similar to the previous case above, the sag-bend area is the location where the maximum utilization occurs, and it also has a low maximum utilization value.

Case 3 WD: 1000m

Max. Effective Tension

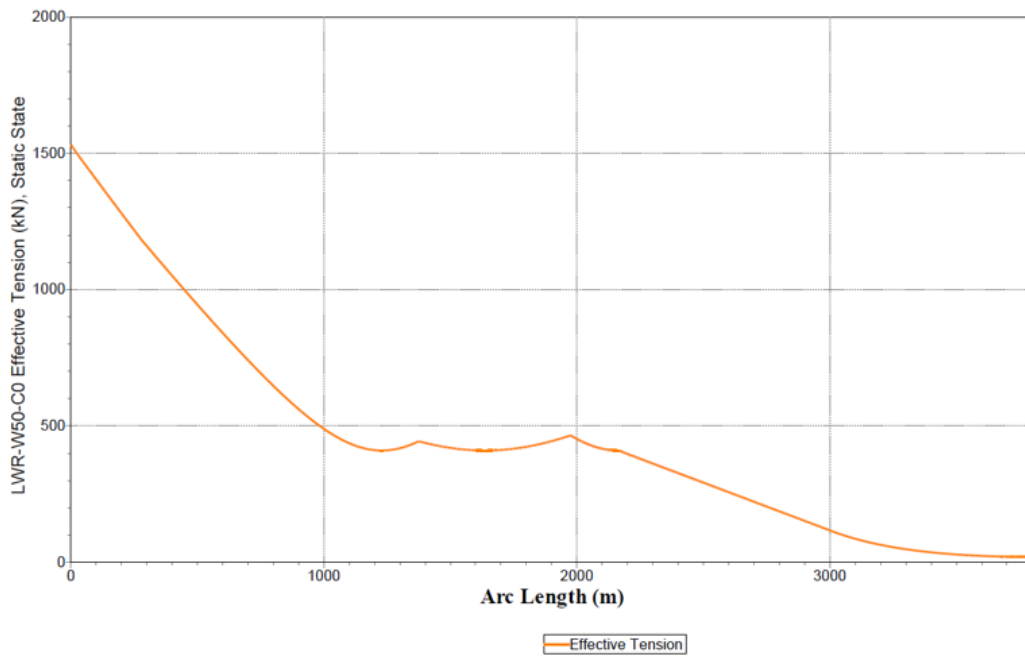


Figure 5.10 Max Effective Tension for Static Analysis

Max Bending Moment

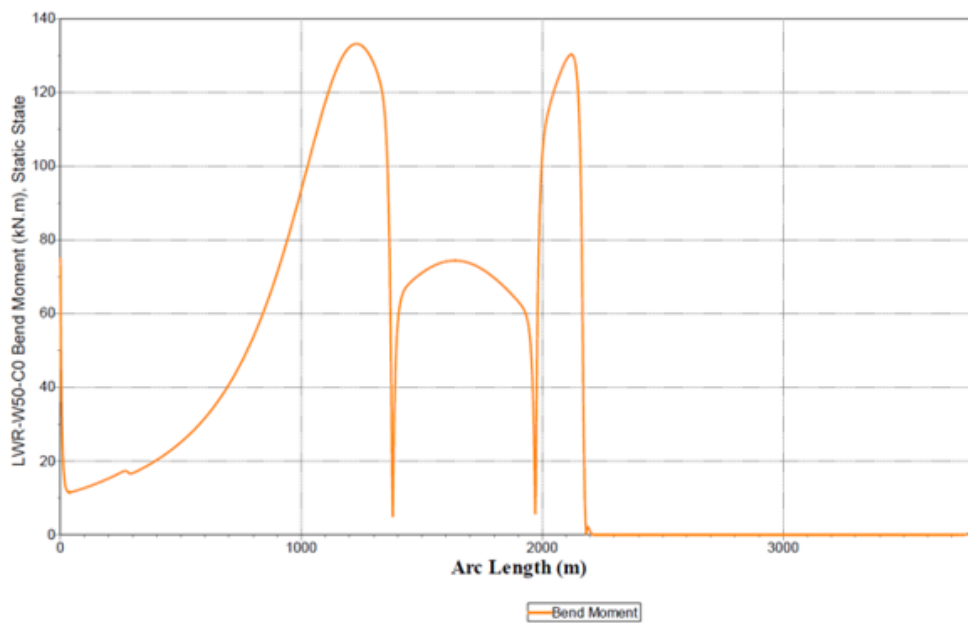


Figure 5.11 Max Bending Moment for Static Analysis

Max Von Mises Stress

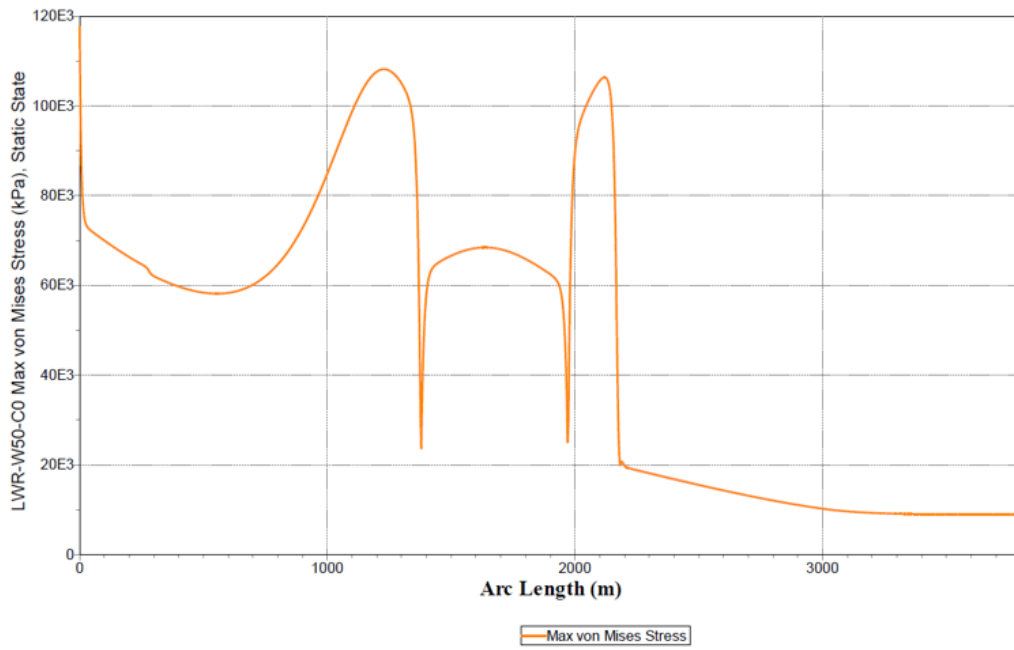


Figure 5.12 Max Von Mises Stress for Static Analysis

Max. DNV LRFD Utilization

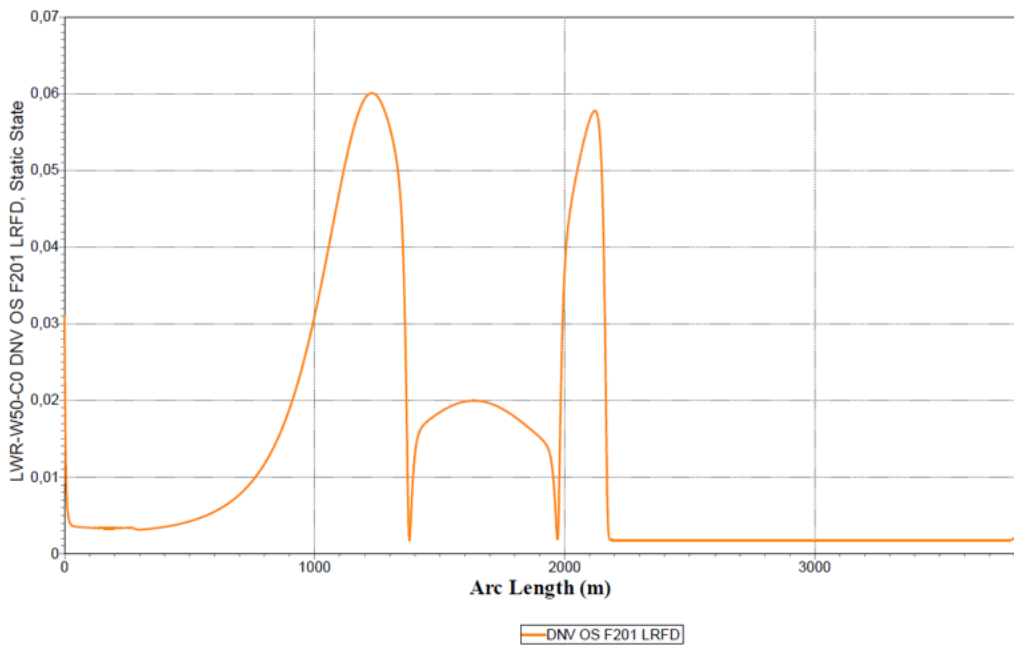


Figure 5.13 Max Utilization for Static Analysis

Table 5.6 Summary Results of Lazy-Wave Riser Nominal Static Analysis

Semisubmersible Nominal Position (Hs:17 m / Tp:19 s) (Wave direction-180⁰)				
Water depth: 1000m				
Top Tension (kN)	1509			
Hang-off Angle (degree)	15			
Critical Locations	Unit	Sag-bend	Hog-bend	TDP
Effective Tension	kN	409,62	409,68	411,27
Bending Moment	kN.m	113,12	74,20	129,3
Von Mises Stresses	MPa	108,16	68,37	105,7
DNV Utilization	-	0,06	0,02	0,057

Result Discussion of the Static analysis

Similar to the previous case, the sag-bend area is the location where the maximum utilization occurs, and it also has a low maximum utilization value. The effective tension, in this case, is much higher when compared with the previous cases.

5.3.2 Dynamic Analysis

During the dynamic analysis, the riser response to both the wave (100 years) and current (10 years) is analyzed. The starting point of this calculation is the static equilibrium. Dynamic simulation weighs in the vessel's RAO over a specific time.

Table 5.7 illustrates the effective tension, von Mises stress and bending moment at critical sections (riser top, arch bend, and touchdown area) of LWR for each load:

Table 5.7 Summary Results of Lazy-Wave Riser Nominal Dynamic Analysis

Semisubmersible Nominal Position (Hs:17 m / Tp:19 s) (Wave direction-180°)				
Water depth: 2000m				
Max. Effective Top Tension (kN)	3756			
Critical Locations	Unit	Sag-bend	Hog-bend	TDP
Effective Tension	kN	820,8	705,3	643,2
Bending Moment	kN.m	245,6	146,7	137,6
Von Mises Stresses	MPa	183,3	123,2	108,4
DNV Utilization	-	0,23	0,08	0,006
Water depth: 1500m				
Max. Effective Top Tension (kN)	3013			
Critical Locations	Unit	Sag-bend	Hog-bend	TDP
Effective Tension	kN	892,9	785,3	755,27
Bending Moment	kN.m	241,3	123,7	121,2
Von Mises Stresses	MPa	186,4	110,7	101,6
DNV Utilization	-	0,21	0,06	0,07
Water depth: 1000m				
Max. Effective Top Tension (kN)	2376			
Critical Locations	Unit	Sag-bend	Hog-bend	TDP
Effective Tension	kN	1005,5	928,2	941,6
Bending Moment	kN.m	186,1	122,8	112,1
Von Mises Stresses	MPa	150,4	103	94,2
DNV Utilization	-	0,13	0,05	0,06

Case 1 WD: 2000m

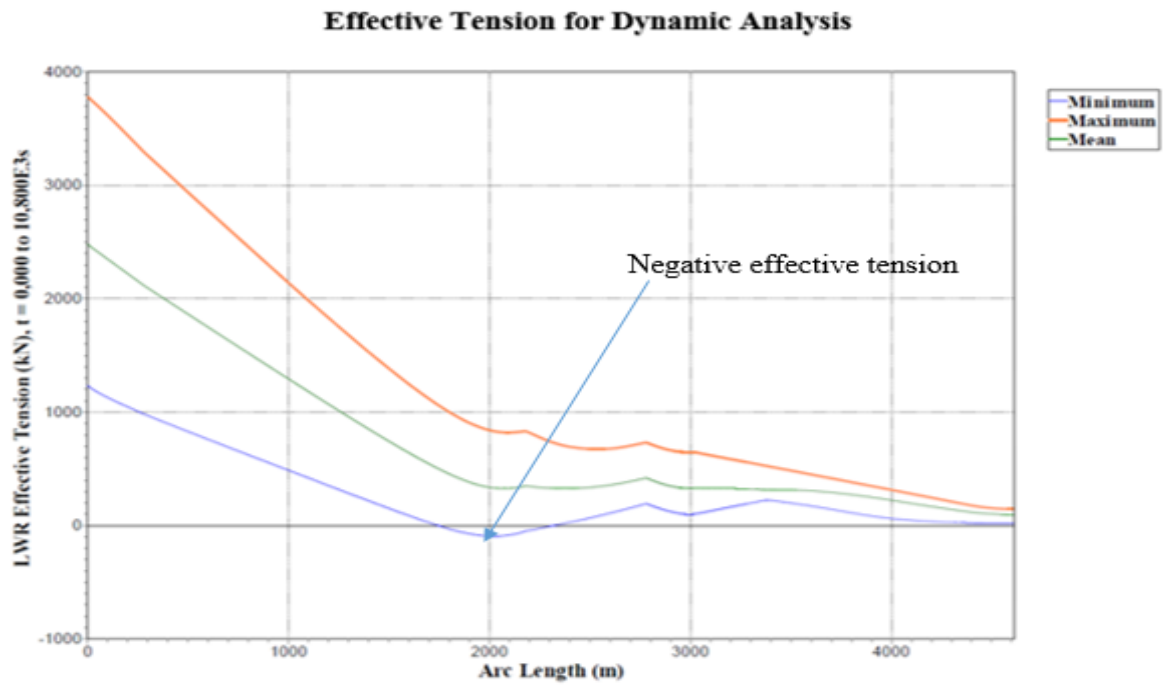


Figure 5.14 Riser Effective Tension for (WD: 2000m)

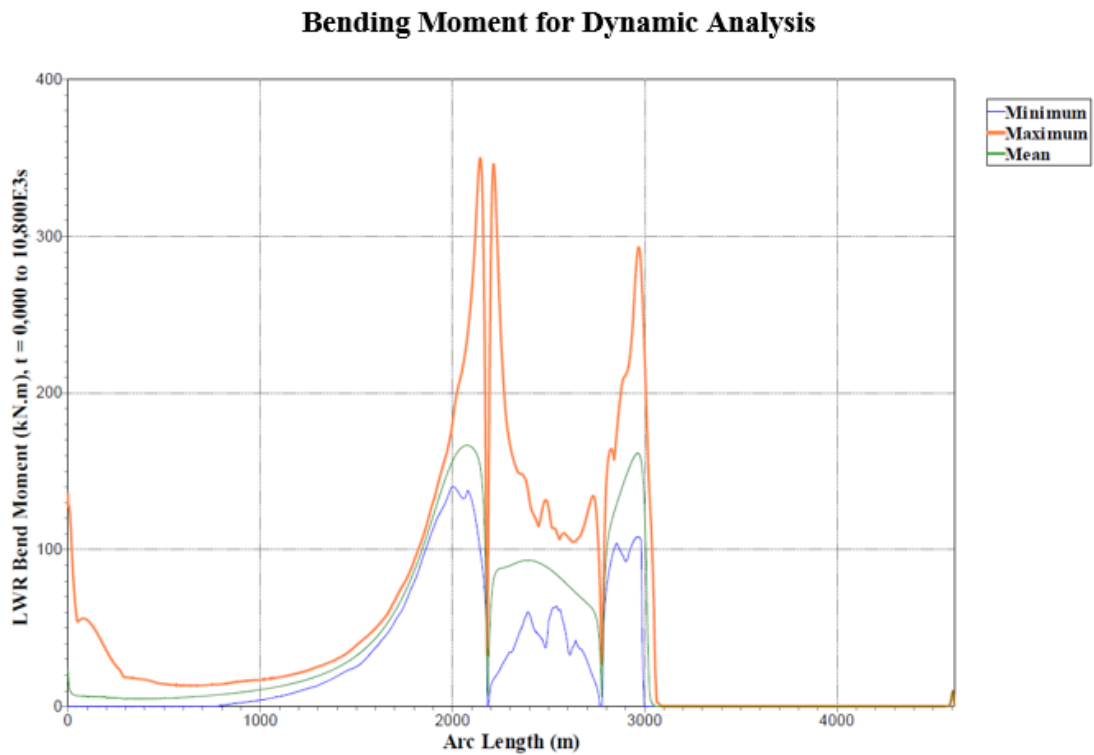


Figure 5.15 Riser Bending Moment (WD: 2000m)

Von Mises Stress for Dynamic Analysis

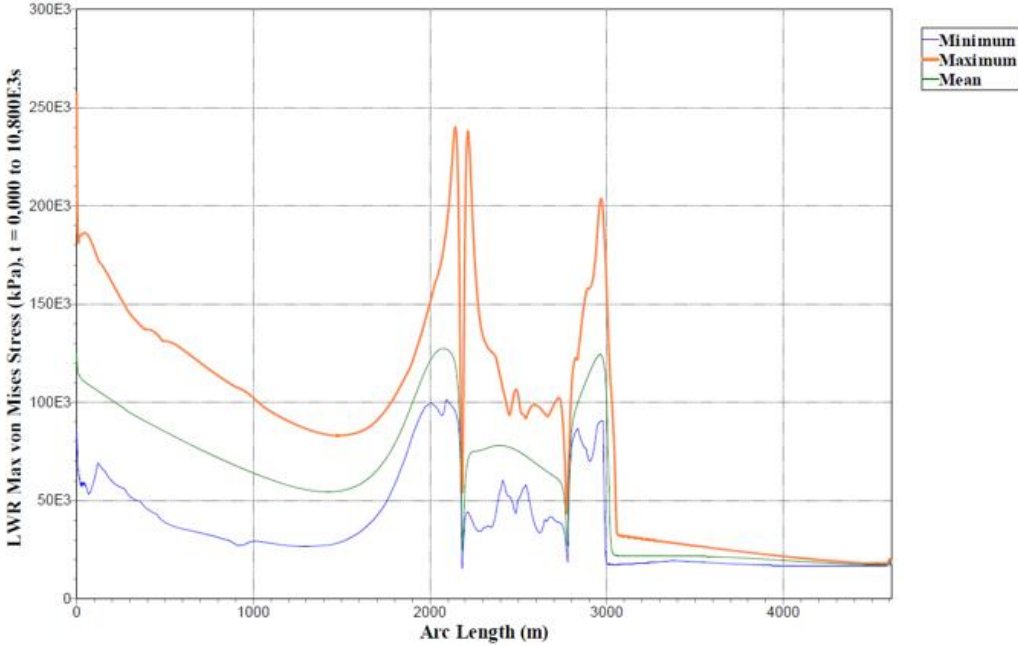


Figure 5.16 Riser Von Mises Stress (WD: 2000m)

LRFD Utilization for Dynamic Analysis

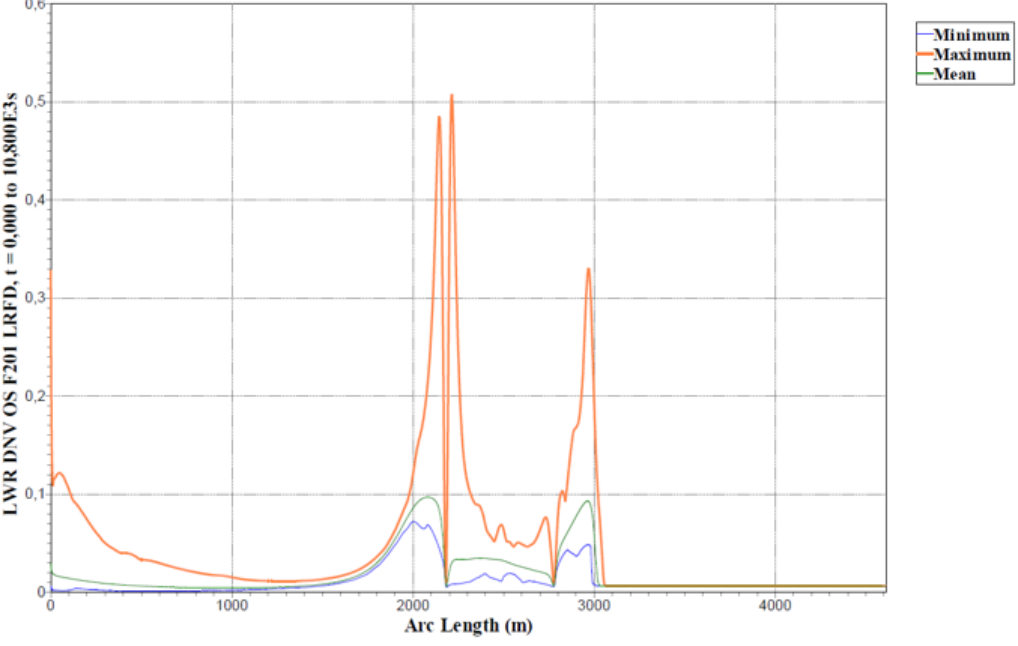


Figure 5.17 Riser Utilization (WD: 2000m)

Case 2 WD: 1500m

Effective Tension for Dynamic Analysis

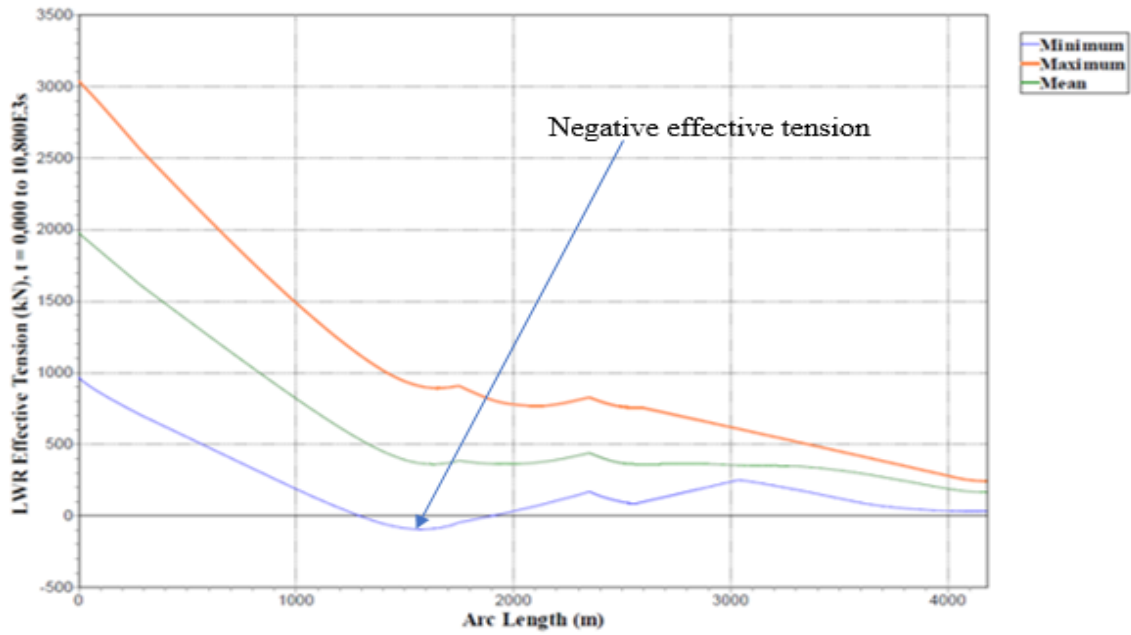


Figure 5.18 Riser Effective Tension (WD: 1500m)

Bending Moment for Dynamic Analysis

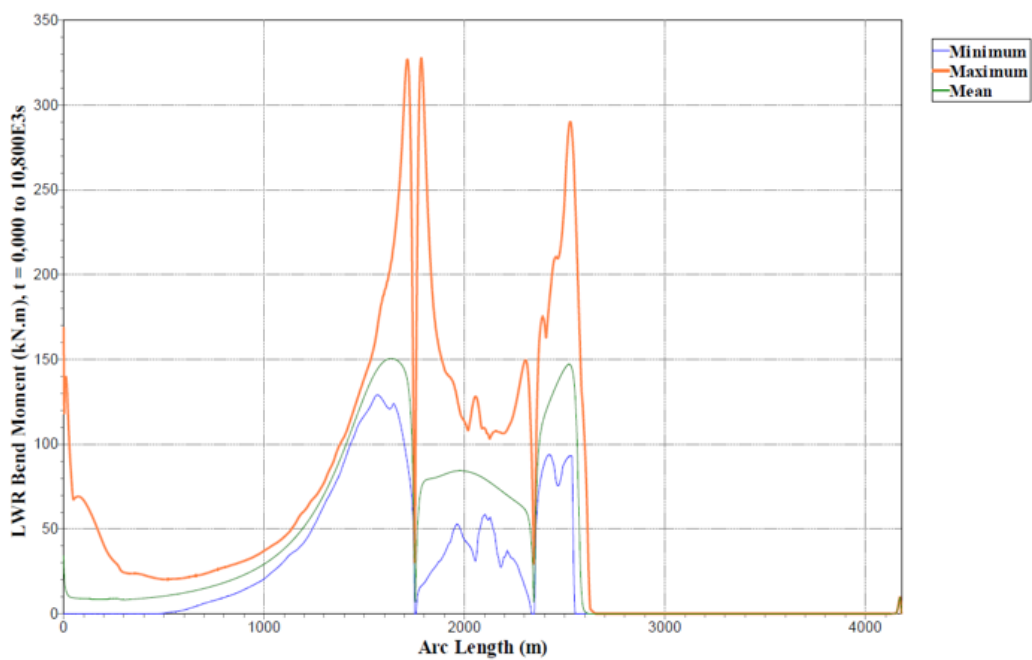


Figure 5.19 Riser Bending Moment (WD: 1500m)

Von Mises Stress for Dynamic Analysis

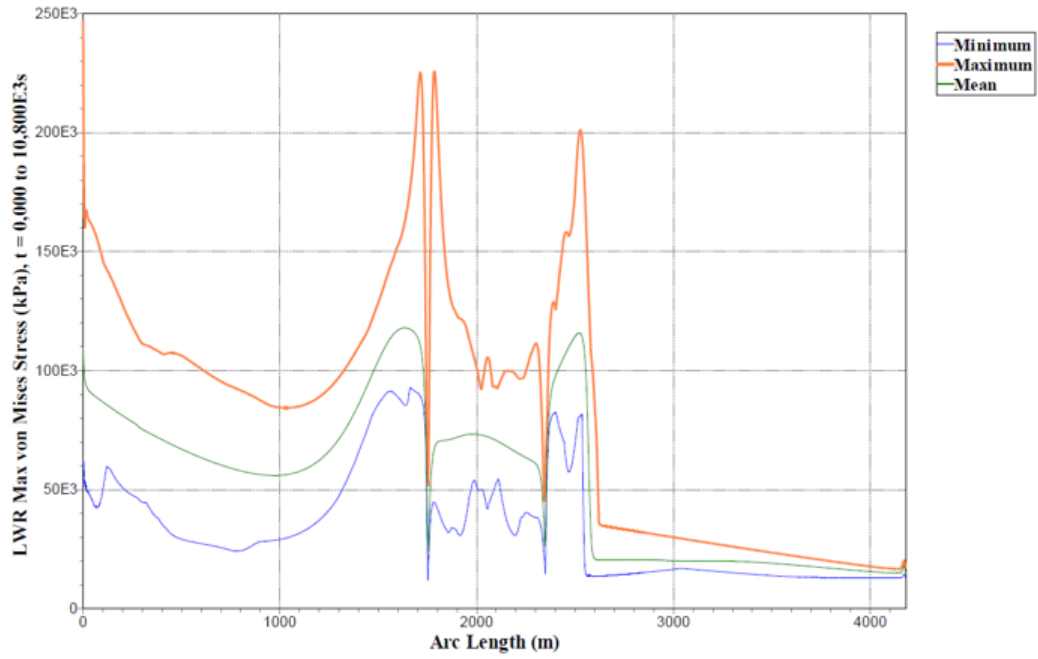


Figure 5.20 Riser Von Mises Stress (WD 1500m)

LRFD Utilization for Dynamic Analysis

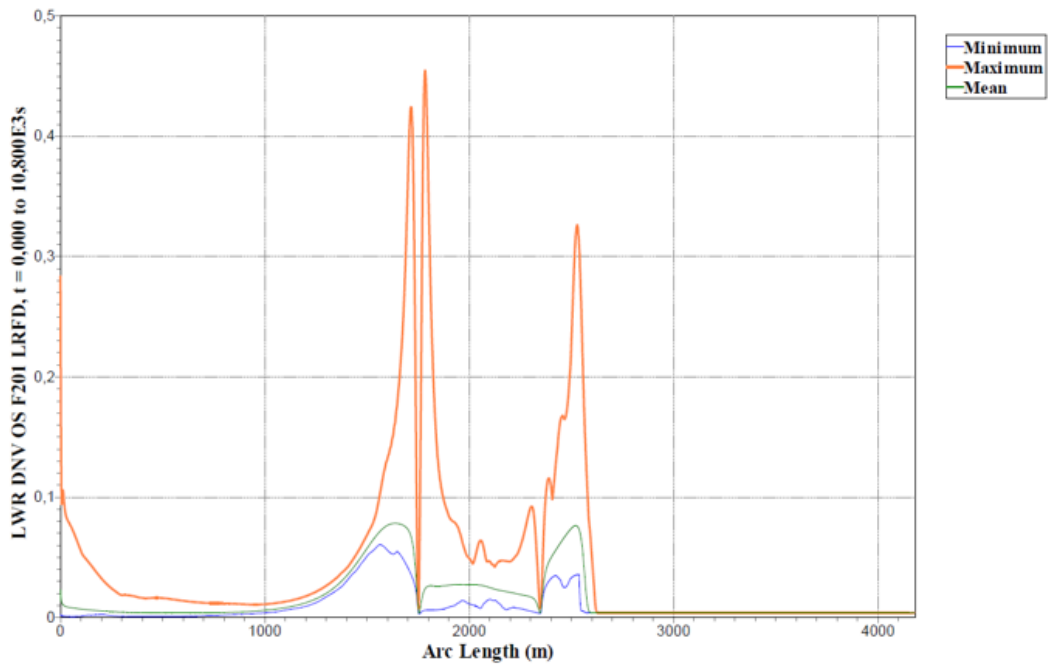


Figure 5.21 Riser Utilization (WD: 1500m)

Case 3 WD: 1000m

Effective Tension for Dynamic Analysis

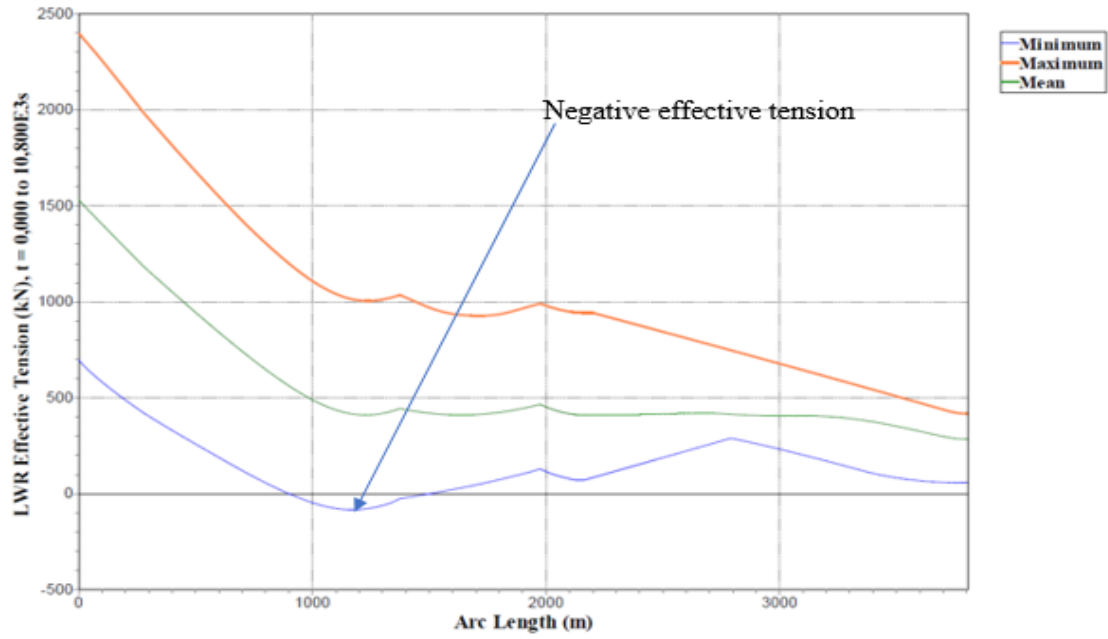


Figure 5.22 Riser Effective Tension (WD: 1000m)

Bending Moment Dynamic Analysis

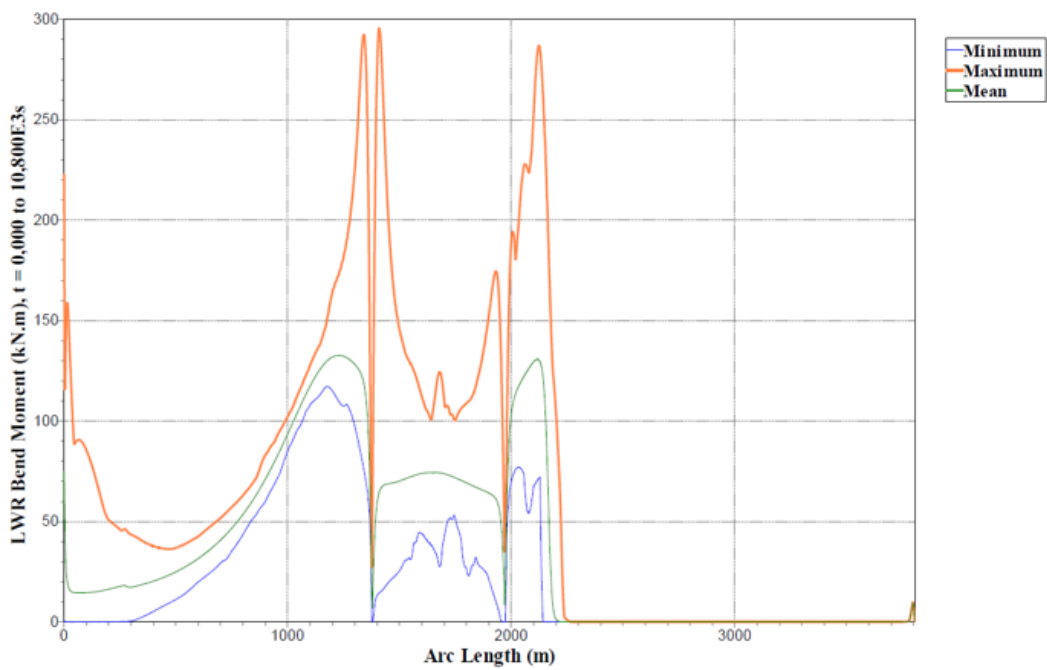


Figure 5.23 Riser Bending Moment (WD: 1000m)

Von Mises Stress for Dynamic Analysis

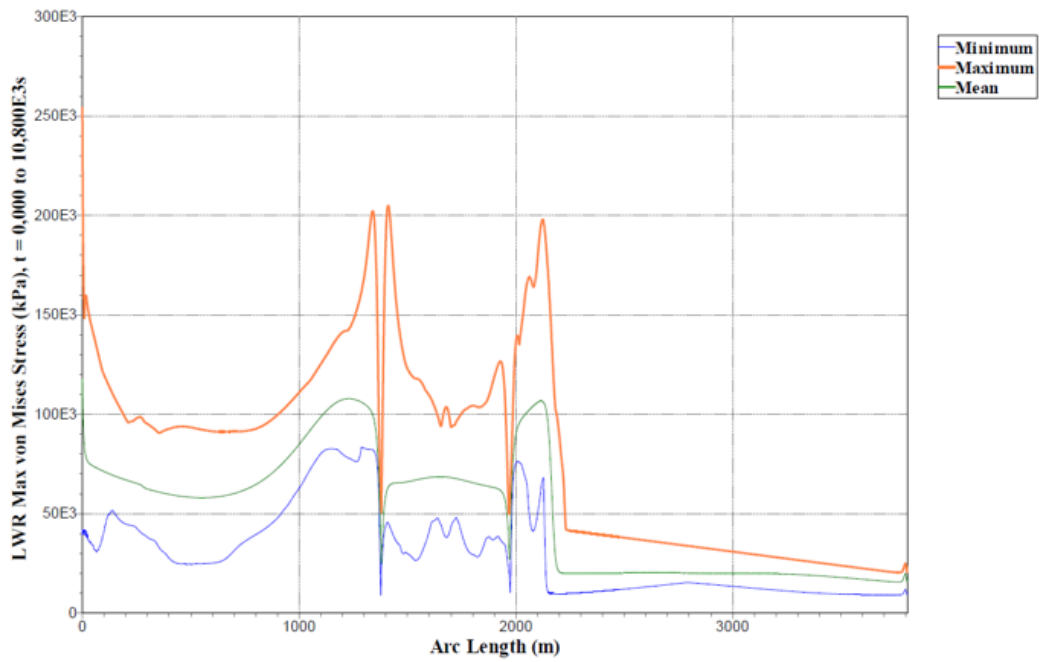


Figure 5.24 Riser Bending Moment (WD: 1000m)

LRFD Utilization for Dynamic Analysis

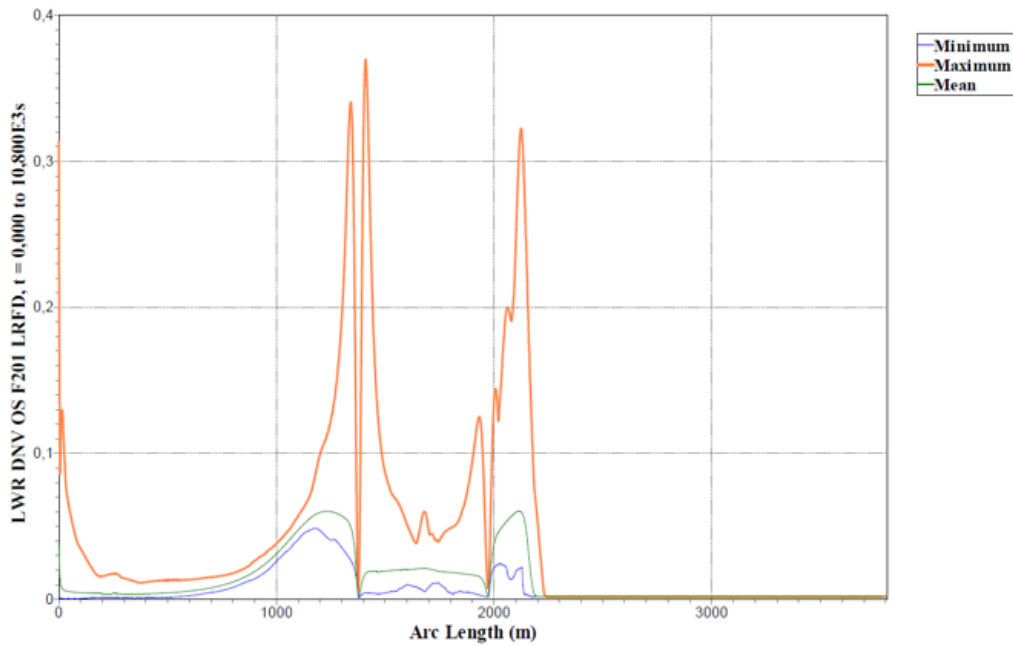


Figure 5.25 Riser Utilization (WD: 1000m)

Result Discussion of the Dynamic analysis

Analysis has been performed for the 100 years wave, and 10 years current comparison has been made with water depths of 1000m, 1500, 2000m.

The dynamic analysis clearly shows differing values when compared to the values from the static configuration. There is a significant jump in the ineffective tension, bending moment, and higher utilization factor. Thus, suggesting a strong correlation between the environmental loads and overall performance of the riser. The maximum bending moment is a higher value at the sag-bend all the three cases. The bending moment is also higher at 2000m water depth as opposed to the other two water depth. The effective tension at the high sag bend area is comparable with hog-bend and TDP.

Moreover, as the water depth decreases the effective tension increases in all locations, the Maximum LRFD utilization value is 23%, 21% and 13% at the sag-bend of the LWR.

All configurations are acceptable as the utilization is less than 1, which means that the maximum stress in the riser is lower than SMYS, and hence the design is safe.

Excessive compression (negative tension) leads to failure and shall be avoided at the sag bend region or be minimal for all three cases as described in section 4.8.2.

It can be concluded that extreme response is seen in the case of LWR in 2000 m water depth.

6. Conclusion

In this thesis, 10" production riser made from X65 grade carbon steel riser material was optimized, while a lazy wave riser (LWR) configuration was investigated. Several parameter adjustments could have been implemented to improve the LRFD utilization. The strong performance of an LWR connected to a semisubmersible deployed in NCS area at water depths of 2000m, 1500m and 1000m has been presented.

The riser modeling and analyses have been performed using the OrcaFlex computer program. Based on the results obtained from the static and dynamic analysis, the bending moment and von Mises stress at the sag bend, hog bend and riser touchdown area are critical, and the combined stresses are the limiting design criteria.

The maximum stress and the maximum stress utilization factor along the riser were both observed at 180-degree wave direction with respect to the vessel, which is giving the

maximum downward riser motion. With this LWR configuration for the worst sea states and the three water depths analyzed, maximum LRFD utilization values of 23%, 21%, and 13% were observed. These values are considered low when located in the sag bend area. In the extreme weather conditions, the maximum von Mises stresses values of 183.3 MPa, 186.3 MPa, and 150.4 MPa were observed at this location, which is below the allowable limit, and therefore the configurations are considered safe.

In the extreme response analysis study, negative minimum tension values were identified at the sag bend area, the maximum values of the compression forces for design is 94kN, 91kN, and 83kN, respectively. The compressive force due to the vessel movement was handled well due to the presence of the arch shape in the lazy wave riser, which supports the compressive force. Also, a further refinement of the riser will help reduce the compression force at the sag bend area.

References

- Achenbach, E. & Heinecke, E. (1981). On vortex shedding from smooth and rough cylinders in the range of Reynolds numbers 6×10^3 to 5×10^6 . *Journal of fluid mechanics*, 109, 239-251.
- Angelakis, A. N.; Mays, L. W.; Koutsoyiannis, D & Mamassis, N. (2012). *Evolution of Water Supply Through the Millennia*. Iwa Publishing (published January 1, 2012). pp. 202–203. ISBN 978-1843395409
- API 1998. Design of Risers for Floating Production Systems (FPSs) and Tension-Leg Platforms (TLPs). *Recommended Practice, API-RP-2RD*. American Petroleum Institute.
- Bai, Y. & Bai, Q. (2005). *Subsea pipelines and risers*. , Amsterdam ; Oxford: Elsevier.
- Balmoral. 2014. Distributed Buoyancy Modules [Online]. Balmoral Offshore Engineering. Available: <http://www.balmoral-offshore-engineering/2-surf-distributed-buoyancy.php> [Accessed 06 June 2014].
- Case, J., Chilver, A & Ross, C. T. (1999). *Strength of materials and structures*. 4th ed. Arnold Publisher; 1999
- Carter, B. & Ronalds, B. (1998). *Deepwater riser technology*. Paper presented at the SPE Asia Pacific Oil and Gas Conference and Exhibition.
- Dikdogmus, H. (2012). *Riser Concepts for Deep Waters*. Master thesis. Institutt for Marin Teknikk, Trondheim, Norway.
- DNV-OS-F201 (2010a). *Offshore Standard Dynamic Risers*. Det Norske Veritas, Høvik, Oslo.
- DNV. (2010b). *DNV-RP-C205: Environmental Conditions and Environmental Loads*. Norway: Det Norske Veritas, Høvik, Oslo.
- DNV-OSS-302 (2010c). *Offshore service specification: offshore riser systems*. Norway: Det Norske Veritas, Høvik, Oslo.
- Felisita, A. 2017. *On the Application of Steel Lazy Wave Riser for Deepwater Locations with Harsh Environments*. Philosophiae Doctor thesis, Faculty of Science and Technology, University of Stavanger.
- Felisita, A., Gudmestad, O. T., Karunakaran, D. & Martinsen, L. O. (2017). Review of steel lazy wave riser concepts for the north Sea. *Journal of Offshore Mechanics and Arctic Engineering*, 139(1), 011702.
- Gardner, G. (2017). *Managing the Threat of Flexible Riser Outer Sheath Damage*. Web Site, Retrieved from <https://2h offshore.com/blog/flexible-riser-outer-sheath-damage/>
- Genesis. (2019). Riser Analysis. Web Site, Retrieved from <http://www.genesisoilandgas.com/Services/Specialist-Technical-Services/Advanced-Mechanical-and-Subsea-Design/Riser-Analysis/>
- Grealish, F., Kavanagh, K., Connaire, A. & Batty, P. (2007). *Advanced nonlinear analysis methodologies for SCRs*. Paper presented at the Offshore Technology Conference, Paper OTC-18922.
- Green, K. P. & Jackson, T. (2015). Pipelines are the safest way to transport oil and gas. *The National Post*. <https://www.fraserinstitute.org/article/pipelines-are-safest-way-transport-oil-and-gas>
- Gudmestad, O. (2015). *Marine technology and operations: theory & practice*. WIT Press.
- Han, C. J. & Yan, T. (2010). The Study on Vibration of Marine Riser under Deep Water. *Advanced Materials Research*, 97-101, 2816-2819. doi:10.4028/www.scientific.net/AMR.97-101.2816
- Hariharan, M. & Thethi, R. (2007). *Drilling Riser Management In Deepwater Environments*. Paper presented at the The 7th International Oil & Gas Conference and Exhibition, New Delhi, India.
- Huang, S., & Hatton, S. (1996). Rigid bottom weighted large diameter risers -concept, analysis and design. *Technologies for Deep Hostile Seas*. Aberdeen. United Kingdom
- Haver, S., 2007. A Discussion of Long Term response versus Mean Maximum Response of the Selected Design Sea State, Paper No: OMAE2007-29552. Proceedings of the 26 th international Conference on offshore Mechanics and Arctic Engineering (OMAE). ASME, San Diego, California, USA.
- Hoffman, J., Yun, H., Modi, A. & Pearce, R. (2010). Parque das Conchas Pipeline, Flowline and Riser System Design, Installation and Challenges. Paper presented at the Offshore Technology Conference, Paper OTC-20650-MS

- Hopkins, P. (2015). *Recent Lazy Wave Riser Experience*. Paper presented at the Offshore Pipeline Technology Conference.
- Howells, H. & Hatton, S. A. (1997). *Challenges for Ultra-Deep Water Riser Systems*. Floating Production Systems. IIR, London.
- Ismail, N., Nielsen, R. & Kanarellis, M. (1992). *Design Considerations for Selection of Flexible Riser Configuration*. Paper presented at the Energy-Sources Technology Conference and Exhibition.
- Journee, J. M. J. & Massie, W. W. (2001). *Offshore Hydrodynamics* (1st ed.). Delft, Netherland: Delft University of Technology.
- Kalman, M., Yu, L., Durr, C. & Suarez, J. (2014). *Qualification of Unbonded Flexible Pipe to API and DNV Standards*. Paper presented at the Offshore Technology Conference, Paper OTC-25092-MS.
- Karunakaran, D. & Frønsdal, M. (2016). *Steel Lazy Wave Riser with Tether for FPSO with Disconnectable Turret for Iceberg Conditions*. Paper presented at the Arctic Technology Conference, St Johns, Newfoundland, Canada, Paper OTC-27390-MS.
- Karunakaran, D., Meling, T. S., Kristoffersen, S. & Lund, K. M. (2005). *Weight-Optimized SCRs for Deepwater Harsh Environments*. Paper presented at the Offshore Technology Conference, Paper OTC-17224-MS.
- Karunakaran, D., Nordsve, N. T. & Olufsen, A. (1996). *An efficient metal riser configuration for ship and semi based production systems*. Paper presented at the The Sixth International Offshore and Polar Engineering Conference, Proceedings Vol 2, pp.156-162.
- Kenny, J. P. (1993). Structural analysis of pipeline spans. *HSE Books, OTI, 93*, 613.
- Knapstad, B. (2017). *Optimisation of Steel Lazy Wave Risers*. (Master Thesis), University of Stavanger, Norway.
- Legras, J.-L., Karunakaran, D. N. & Jones, R. L. (2013). *Fatigue enhancement of scr: Design applying weight distribution and optimized fabrication*. Paper presented at the Offshore Technology conference, Paper OTC-23945-MS.
- Li, S. (2014). *Response Analysis of the Deepwater Steel Lazy-wave Riser for the Turret Moored Floating Production Storage Off-loading System*. (Master Thesis) Florida Institute of Technology, Melbourne, Florida
- Luppi, A., Cousin, G. & O'Sullivan, R. (2014). *Deepwater Hybrid Riser Systems*. Paper presented at the Offshore Technology Conference-Asia. OTC-24802-MS.
- Miller, C. A. (2017). Risers Introduction. *Encyclopedia of Maritime and Offshore Engineering*, 1-11. John Wiley & Sons, Ltd.
- Nakhaee, A. (2010). *Study of the fatigue life of steel catenary risers in interaction with the seabed* (Vol. 72). PhD Thesis, Texas A&M University.
<http://oaktrust.library.tamu.edu/bitstream/handle/1969.1/ETD-TAMU-2010-12-9016/NAKHAEE DISSERTATION.pdf>
- NORSOK STANDARD. (2007). N-003: Action and Action Effects. Norway: Standards Norway.
- NORSOK STANDARD. (2016). N-003: Action and Action Effects. Norway: Standards Norway.
- Oil States Industries. (2019). Retrieved from <https://oilstates.com/production-platform-systems/semi-submersibles/riser-receptacles-pull-in-equipment/>
- OrcaFlexManual. (2012). <http://www.orcina.com/SoftwareProducts/OrcaFlex/Documentation>
- Orimolade, A. P., Karunakaran, D., & Meling, T.S. (2015). Steel lazy wave risers from turret moored FPSO for deepwater harsh environment. ASME 2015 34th International Conference on Ocean, Offshore and Arctic Engineering, American Society of Mechanical Engineers. OMAE2015-41004.
- Pangaea Drilling. (2019). Composite Tubular Experience. <http://pangaeadrillingtech.com/composite-drilling-risers>
- Petromin (2012). An Innovative Flexible Riser Solution for Large Diameter, Ultra-deepwater Asian Fields. Technology. Petromin Pipeliner
- Shell. (2018). Retrieved from <https://www.shell.com/about-us/major-projects/vito.html>
- Song, R. & Stanton, P. (2007). Deepwater Tieback SCR: Unique Design Challenges and Solutions. Offshore Technology Conference. Houston, Texas.

- Sparks, C. P., Cabillic, J. P. & Schawann, J.-C. (1983). Longitudinal resonant behavior of very deep water risers. *Journal of Energy Resources Technology*, 105(3), 282-289.
- Sparks, C. P. (2007). Fundamentals of marine riser mechanics: basic principles and simplified analyses, PennWell, Tulsa, Okla.
- Sumer, B. M. & Fredsøe, J. (2006). *Hydrodynamics around cylindrical structures* (Vol. 26): World scientific.
- Taggart, S. & Tognarelli, M. A. (2008). *Offshore Drilling Riser VIV Suppression Devices: What's Available to Operators?* Paper presented at the ASME 2008 27th International Conference on Offshore Mechanics and Arctic Engineering, Paper No. OMAE2008-57047, pp. 527-537;
- Taheri, A. & Siahtiri, R. (2017). Effect of Riser-Seabed Interaction on the Dynamic Behavior of Risers. *Journal of Oil, Gas and Petrochemical Technology*, 4, 40-54.
- Tenaris. (2019). *Hybrid Risers Systems*. Web Site, Retrieved from <http://www.tenaris.com/en/Products/OffshoreLinePipe/Risers/HybridRisersSystems.aspx>
- Vikestad, K. (1998). *Multi-frequency response of a cylinder subjected to vortex shedding and support motions*: Book, Norwegian University of Science and Technology Trondheim, ISBN 8247102358
- Xie, J. (2008): *Weight-optimised Steel Catenary Risers and their Applications in harsh Deepwater Environment*. Ph.D. thesis, Department of Naval Architecture and Marine Engineering, Universities of Glasgow and Strathclyde.

Appendix A: Wall Thickness Calculation

DNV-OS-F101 version
 DNV-OS-F101 2007 Code check are done according to the 2007 version of DNV-OS-F101.

Kilometer Post
 Start End

Material Input
 SMYS [MPa]
 SMTS [MPa]
 f_y temp [MPa]
 f_u temp [MPa]
 Young's modulus [GPa]
 Poisson's ratio [-]
 Anisotropy factor [-]
 Hardening factor [-]
 Fabrication factor [-]
 Suppl. req. U fulfilled

Load Input

	Pressure [barg]	@ level [m]	Content mass density [kg/m ³]
Design	<input type="text" value="344"/>	<input type="text" value="-2000"/>	<input type="text" value="800"/>
System test	<input type="text" value="397"/>	<input type="text" value="-2000"/>	<input type="text" value="1025"/>
Incidental to design pressure ratio [-] <input type="text" value="1.1"/>			
Water depth [m] <input type="text" value="2000"/>		and mass density [kg/m ³] <input type="text" value="1025"/>	
	Functional	Environmental	
Moment [kNm]	<input type="text" value="100"/>	<input type="text" value="80"/>	
Axial force [kN]	<input type="text" value="50"/>	<input type="text" value="20"/>	
Strain [%]	<input type="text" value="0.43"/>	<input type="text" value="0"/>	
Load condition factor [-] <input type="text" value="0.85"/>			

Geometry Input
 Steel diameter [mm]
 Steel thickness [mm] D/t = 11.8
 Fabrication tolerance [%]
 Corrosion allowance [mm]
 Ovality [%]
 Girth weld factor [-]

Design Input

Failure mode	Condition	Safety class	Corr.	Der.	Calc.	t _{req} [mm]	Utilisation [-]	Utilisation [-]
Burst	Operation	<input type="text" value="High"/>	<input checked="" type="checkbox"/>	<input checked="" type="checkbox"/>	<input checked="" type="checkbox"/>	<input type="text" value="7.51"/>	<input type="text" value="0.311"/>	<input type="text" value="0.311"/>
Burst	System test	System test	<input checked="" type="checkbox"/>	<input checked="" type="checkbox"/>	<input checked="" type="checkbox"/>	<input type="text" value="6.61"/>	<input type="text" value="0.275"/>	<input type="text" value="0.275"/>
Collapse	<input type="text" value="Empty"/>	<input type="text" value="High"/>	<input checked="" type="checkbox"/>	<input checked="" type="checkbox"/>	<input checked="" type="checkbox"/>	<input type="text" value="18.35"/>	<input type="text" value="0.642"/>	<input type="text" value="0.642"/>
Propagating buckling	<input type="text" value="Empty"/>	<input type="text" value="High"/>	<input checked="" type="checkbox"/>	<input checked="" type="checkbox"/>	<input checked="" type="checkbox"/>	<input type="text" value="26.49"/>	<input type="text" value="1.039"/>	<input type="text" value="1.039"/>
Load comb., LCC, lc = a					<input checked="" type="checkbox"/>	<input type="text" value="7.85"/>	<input type="text" value="0.061"/>	<input type="text" value="0.061"/>
Load comb., LCC, lc = b					<input checked="" type="checkbox"/>	<input type="text" value="9.22"/>	<input type="text" value="0.091"/>	<input type="text" value="0.091"/>
Load comb., DCC, lc = a					<input type="checkbox"/>	<input type="text" value="3.01"/>	<input type="text" value="0.101"/>	<input type="text" value="0.101"/>
Load comb., DCC, lc = b					<input type="checkbox"/>	<input type="text" value="2.97"/>	<input type="text" value="0.092"/>	<input type="text" value="0.092"/>

Figure A.1: Wall Thickness Calculation for LWR (2000m WD)

DNV-OS-F101 version
 DNV-OS-F101 2007 Code check are done according to the 2007 version of DNV-OS-F101.

Kilometer Post
 Start End

Material Input
 SMYS [MPa]
 SMTS [MPa]
 f_y temp [MPa]
 f_u temp [MPa]
 Young's modulus [GPa]
 Poisson's ratio [-]
 Anisotropy factor [-]
 Hardening factor [-]
 Fabrication factor [-]
 Suppl. req. U fulfilled

Load Input

	Pressure [barg]	@ level [m]	Content mass density [kg/m ³]
Design	<input type="text" value="344"/>	<input type="text" value="-1500"/>	<input type="text" value="800"/>
System test	<input type="text" value="397"/>	<input type="text" value="-1500"/>	<input type="text" value="1025"/>
Incidental to design pressure ratio [-] <input type="text" value="1.1"/>			
Water depth [m] <input type="text" value="1500.0"/> and mass density [kg/m ³] <input type="text" value="1025"/>			
	Functional		Environmental
Moment [kNm]	<input type="text" value="100"/>	<input type="text" value="80"/>	
Axial force [kN]	<input type="text" value="50"/>	<input type="text" value="20"/>	
Strain [%]	<input type="text" value="0.43"/>	<input type="text" value="0"/>	
Load condition factor [-]	<input type="text" value="0.85"/>		

Geometry Input
 Steel diameter [mm]
 Steel thickness [mm] D/t = 11.8
 Fabrication tolerance [%]
 Corrosion allowance [mm]
 Ovality [%]
 Girth weld factor [-]

Design Input

Failure mode	Condition	Safety class	Corr.	Der.	Calc. t _{req} [mm]	Utilisation [-]	Utilisation [-]
Burst	Operation	<input type="text" value="High"/>	<input checked="" type="checkbox"/>	<input checked="" type="checkbox"/>	<input type="text" value="9.73"/>	<input type="text" value="0.400"/>	<div style="width: 40%;"></div>
Burst	System test	System test	<input checked="" type="checkbox"/>	<input checked="" type="checkbox"/>	<input type="text" value="8.37"/>	<input type="text" value="0.346"/>	<div style="width: 34.6%;"></div>
Collapse	<input type="text" value="Empty"/>	<input type="text" value="High"/>	<input checked="" type="checkbox"/>	<input checked="" type="checkbox"/>	<input type="text" value="15.25"/>	<input type="text" value="0.482"/>	<div style="width: 48.2%;"></div>
Propagating buckling	<input type="text" value="Empty"/>	<input type="text" value="High"/>	<input checked="" type="checkbox"/>	<input checked="" type="checkbox"/>	<input type="text" value="23.08"/>	<input type="text" value="0.779"/>	<div style="width: 77.9%;"></div>
Load comb., LCC, lc = a					<input checked="" type="checkbox"/>	<input type="text" value="8.36"/>	<input type="text" value="0.066"/>
Load comb., LCC, lc = b					<input checked="" type="checkbox"/>	<input type="text" value="9.47"/>	<input type="text" value="0.096"/>
Load comb., DCC, lc = a	<input type="text" value="System test"/>	<input type="text" value="High"/>	<input type="checkbox"/>	<input type="checkbox"/>	<input checked="" type="checkbox"/>	<input type="text" value="2.93"/>	<input type="text" value="0.088"/>
Load comb., DCC, lc = b					<input checked="" type="checkbox"/>	<input type="text" value="2.89"/>	<input type="text" value="0.081"/>

Figure A.2: Wall Thickness Calculation for LWR (1500m WD)

DNV-OS-F101 version
 DNV-OS-F101 2007 Code check are done according to the 2007 version of DNV-OS-F101.

Kilometer Post
 Start End

Material Input
 SMYS [MPa]
 SMTS [MPa]
 f_y temp [MPa]
 f_u temp [MPa]
 Young's modulus [GPa]
 Poisson's ratio [-]
 Anisotropy factor [-]
 Hardening factor [-]
 Fabrication factor [-]
 Suppl. req. U fulfilled

Load Input

	Pressure [barg]	@ level [m]	Content mass density [kg/m ³]
Design	<input type="text" value="344"/>	<input type="text" value="-1000"/>	<input type="text" value="800"/>
System test	<input type="text" value="397"/>	<input type="text" value="-1000"/>	<input type="text" value="1025"/>
Incidental to design pressure ratio [-]	<input type="text" value="1.1"/>		
Water depth [m]	<input type="text" value="1000"/>	and mass density [kg/m ³]	<input type="text" value="1025"/>
	Functional	Environmental	
Moment [kNm]	<input type="text" value="100"/>	<input type="text" value="80"/>	
Axial force [kN]	<input type="text" value="50"/>	<input type="text" value="20"/>	
Strain [%]	<input type="text" value="0.43"/>	<input type="text" value="0"/>	
Load condition factor [-]	<input type="text" value="0.85"/>		

Geometry Input
 Steel diameter [mm]
 Steel thickness [mm] D/t = 11.8
 Fabrication tolerance [%]
 Corrosion allowance [mm]
 Ovality [%]
 Girth weld factor [-]

Design Input

Failure mode	Condition	Safety class	Corr.	Der.	Calc.	t _{req} [mm]	Utilisation [-]	Utilisation [-]
Burst	Operation	<input type="text" value="High"/>	<input checked="" type="checkbox"/>	<input checked="" type="checkbox"/>	<input checked="" type="checkbox"/>	<input type="text" value="12.00"/>	<input type="text" value="0.488"/>	<div style="width: 48.8%;"></div>
Burst	System test	System test	<input checked="" type="checkbox"/>	<input checked="" type="checkbox"/>	<input checked="" type="checkbox"/>	<input type="text" value="10.16"/>	<input type="text" value="0.416"/>	<div style="width: 41.6%;"></div>
Collapse	<input type="text" value="Empty"/>	<input type="text" value="High"/>	<input checked="" type="checkbox"/>	<input checked="" type="checkbox"/>	<input checked="" type="checkbox"/>	<input type="text" value="12.22"/>	<input type="text" value="0.321"/>	<div style="width: 32.1%;"></div>
Propagating buckling	<input type="text" value="Empty"/>	<input type="text" value="High"/>	<input checked="" type="checkbox"/>	<input checked="" type="checkbox"/>	<input checked="" type="checkbox"/>	<input type="text" value="19.11"/>	<input type="text" value="0.519"/>	<div style="width: 51.9%;"></div>
Load comb., LCC, lc = a					<input checked="" type="checkbox"/>	<input type="text" value="9.11"/>	<input type="text" value="0.073"/>	<div style="width: 7.3%;"></div>
Load comb., LCC, lc = b					<input checked="" type="checkbox"/>	<input type="text" value="10.04"/>	<input type="text" value="0.102"/>	<div style="width: 10.2%;"></div>
Load comb., DCC, lc = a	<input type="text" value="System tes"/>	<input type="text" value="High"/>	<input type="checkbox"/>	<input type="checkbox"/>	<input checked="" type="checkbox"/>	<input type="text" value="2.87"/>	<input type="text" value="0.079"/>	<div style="width: 7.9%;"></div>
Load comb., DCC, lc = b					<input checked="" type="checkbox"/>	<input type="text" value="2.84"/>	<input type="text" value="0.072"/>	<div style="width: 7.2%;"></div>

Reports

Information

Figure A.3: Wall Thickness Calculation for LWR (1000m WD)

Appendix B: Sensitivity Studies for Steel Catenary Riser- OrcaFlex Example

B.1 Introduction

Before the Lazy Wave Riser (LWR) study reported in this thesis, an OrcaFlex steel catenary riser (SCR) study was carried out. This study attempted to identify the different trends in the design when the design basis changes and will be reported here as background for our analysis of the lazy wave risers back.

The analysis studies are done on different configurations, which includes different water depths and physical conditions. Changing the water depth correspondingly increases the von Mises Stress and Bending moment. Therefore the task will focus on these parameters and how each parameter affects the performance of the riser. OrcaFlex is the program used for this analytical process.

The factors affecting the performance of the riser system includes:

1. Component properties of the riser system
2. Adjoining facilities behavior (Example: Floating semisubmersible platform with properties as the default semisubmersible as given in the Orca flex software)
3. Environmental conditions in the deployment area

The above factors form the input parameters for a riser design and analysis operation. Therefore, precise prior knowledge of these parameters is essential when conducting system analysis.

B.2 Riser Material Properties for SCR

Table B.1 Riser Properties for SCR

Parameter	Design Value	Unit
Internal diameter	250	mm
Riser Wall Thickness	15	mm
Riser material	Carbon Steel, grade X65	-
Steel Material Density	7850	kg/m ³
Young's modulus E	212000	MPa
Specified Minimum Yield Strength (SMYS)	448.16	MPa
Allowable Stress	437	MPa
Poisson Ratio	0.3	
Design Pressure	34,5	MPa

B.3 Environmental Data

Water Depth

200 m, 350m, and 500 m are the water depth values used in the studies. The sea water density is assumed to be constant throughout at 1025 kg/m³.

Wave data

For this study, the following sea states are considered:

Wave height, H_s 2m, 5m and 10m

Wave peak period, $T_p = 20s$ and $21s$

The Dynamic analysis results with regard to the riser configurations are von Mises Stress and static Bending moments for these varying parameters and how each parameter affects the performance of the SCR riser model.

Table B.2: Dynamic Analysis Results for SCRs

Water depth (m)	Hs (m)	Tp (s)	Max von Mises Stress (MPa)	Max Bending Moment (kN.m)
Case A: 200	2	20	410	180
		21	430	210
	5	20	422	200
		21	580	320
	10	20	446	230
		21	1700	1100
Case B: 350	2	20	415	200
		21	440	230
	5	20	432	220
		21	590	340
	10	20	450	240
		21	1378	805
Case C: 500	2	20	430	230
		21	465	250
	5	20	452	240
		21	610	360
	10	20	480	268
		21	1140	670

Case A WD: 200m

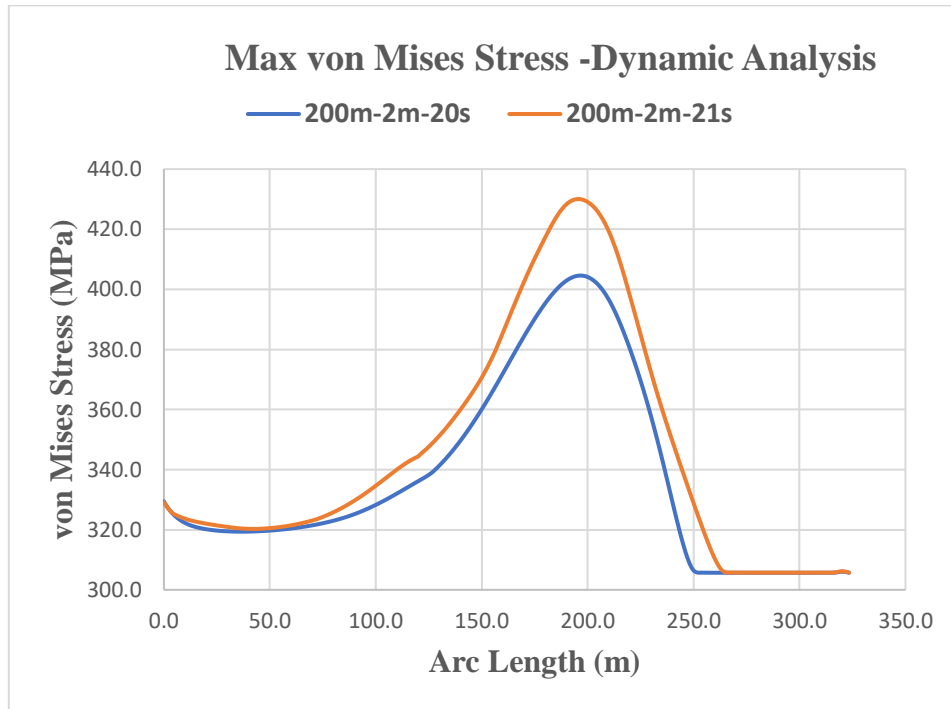


Figure B.1: Max von Mises Stress-Dynamic Analysis (200m-2m-20s / 200m-2m-21s)

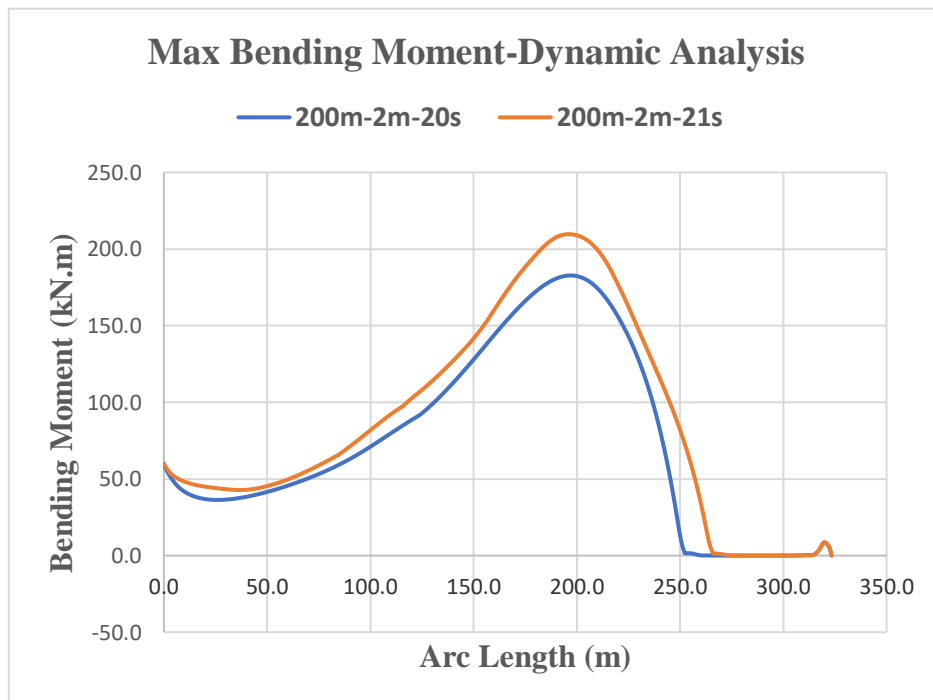


Figure B.2: Max Bending Moment-Dynamic Analysis (200m-2m-20s / 200m-2m-21s)

The von Mises stress in Figure B.1 for wave period 21s is significantly larger than the wave period 20s at a similar water depth of 200 m and a wave height of 2 m. The increase in the von Mises stress can be accounted due to the increase in the wave period. When the wave period increases from 20s to 21s, the response of the semisubmersible is larger due to resonance in heave with waves of 21s period, see chapter 4.3 and were at 200m, the touchdown point, the largest von Misses stress and bending moment is observed.

Following this analysis, we will consider other water depths and wave heights as shown below in Figures B.3 to Figure B.16

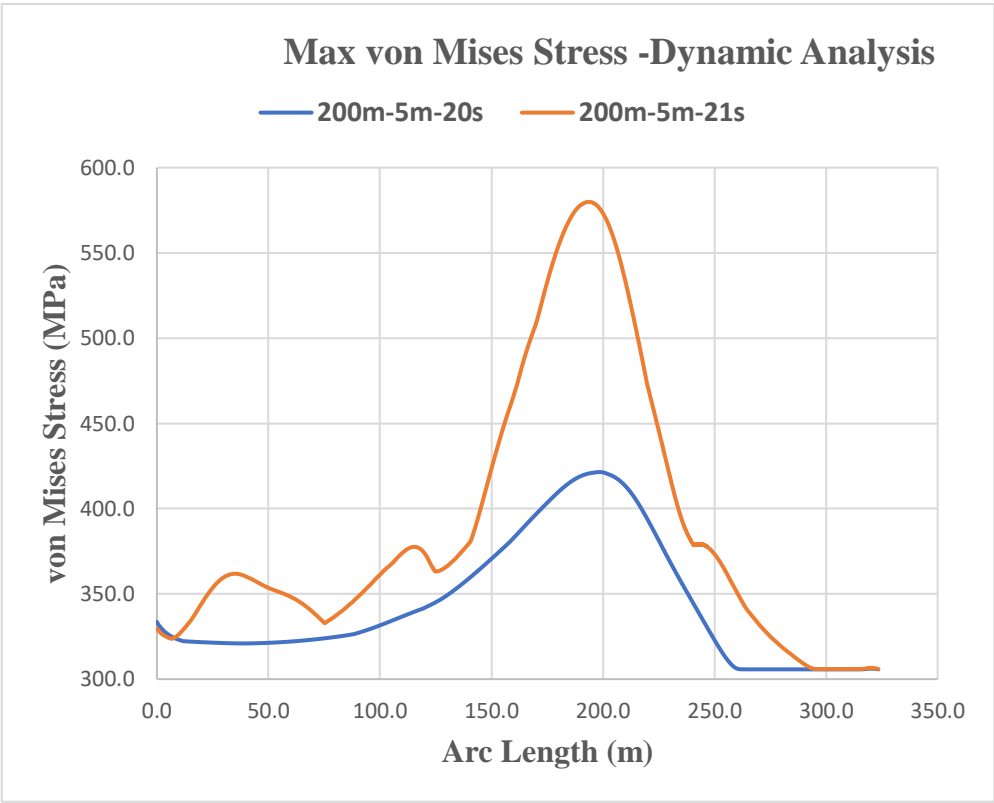


Figure B.3: Max von Mises Stress-Dynamic Analysis (200m-5m-20s / 200m-5m-21s)

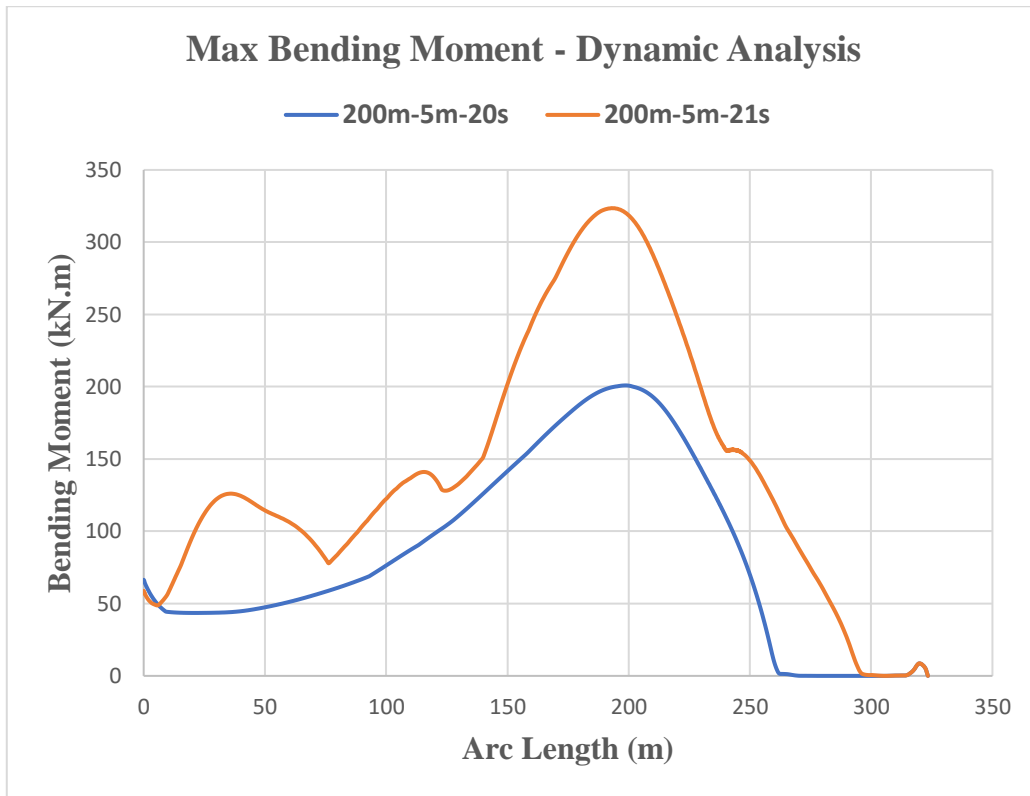


Figure B.4: Max Bending Moment-Dynamic Analysis (200m-5m-20s / 200m-5m-21s)

For waves of 5m height, we find from Figure B.3 that the von Mises stresses and Figure B.4 Bending moments are smooth curves in case of wave periods of 20s. At resonance, when the wave period is 21s, the stresses and Bending moments increase considerably, and the riser behavior is not acceptable, the bending moment even goes beyond zero kN.m, see Figure B.4.

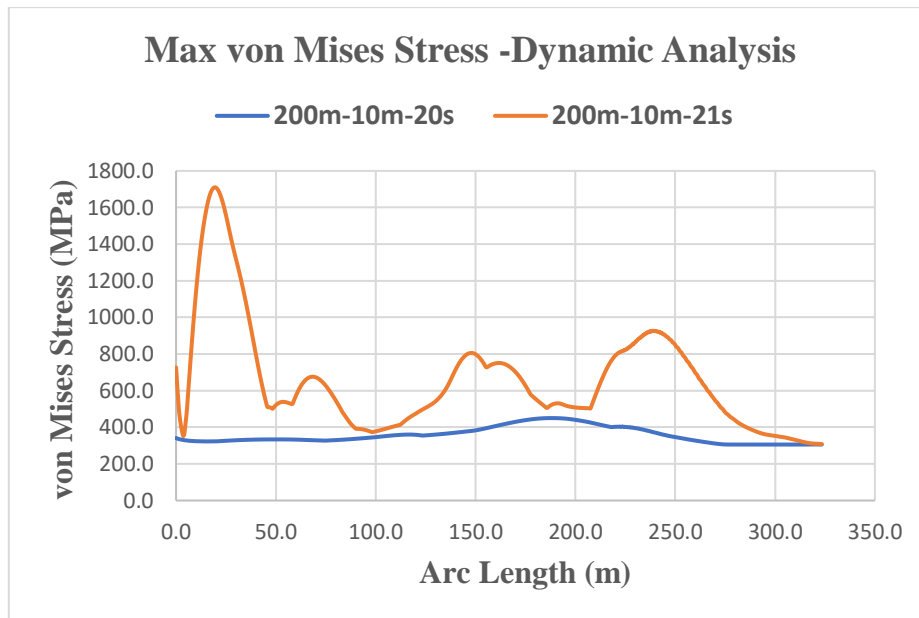


Figure B.5: Max von Mises Stress-Dynamic Analysis (200m-10m-20s / 200m-10m-21s)

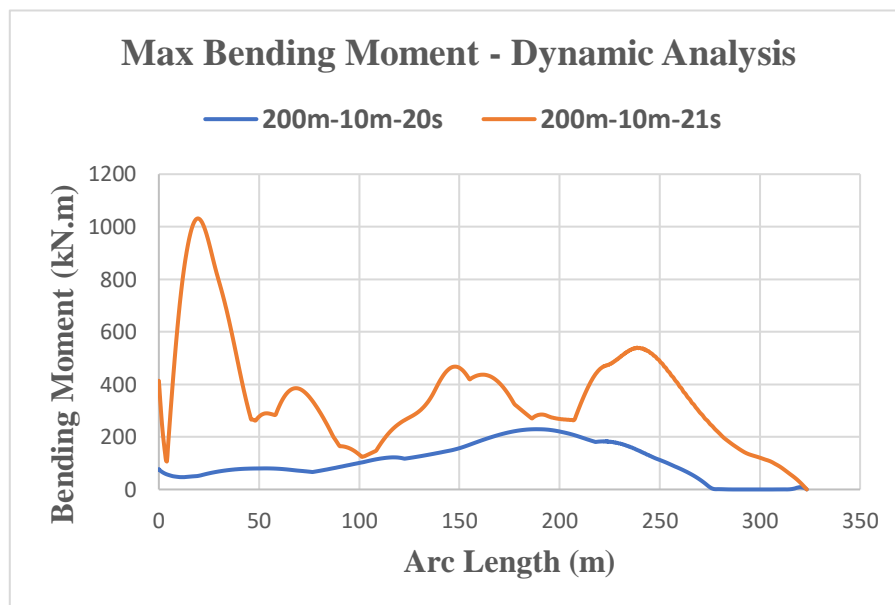


Figure B.6: Max Bending Moment-Dynamic Analysis (200m-10m-20s / 200m-10m-21s)

For waves of 10m height, we find from Figure B.5 that the von Mises stresses and Figure B.6 Bending moments increase considerably, there are sharp changes in the curves, and the riser behavior is not acceptable in case of wave periods of 20s. While Figure B.5 and B.6 is also unstable, when the wave period is 21s (at resonance), as the stresses and Bending moments displays an inconsistent behavior and where at 15m, the topside, the largest von Misses stress and bending moment is observed.

Case B WD: 350m

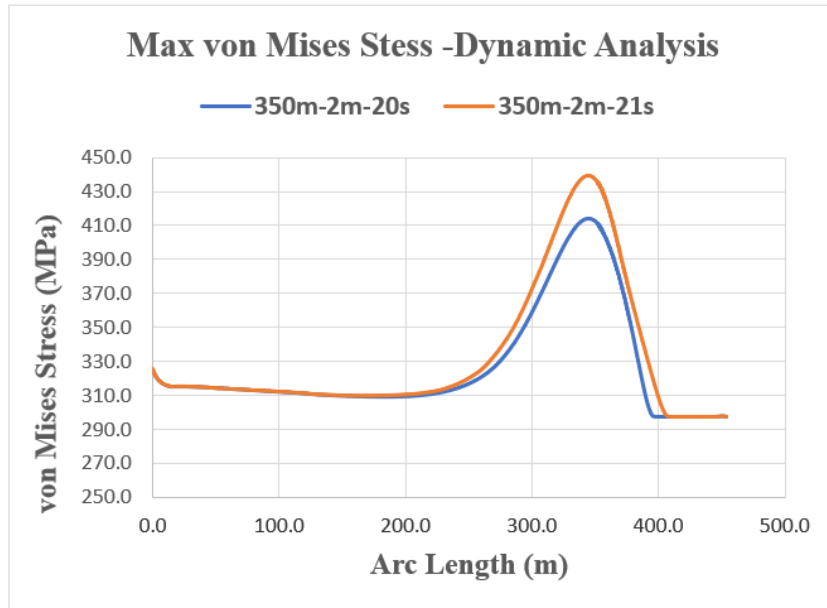


Figure B.7: Max von Mises Stress-Dynamic Analysis (350m-2m-20s / 350m-2m-21s)

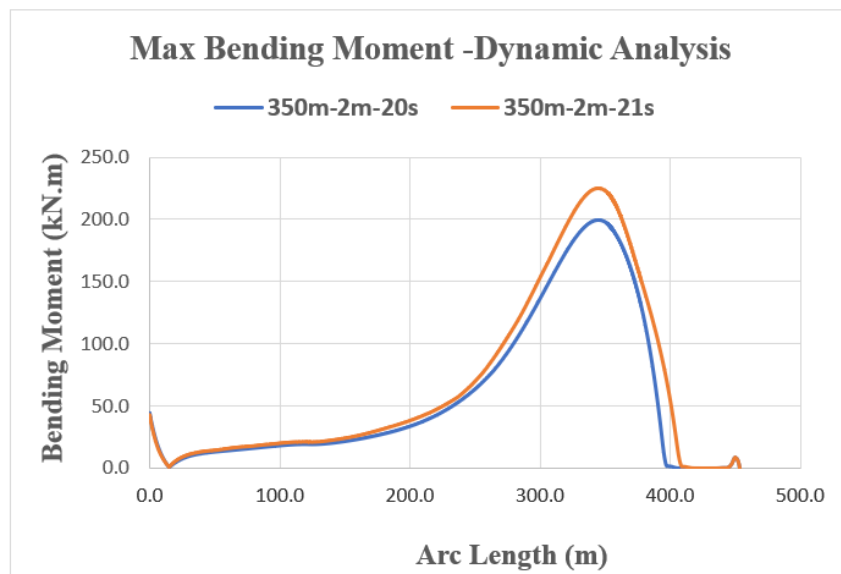


Figure B.8: Bending Moment-Dynamic Analysis (350m-2m-20s / 350m-2m-21s)

A check of whether the allowable stress is exceeded will be presented in Chapter 3.10. Similar to Figure B.1 explanations above, the increase in the von Mises stress can be accounted for due to the increase in the wave period. When the wave period increases from the 20s to 21s, the response of the semisubmersible is larger due to resonance in heave with waves of 21s period, see Chapter 4.3. Where at 340m, the touchdown point, the largest von Mises stress and bending moment is observed.

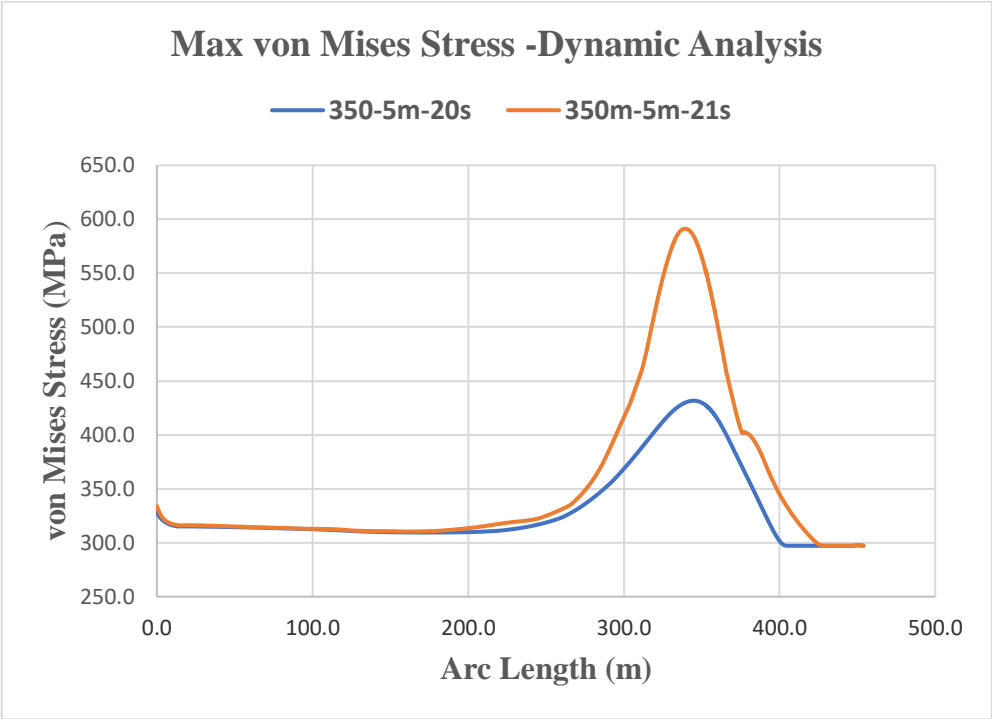


Figure B.9: Max von Mises Stress-Dynamic Analysis (350m-5m-20s / 350m-5m-21s)

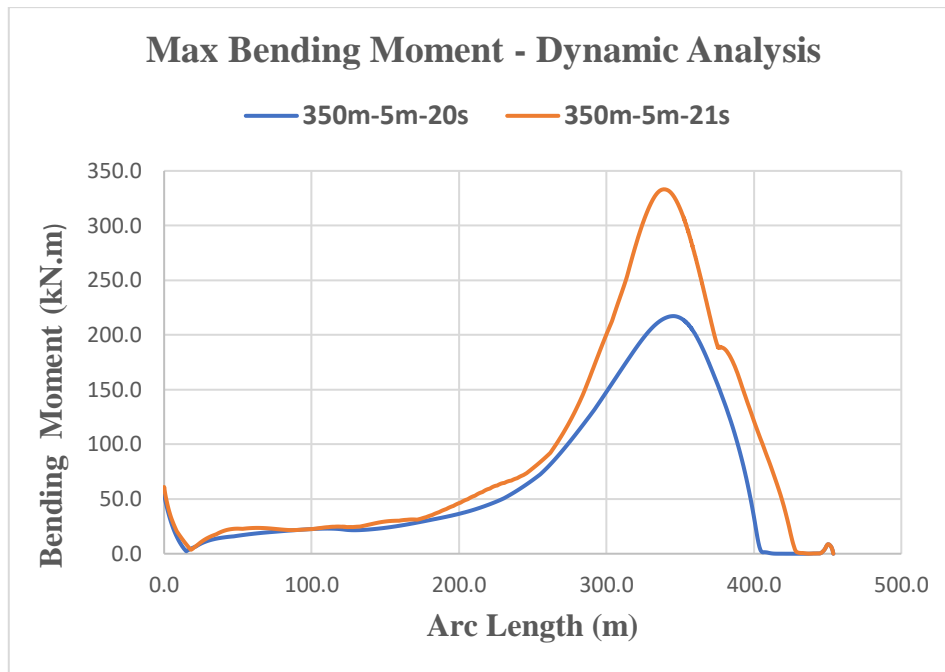


Figure B.10: Bending Moment-Dynamic Analysis (350m-5m-20s / 350m-5m-21s)

For waves of 5m height, we find that the von Mises stresses and Bending moments are smooth curves in case of wave periods of the 20s. At resonance, when the wave period 21s is stresses and Bending moments increase considerably, and the riser behavior is not acceptable, see Figures B.9 and B.10.

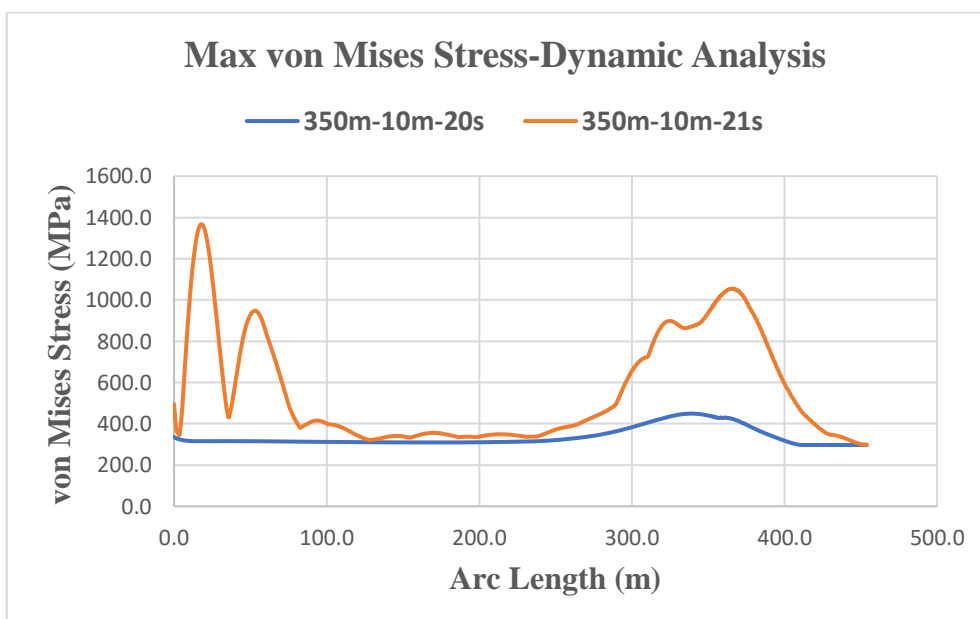


Figure B.11: Max von Mises Stress-Dynamic Analysis (350m-10m-20s / 350m-10m-21s)

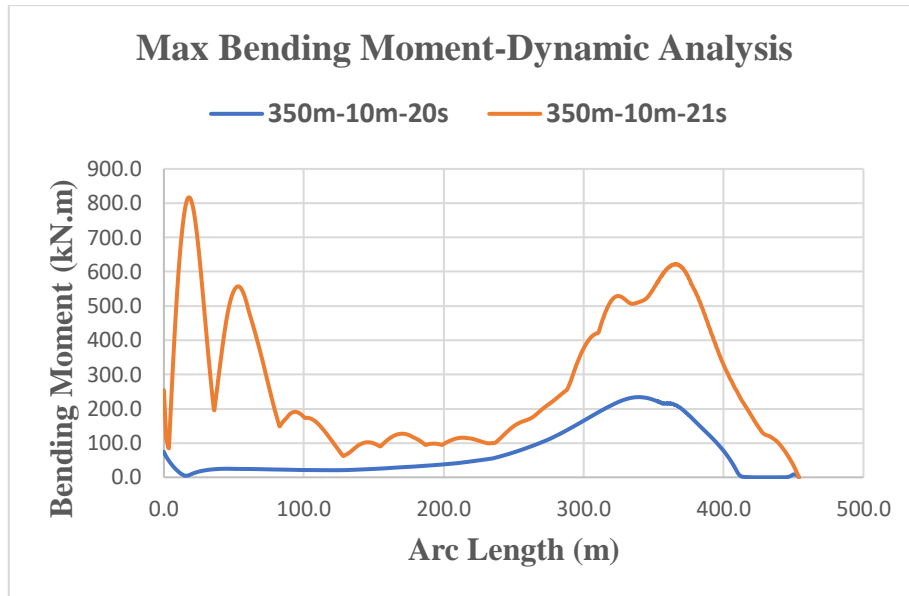


Figure B.12: Max Bending Moment -Dynamic Analysis (350m-10m-20s / 350m-10m-21s)

Similar to Figure B.5 and B.6 explanations above, the increase in the von Mises stress and Bending Moment can be accounted for due to the increase in the wave period. Riser behavior is not acceptable.

Case C WD: 500m

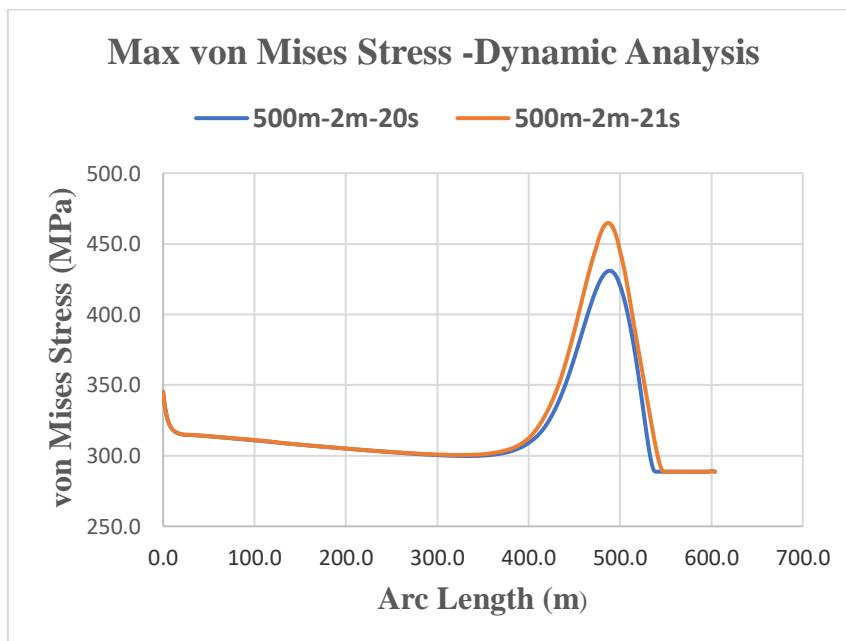


Figure B.13: Max von Mises Stress-Dynamic Analysis (500 m-2m-20s / 500 m-2m-21s)

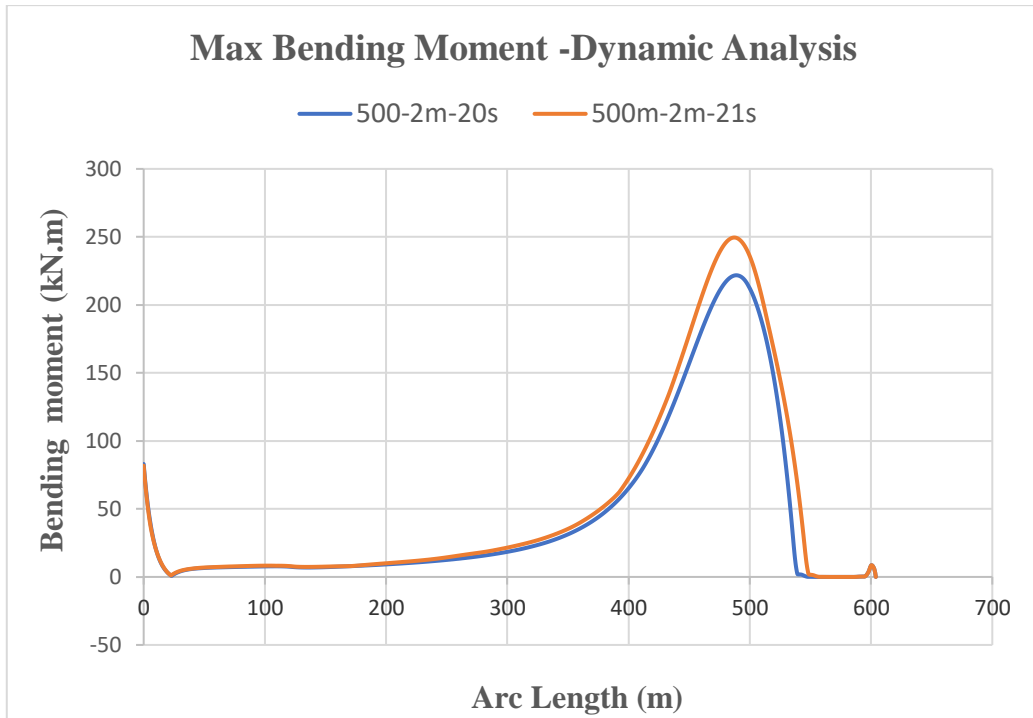


Figure B.14: Max Bending Moment -Dynamic Analysis (500m-2m-20s / 500m-2m-21s)

Similar to Figure B.1 and B.2 explanations above, the increase in the von Mises stress and Bending Moment can be accounted for due to the increase in the wave period. When the wave period increases from the 20 s to 21s, the response of the semisubmersible is larger due to resonance in heave with waves of 21s the period, see chapter 4.3

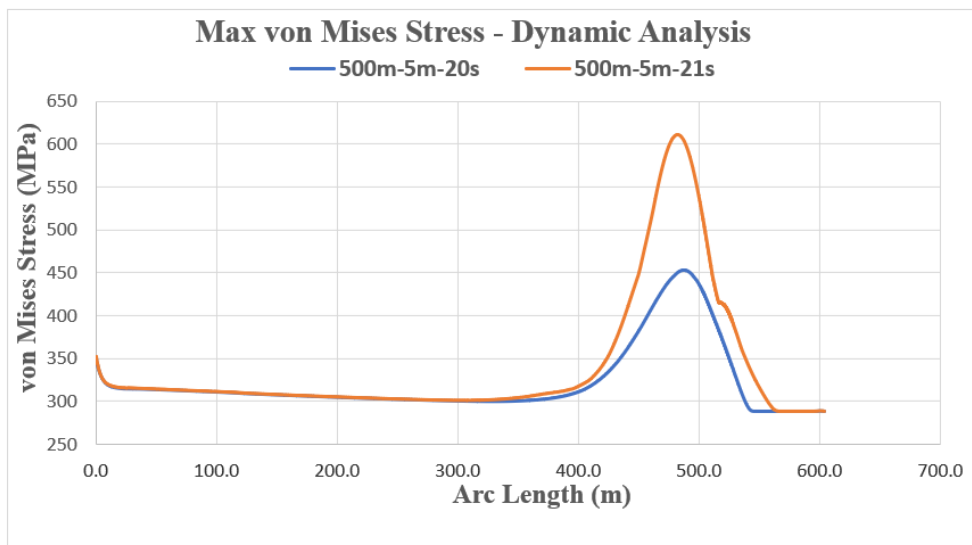


Figure B.15: Max von Mises Stress-Dynamic Analysis (500 m-5m-20s / 500 m-5m-21s)

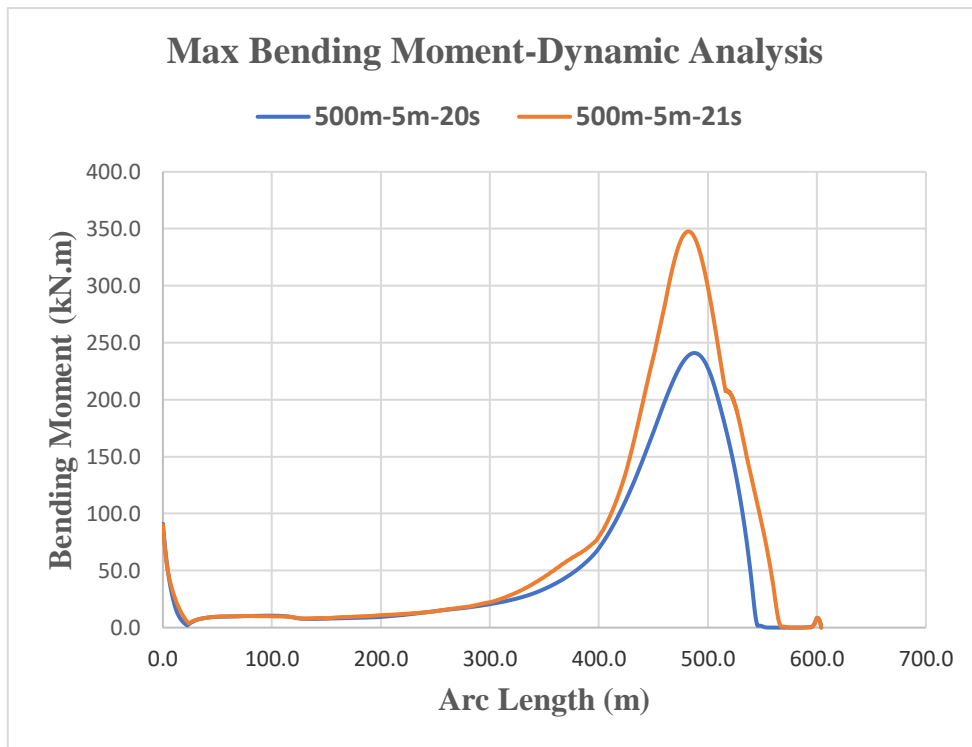


Figure B.16: Max Bending Moment -Dynamic Analysis (500m-2m-20s / 500m-2m-21s)

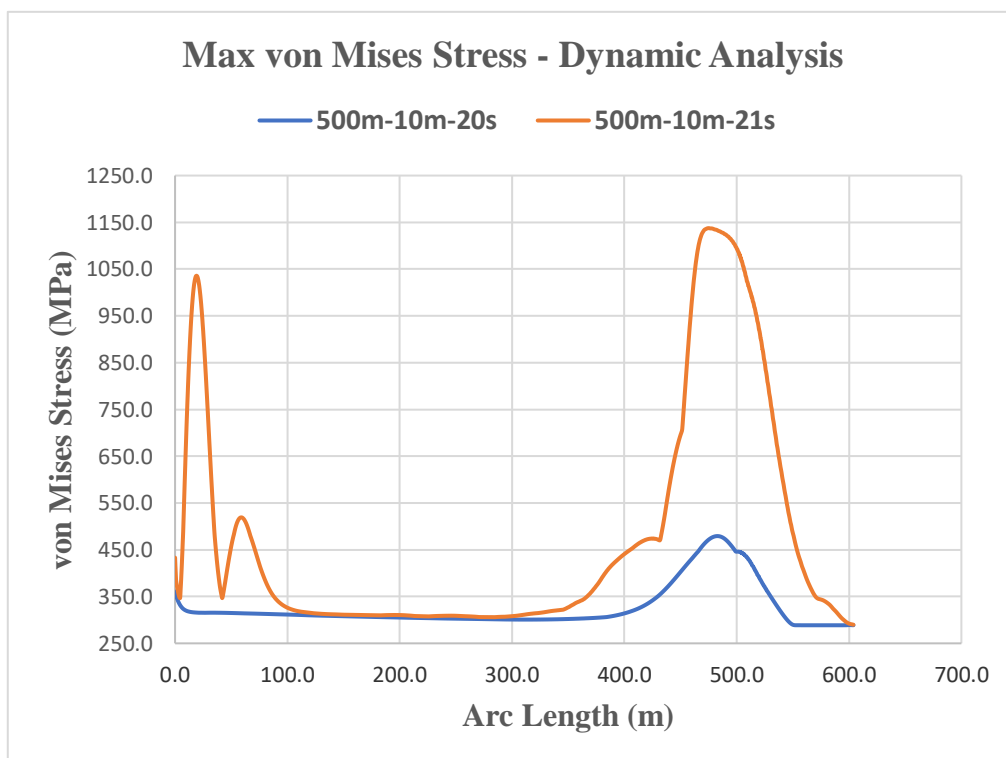


Figure B.17: Max von Mises Stress-Dynamic Analysis (500 m-10m-20s / 500 m-10m-21s)

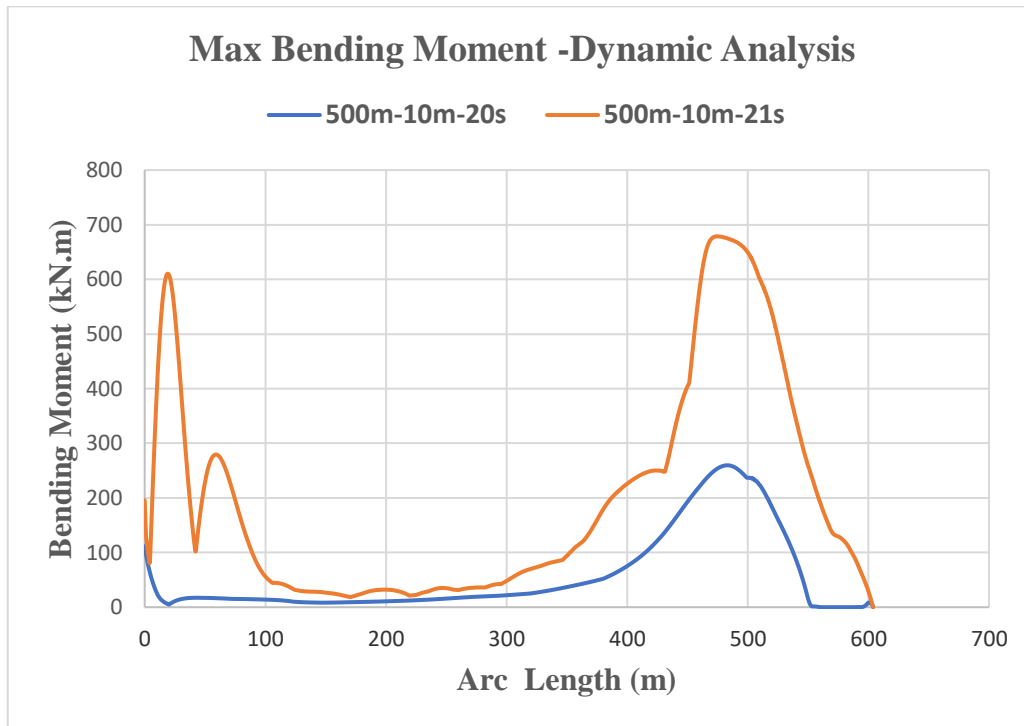


Figure B.18: Max Bending Moment -Dynamic Analysis (500m-10m-20s / 500m-10m-21s)

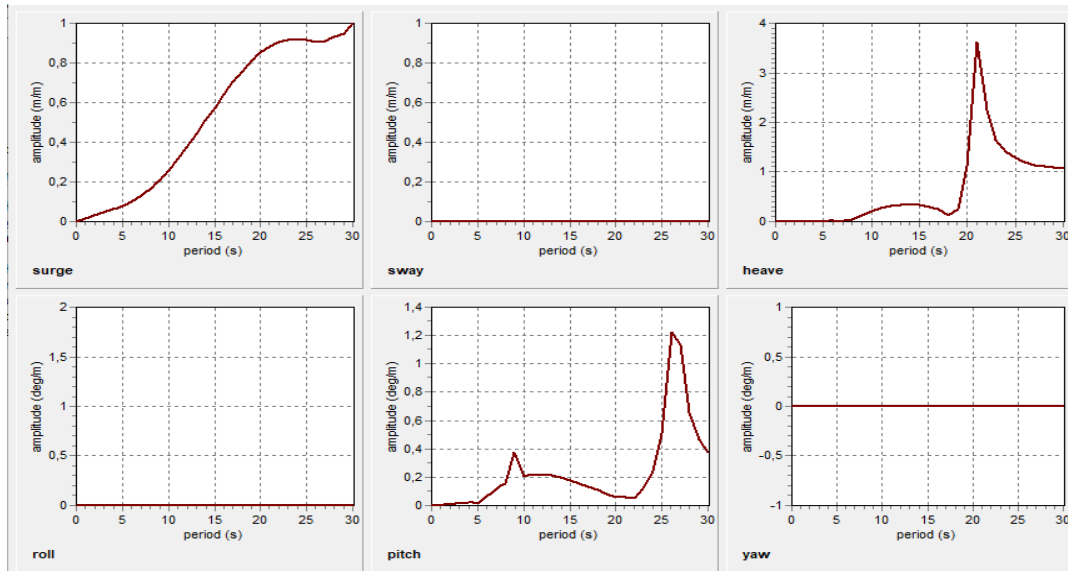
For waves of 10m height, we find from Figure B.17 and B.18 that the von Mises stresses and Bending moments increase considerably and the riser behavior is not acceptable in case of wave periods of 20 s. While the stresses and bending moments in wave period 21 also unstable and stresses and bending moments displays an inconsistent behavior.

B.4 The Response Amplitude Operator, RAO, for a vessel

RAO Data

RAO data are available (OrcaFlex Manual, 2012) for directions of RAO: 0, 45, 90,135,180 degrees. These data are available from one typical semi-submersible data for periods (T) 20 s to 21 s. All these directions are implemented in the parametric study in this thesis.

0 DEGREE



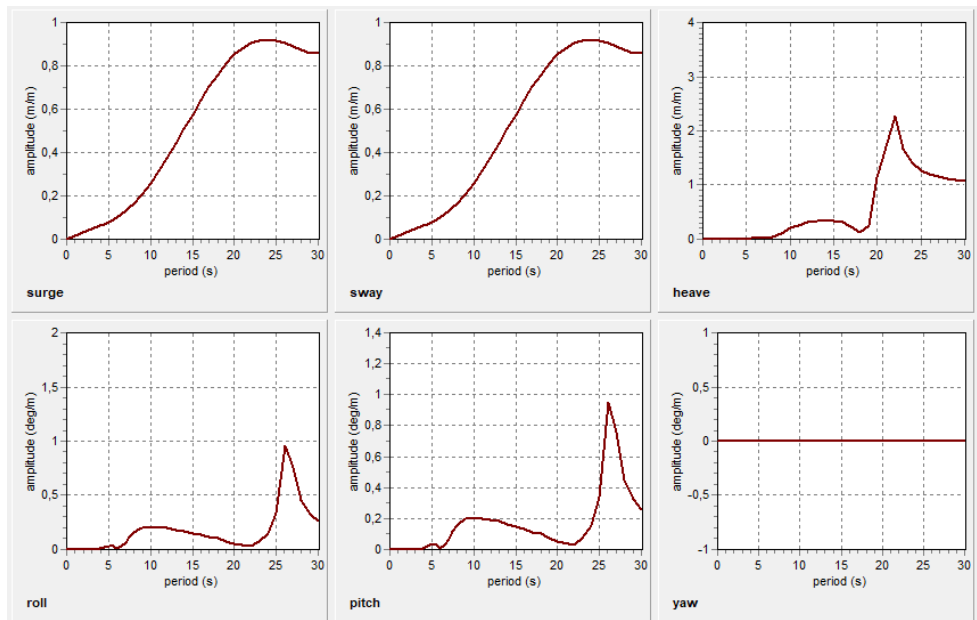
0° 45° 90° 135° 180°

Periods: 33

Period (s)	Surge		Sway		Heave		Roll		Pitch		Yaw	
	Ampl. (m/m)	Phase (deg)	Ampl. (m/m)	Phase (deg)	Ampl. (m/m)	Phase (deg)	Ampl. (deg/m)	Phase (deg)	Ampl. (deg/m)	Phase (deg)	Ampl. (deg/m)	Phase (deg)
0,00	0,000	0,0	0,000	0,0	0,000	0,0	0,000	0,0	0,000	0,0	0,000	0,0
4,00	0,063	267,8	0,000	0,0	0,0060	12,8	0,000	0,0	0,025	-97,2	0,000	0,0
4,50	0,071	246,3	0,000	0,0	0,0010	-8,1	0,000	0,0	0,023	-117,3	0,000	0,0
5,00	0,079	66,5	0,000	0,0	0,0070	164,4	0,000	0,0	0,015	13,2	0,000	0,0
5,50	0,089	71,1	0,000	0,0	0,018	-170,4	0,000	0,0	0,044	69,3	0,000	0,0
6,00	0,100	75,9	0,000	0,0	0,014	-148,6	0,000	0,0	0,065	75,5	0,000	0,0
6,50	0,114	83,9	0,000	0,0	0,010	-156,0	0,000	0,0	0,085	82,8	0,000	0,0
7,00	0,129	90,6	0,000	0,0	0,011	0,81	0,000	0,0	0,116	90,7	0,000	0,0
7,50	0,145	94,1	0,000	0,0	0,025	-18,5	0,000	0,0	0,141	95,5	0,000	0,0
8,00	0,164	92,3	0,000	0,0	0,042	-25,4	0,000	0,0	0,154	101,2	0,000	0,0
9,00	0,207	279,9	0,000	0,0	0,124	-22,2	0,000	0,0	0,377	96,1	0,000	0,0
10,00	0,257	276,1	0,000	0,0	0,213	-12,5	0,000	0,0	0,207	95,9	0,000	0,0
11,00	0,314	274,5	0,000	0,0	0,278	-5,7	0,000	0,0	0,218	91,0	0,000	0,0
12,00	0,376	273,7	0,000	0,0	0,317	-2,2	0,000	0,0	0,216	92,0	0,000	0,0
13,00	0,441	273,3	0,000	0,0	0,337	-0,87	0,000	0,0	0,213	92,0	0,000	0,0
14,00	0,508	273,1	0,000	0,0	0,350	-0,65	0,000	0,0	0,202	88,8	0,000	0,0
15,00	0,575	273,0	0,000	0,0	0,335	-1,2	0,000	0,0	0,176	90,4	0,000	0,0
16,00	0,641	272,9	0,000	0,0	0,304	-2,8	0,000	0,0	0,155	88,7	0,000	0,0
17,00	0,703	272,9	0,000	0,0	0,245	-7,8	0,000	0,0	0,135	87,0	0,000	0,0
18,00	0,760	272,9	0,000	0,0	0,131	-34,3	0,000	0,0	0,108	83,3	0,000	0,0
19,00	0,809	273,0	0,000	0,0	0,253	-133,6	0,000	0,0	0,078	80,0	0,000	0,0
20,00	0,851	273,1	0,000	0,0	1,119	-139,3	0,000	0,0	0,056	58,0	0,000	0,0
21,00	0,883	273,5	0,000	0,0	3,612	-74,2	0,000	0,0	0,061	17,1	0,000	0,0
22,00	0,905	273,3	0,000	0,0	2,258	-20,2	0,000	0,0	0,054	-31,5	0,000	0,0
23,00	0,918	273,6	0,000	0,0	1,648	-9,5	0,000	0,0	0,120	-59,4	0,000	0,0
24,00	0,921	274,2	0,000	0,0	1,405	-5,7	0,000	0,0	0,246	-63,5	0,000	0,0
25,00	0,916	276,3	0,000	0,0	1,279	-3,9	0,000	0,0	0,506	-57,2	0,000	0,0
26,00	0,904	286,6	0,000	0,0	1,199	-3,0	0,000	0,0	1,223	-21,7	0,000	0,0
27,00	0,910	285,2	0,000	0,0	1,147	-2,3	0,000	0,0	1,137	52,1	0,000	0,0
28,00	0,930	276,0	0,000	0,0	1,118	-1,9	0,000	0,0	0,657	75,0	0,000	0,0
29,00	0,950	274,2	0,000	0,0	1,094	-1,6	0,000	0,0	0,466	81,4	0,000	0,0
30,00	1,000	270,0	0,000	0,0	1,078	-1,4	0,000	0,0	0,375	84,7	0,000	0,0
Infinity	1,000	270,0	0,000	0,0	1,000	-1,4	0,000	0,0	0,377	84,9	0,000	0,0

Figure B.19: Vessel RAO, s (Response Amplitude Operators) for 0 Degree.

45 DEGREE



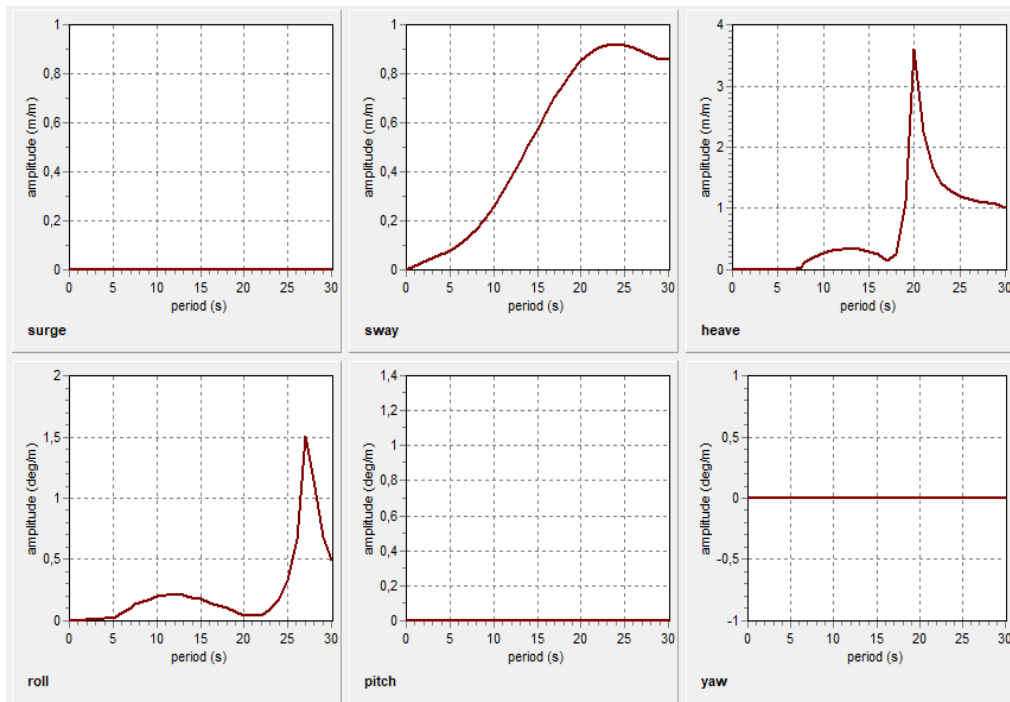
0° 45° 90° 135° 180°

Periods: 33

Period (s)	Surge		Sway		Heave		Roll		Pitch		Yaw	
	Ampl. (m/m)	Phase (deg)	Ampl. (m/m)	Phase (deg)	Ampl. (m/m)	Phase (deg)	Ampl. (deg/m)	Phase (deg)	Ampl. (deg/m)	Phase (deg)	Ampl. (deg/m)	Phase (deg)
0,00	0,000	0,0	0,000	0,0	0,000	0,0	0,000	0,0	0,000	0,0	0,000	0,0
4,00	0,063	34,2	0,063	34,2	0,0080	-44,1	0,0080	36,5	0,0080	36,5	0,000	0,0
4,50	0,071	266,3	0,071	-97,3	0,0050	170,6	0,019	-100,8	0,019	-100,8	0,000	0,0
5,00	0,079	255,5	0,079	-108,1	0,0030	107,3	0,036	-109,4	0,036	-109,4	0,000	0,0
5,50	0,089	250,6	0,089	-113,0	0,017	136,5	0,027	-115,7	0,027	-115,7	0,000	0,0
6,00	0,100	258,1	0,100	-105,5	0,018	164,6	0,010	-112,2	0,010	-112,2	0,000	0,0
6,50	0,114	317,3	0,114	-46,6	0,021	178,6	0,028	48,2	0,028	48,2	0,000	0,0
7,00	0,129	23,8	0,129	23,5	0,016	9,5	0,065	56,1	0,065	56,1	0,000	0,0
7,50	0,145	46,9	0,145	46,5	0,018	-10,1	0,115	63,6	0,115	63,6	0,000	0,0
8,00	0,164	19,7	0,164	11,9	0,046	-16,0	0,157	75,1	0,157	75,1	0,000	0,0
9,00	0,207	270,5	0,207	-93,1	0,113	-17,7	0,196	86,4	0,196	86,4	0,000	0,0
10,00	0,257	273,1	0,257	-90,6	0,203	-10,6	0,199	91,1	0,199	91,1	0,000	0,0
11,00	0,314	273,4	0,314	-90,2	0,261	-4,9	0,199	92,6	0,199	92,6	0,000	0,0
12,00	0,376	273,3	0,376	-90,3	0,306	-1,9	0,195	90,8	0,195	90,8	0,000	0,0
13,00	0,441	273,1	0,441	-90,5	0,335	-0,74	0,184	91,2	0,184	91,2	0,000	0,0
14,00	0,508	273,0	0,508	-90,6	0,338	-0,56	0,164	92,1	0,164	92,1	0,000	0,0
15,00	0,575	272,9	0,575	-90,7	0,329	-1,1	0,151	91,2	0,151	91,2	0,000	0,0
16,00	0,641	272,9	0,641	-90,7	0,306	-2,7	0,135	88,9	0,135	88,9	0,000	0,0
17,00	0,703	272,9	0,703	-90,7	0,241	-7,4	0,114	88,8	0,114	88,8	0,000	0,0
18,00	0,760	272,9	0,760	-90,7	0,126	-33,2	0,100	85,8	0,100	85,8	0,000	0,0
19,00	0,809	272,9	0,809	-90,7	0,251	-134,8	0,076	81,4	0,076	81,4	0,000	0,0
20,00	0,851	273,0	0,851	-90,6	1,134	-143,4	0,051	70,5	0,051	70,5	0,000	0,0
22,00	0,905	273,2	0,905	-90,4	2,282	-19,2	0,033	-7,9	0,033	-7,9	0,000	0,0
23,00	0,918	273,4	0,918	-90,3	1,658	-8,8	0,073	-57,2	0,073	-57,2	0,000	0,0
24,00	0,921	274,0	0,921	-90,0	1,410	-5,4	0,152	-63,9	0,152	-63,9	0,000	0,0
25,00	0,916	275,9	0,916	-89,2	1,272	-3,8	0,340	-59,9	0,340	-59,9	0,000	0,0
26,00	0,904	287,2	0,904	-86,7	1,205	-2,9	0,954	-26,4	0,954	-26,4	0,000	0,0
27,00	0,888	281,8	0,888	-72,3	1,148	-2,3	0,761	63,2	0,761	63,2	0,000	0,0
28,00	0,872	275,6	0,872	-79,6	1,120	-1,8	0,449	74,9	0,449	74,9	0,000	0,0
29,00	0,859	274,0	0,859	-88,1	1,090	-1,6	0,323	82,9	0,323	82,9	0,000	0,0
30,00	0,856	273,5	0,856	-89,6	1,071	-1,3	0,261	85,2	0,261	85,2	0,000	0,0
Infinity	0,856	270,8	0,609	-88,7	1,000	-1,3	0,259	86,5	0,259	86,5	0,000	0,0

Figure B.20: Vessel RAO, s (Response Amplitude Operators) for 45 Degree.

90 DEGREE



7° 45° 90° 135° 180°

Periods: 33

Period (s)	Surge		Sway		Heave		Roll		Pitch		Yaw	
	Ampl. (m/m)	Phase (deg)	Ampl. (m/m)	Phase (deg)	Ampl. (m/m)	Phase (deg)	Ampl. (deg/m)	Phase (deg)	Ampl. (deg/m)	Phase (deg)	Ampl. (deg/m)	Phase (deg)
0,00	0,000	0,0	0,000	0,0	0,000	0,0	0,000	0,0	0,000	0,0	0,000	0,0
4,00	0,000	0,0	0,063	-95,9	0,0080	-8,3	0,024	84,8	0,000	0,0	0,000	0,0
4,50	0,000	0,0	0,071	-117,3	0,0070	165,2	0,020	65,7	0,000	0,0	0,000	0,0
5,00	0,000	0,0	0,079	66,5	0,016	-172,9	0,016	195,1	0,000	0,0	0,000	0,0
5,50	0,000	0,0	0,089	71,1	0,0080	-148,2	0,044	250,2	0,000	0,0	0,000	0,0
6,00	0,000	0,0	0,100	75,9	0,0080	-154,8	0,061	260,9	0,000	0,0	0,000	0,0
6,50	0,000	0,0	0,114	83,9	0,010	0,84	0,088	260,6	0,000	0,0	0,000	0,0
7,00	0,000	0,0	0,129	90,6	0,021	-18,0	0,110	270,9	0,000	0,0	0,000	0,0
7,50	0,000	0,0	0,145	94,0	0,042	-25,3	0,140	282,8	0,000	0,0	0,000	0,0
8,00	0,000	0,0	0,164	92,1	0,123	-22,2	0,151	278,2	0,000	0,0	0,000	0,0
9,00	0,000	0,0	0,207	-83,8	0,218	-12,6	0,173	286,3	0,000	0,0	0,000	0,0
10,00	0,000	0,0	0,257	-87,5	0,274	-5,6	0,201	282,6	0,000	0,0	0,000	0,0
11,00	0,000	0,0	0,314	-89,2	0,315	-2,2	0,213	278,1	0,000	0,0	0,000	0,0
12,00	0,000	0,0	0,376	-89,9	0,339	-0,86	0,214	270,2	0,000	0,0	0,000	0,0
13,00	0,000	0,0	0,441	-90,3	0,342	-0,67	0,206	279,2	0,000	0,0	0,000	0,0
14,00	0,000	0,0	0,508	-90,5	0,331	-1,2	0,193	274,8	0,000	0,0	0,000	0,0
15,00	0,000	0,0	0,575	-90,6	0,302	-2,9	0,174	275,1	0,000	0,0	0,000	0,0
16,00	0,000	0,0	0,641	-90,7	0,244	-8,0	0,146	272,1	0,000	0,0	0,000	0,0
17,00	0,000	0,0	0,703	-90,7	0,137	-34,6	0,126	265,3	0,000	0,0	0,000	0,0
18,00	0,000	0,0	0,760	-90,7	0,258	-133,6	0,105	266,9	0,000	0,0	0,000	0,0
19,00	0,000	0,0	0,809	-90,6	1,119	-139,4	0,077	261,8	0,000	0,0	0,000	0,0
20,00	0,000	0,0	0,851	-90,5	3,604	-72,3	0,042	236,1	0,000	0,0	0,000	0,0
21,00	0,000	0,0	0,883	-90,2	2,261	-20,2	0,049	202,0	0,000	0,0	0,000	0,0
22,00	0,000	0,0	0,905	-90,4	1,653	-9,3	0,046	152,2	0,000	0,0	0,000	0,0
23,00	0,000	0,0	0,918	-90,2	1,408	-5,7	0,096	122,4	0,000	0,0	0,000	0,0
24,00	0,000	0,0	0,921	-89,8	1,275	-4,0	0,180	116,6	0,000	0,0	0,000	0,0
25,00	0,000	0,0	0,916	-89,0	1,203	-3,0	0,331	118,1	0,000	0,0	0,000	0,0
26,00	0,000	0,0	0,904	-86,1	1,150	-2,4	0,668	127,1	0,000	0,0	0,000	0,0
27,00	0,000	0,0	0,888	-72,7	1,117	-1,9	1,508	174,5	0,000	0,0	0,000	0,0
28,00	0,000	0,0	0,872	-79,1	1,097	-1,6	1,149	235,4	0,000	0,0	0,000	0,0
29,00	0,000	0,0	0,859	-87,5	1,072	-1,4	0,689	253,8	0,000	0,0	0,000	0,0
30,00	0,000	0,0	0,856	-89,3	1,000	-1,4	0,495	263,7	0,000	0,0	0,000	0,0
Infinity	0,000	0,0	0,856	-88,4	1,069	-1,3	0,493	268,8	0,000	0,0	0,000	0,0

Figure B.21: Vessel RAO, s (Response Amplitude Operators) for 90 Degree.

Appendix C: OrcaFlex Software Description

C.1 Introduction

This chapter is going to elaborate on the description of the OrcaFlex software in general, and the relation to this thesis. In this section, the content will be mainly based on the OrcaFlex Manual version 9.1a.

C.2 General Description about OrcaFlex

OrcaFlex is an analysis program for marine dynamics that is developed by Orcina. Its main purpose is for the static and dynamic analysis of the various offshore system, including marine riser types. Several analyses that are covered in this software are the global analysis, installation, mooring, towed system

The time domain features in this software allow for non-linear time domain analysis. This type of analysis can be performed for a specific section of a system and also for the whole system. It can be used to perform extreme response analyses for different sea states, as well as fatigue analysis of marine risers among the others.

Moreover, modal analysis can be done for individual lines, and Response Amplitude Operators (RAOs) can be calculated for the resulting variable by using Spectral Response Analysis feature in OrcaFlex.

The display in OrcaFlex is in 3D and it can cover multi-line systems, floating lines, and line dynamics after release. The main inputs include regular waves, random waves, and ship motions.

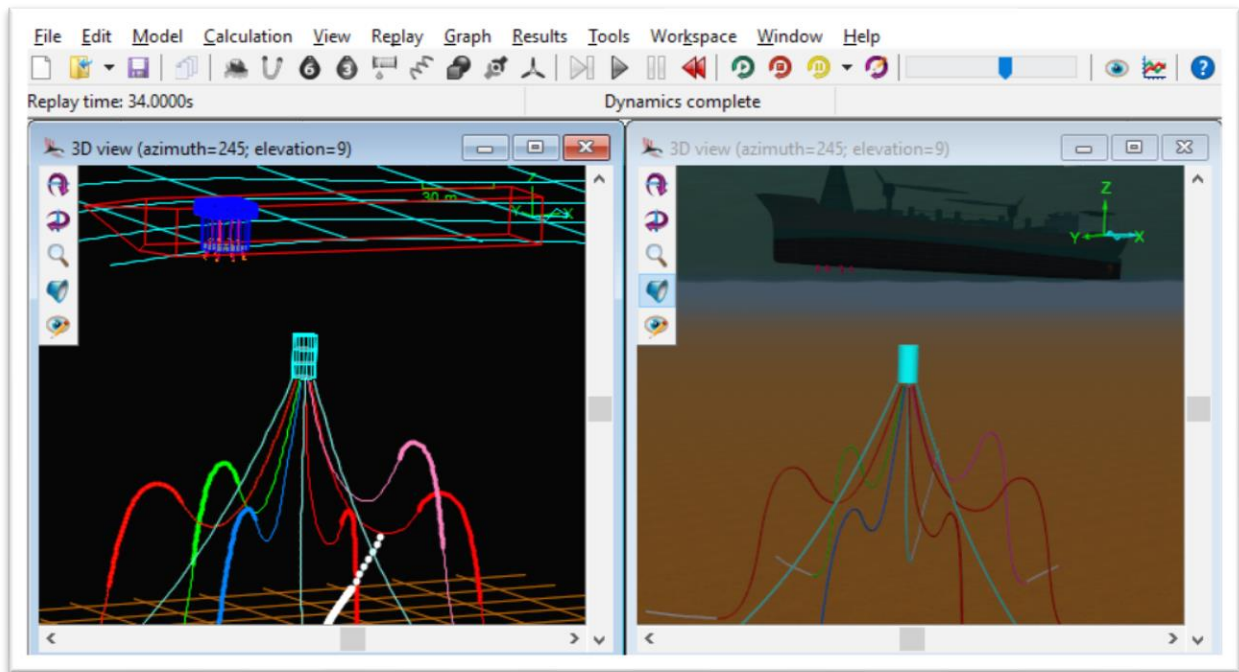


Figure C.1 – 3D View Wire Frame (Orcaflex Manual, 2012).

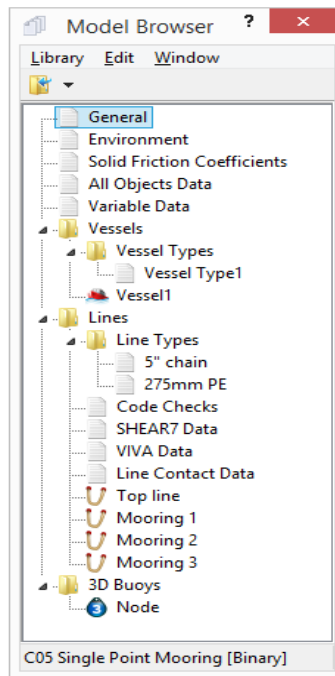


Figure C.2 Model Browser (Orcaflex Manual, 2012).

The menus in OrcaFlex include the general sequence from the static state and also dynamic simulation. The diagram below shows the sequence of simulation and the states that are prevalent together with the actions that are performed.

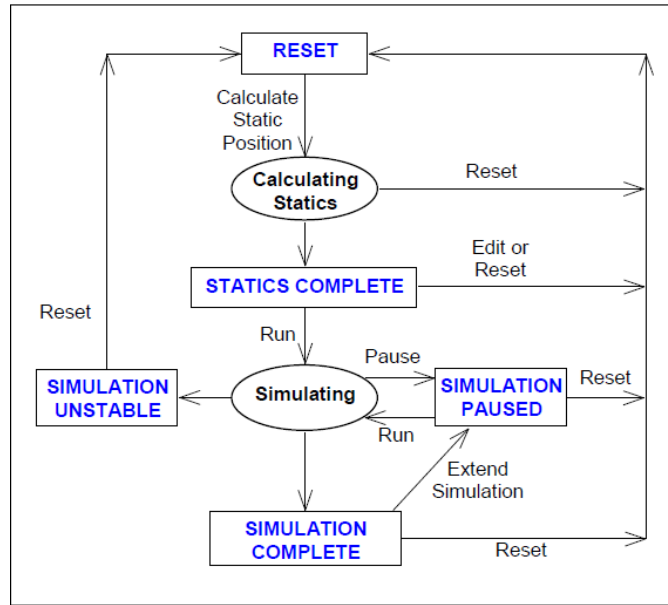


Figure C.3 Model States of OrcaFlex (OrcaFlex Manual, 2012).

C.3 Coordinate System

The coordinate system in OrcaFlex consists of two coordinate systems, the global coordinate system (GX, GY, and GZ) and local coordinate system (x, y, and z). These coordinate systems follow the right-hand rule with generally the Z-axis is pointing upwards for a positive value. Below Figure C.4 and Figure C.5 show the illustration of the coordinate systems, directions, and headings conventions.

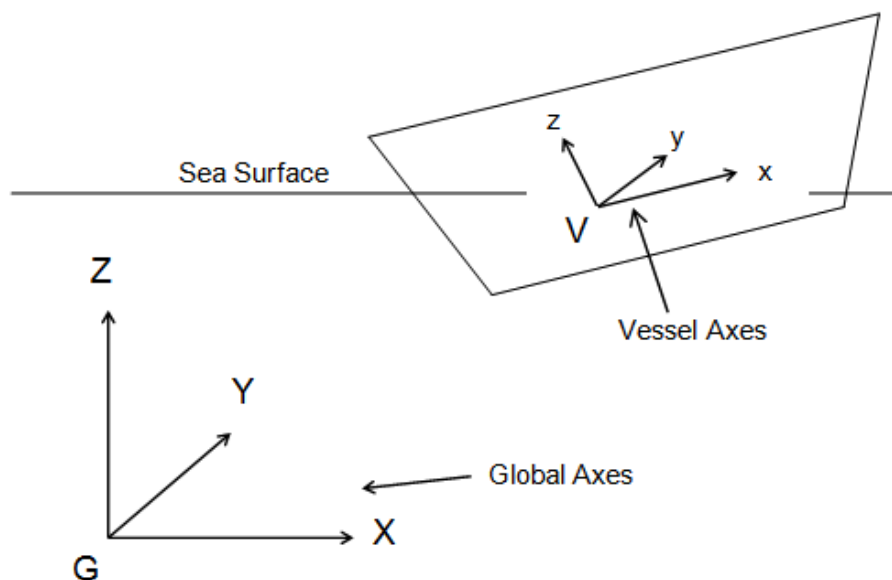


Figure C.4 Coordinate Systems (OrcaFlex Manual, 2012).

The different headings and directions in OrcaFlex, as shown in Figure C.5 below are specified by giving the azimuth angle for each direction, measured in a counterclockwise direction.

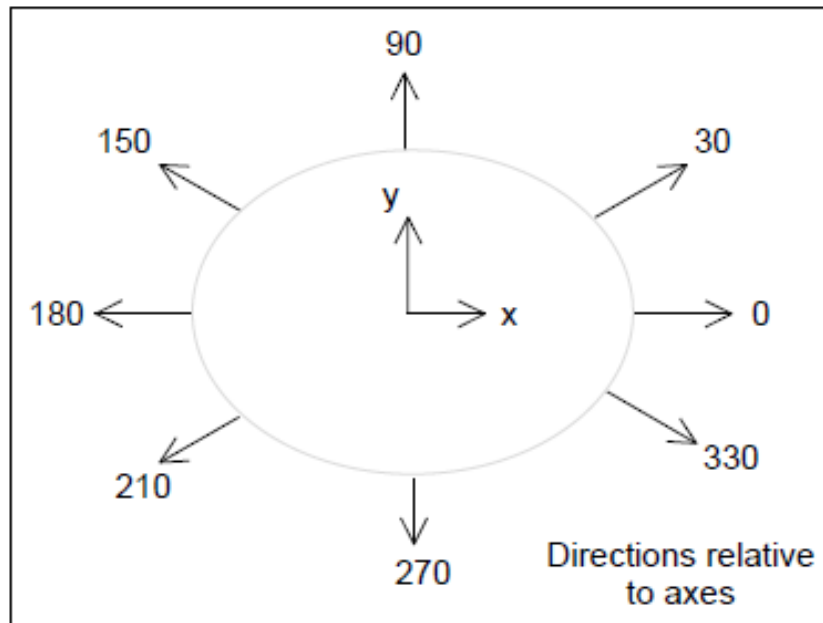


Figure C.5 – Directions and Headings (OrcaFlex Manual, 2012).

C.4 Static and Dynamic Stage

C.4.1 Static Analysis

The static analysis is the initial analysis that provides checking towards the static equilibrium condition of the model. The result of this analysis is used as a starting point for dynamic analysis simulation. In general, the two objectives of static analysis are:

- To determine the equilibrium configuration of the system in static loads, i.e., weight, buoyancy, hydrodynamic drag, etc.
- To prepare the starting configuration for dynamic analysis.

C.4.2 Dynamic Analysis

The dynamic analysis is a time-based simulation for the motions of the model over a certain period of time, from the initial position acquired by the static analysis. A number of consecutive stages in the dynamic analysis represent the period of simulation.

There is a build-up stage prior to the main simulation when the vessel and wave motions are gaining its size from zero to their maximum. This stage provides a smooth start and reduces the simulation time that is generated from static to full dynamic motion. The build-up stage is numbered 0, and its length normally will be set minimum one wave period. Refer below for details.

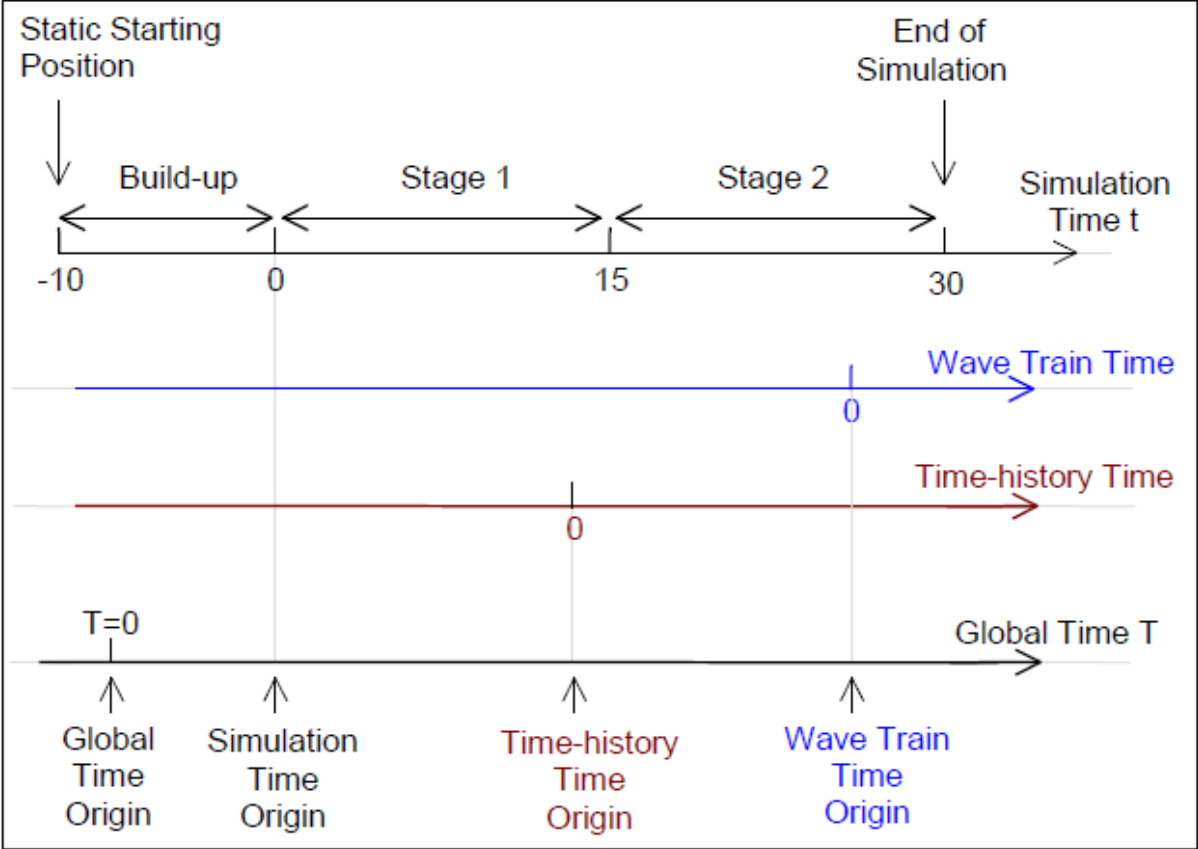


Figure C.6 – Time and Simulation Stages in Dynamic Analysis (OrcaFlex Manual, 2012).